Title
Quantifying the ecosystem-scale emission and deposition fluxes of biogenic volatile organic compounds (BVOC) and their oxidation products above plant canopies

Author
Park, Jeong-Hoo

Publication Date
2012

Peer reviewed|Thesis/dissertation

Quantifying the ecosystem-scale emission and deposition fluxes of biogenic volatile organic compounds (BVOC) and their oxidation products above plant canopies

By

Jeong-Hoo Park

A dissertation submitted in partial satisfaction of the

requirements for the degree of

Doctor of Philosophy

in

Environmental Science, Policy, and Management

in the

Graduate Division

of the

University of California, Berkeley

Committee in charge:

Professor Allen H. Goldstein, Chair

Professor Dennis D. Baldocchi

Professor Ronald C. Cohen

Fall, 2012

Quantifying the ecosystem-scale emission and deposition fluxes of biogenic volatile organic compounds (BVOC) and their oxidation products above plant canopies

Jeong-Hoo Park

Abstract

Quantifying the ecosystem-scale emission and deposition fluxes of biogenic volatile organic compounds (BVOC) and their oxidation products above plant canopies

by

Jeong-Hoo Park

Doctor of Philosophy in Environmental Science, Policy, and Management

University of California, Berkeley

Professor Allen H. Goldstein, Chair

Biogenic volatile organic compounds (BVOC) are one of the most important chemical classes in tropospheric chemistry associated with ozone and secondary organic aerosol formation. Nevertheless, their emission and deposition rates remain unknown for many potentially important plant species due to lack of measurements. Moreover, the number of BVOC species reported for flux measurement by current techniques has been limited to a small fraction of the number of compounds actually emitted or deposited. Thus, large uncertainties still exist in estimating the ecosystem-scale fluxes of BVOCs and their oxidation products (OVOC).

Two intensive field observation campaigns in different vegetation ecosystems took place in summer 2009 and 2010. The Biosphere Effects on AeRosols and Photochemistry EXperiment field campaign during summer 2009 (BEARPEX 2009, June 15 – July 31) was made in a Ponderosa pine plantation on the western slope of the Sierra Nevada Mountain range in California. During summer 2010 (June 25 – July 26), another intensive BVOC concentration and flux measurement campaign was conducted as part of a one-year continuous field campaign (CITRUS 2010, October 2009 – November 2010) in an orange orchard in the Central Valley of California near Visalia.

Through these two field campaigns, this dissertation presents the ecosystem-atmosphere exchange of a wide range of BVOC and OVOC by coupling state of the art VOC measurement techniques (proton transfer reaction mass spectrometry; PTR-MS, and proton transfer reaction – time of flight – mass spectrometry; PTR-TOF-MS) with a well-established micrometeorological approach (eddy-covariance method; EC). Ambient concentrations of BVOC and OVOC were simultaneously measured for investigating fluxes and vertical gradients in both field sites along with the meteorological parameters.

From BEARPEX 2009, I developed an approach of using the flux and gradient relationship from species which could be measured quickly enough to use the EC flux method (e.g. 5 Hz) to determine the eddy diffusivity (K), the apply that K to estimate the flux of species for which

sufficiently fast measurements were not available to use the EC method. In the past, K had been inferred from heat, H_2O and CO_2 which don't have similar exchange characteristics as BVOC, thus I suggest using a universal K derived from multiple BVOC can more accurately be applied where PTR-MS measurements are conducted.

In the CITRUS field campaign we simultaneously used PTR-MS for flux measurements of 3 species and vertical concentration gradient measurements of 27 species, and PTR-TOF-MS for flux and concentration measurements of a much fuller suite of VOCs above the plant canopy. Using the PTR-TOF-MS we demonstrate for the first time that there were significant emission for 27 VOC species for which concentration is commonly measured by PTR-MS, demonstrating not only the strong potential in use of PTR-TOF-MS in EC flux application but also possible underestimation in current knowledge about BVOC emission from land vegetation. For example, acetic acid was missed in flux measurements by the PTR-MS technique; however, acetic acid was here observed to be the third largest emission of any VOC species in the Orange orchard.

I demonstrate for the first time how the application of PTR-TOF-MS can expand our observational capabilities and changes the scope of understanding of VOC exchanges at atmosphere-biosphere interface. Previous work has mostly focused on quantifying emission strength from vegetation for a limited number of BVOC species. However, the results from flux measurements performed during CITRUS 2010 show the existence of significant deposition flux of BVOC and their oxidation products in addition to their emissions. Additionally, active ecosystem-atmosphere exchanges of the vast majority of the VOCs observed (at least 494 species) were discovered by applying a new approach (time shifted absolute value covariance). Through this measurement and analysis, I proved the existence of ecosystem-scale exchanges of species showing vast majority of VOC have bi-directional flux - both upward and downward. This observation is unprecedented, and revealed that most VOC species have at least some active exchange between the biosphere and atmosphere.

The observational evidence of active VOC exchanges in two independent ecosystems in this dissertation provides significant insights of interaction between the biosphere and atmosphere, coupling the VOC exchange and photochemistry within and above the plant canopy.

Table of Contents

List of Figures

List of Tables

Chapter 1: Introduction

1.1 Biogenic volatile organic compound (BVOC)

Volatile organic compounds (VOC) are emitted into the earth's atmosphere from biogenic (BVOC) and anthropogenic (AVOC) sources, and they play a critical role in regional and global atmospheric chemistry through the formation of tropospheric ozone (O_3) by reacting with nitrogen oxides in the presence of sunlight, and the production of secondary organic aerosol (SOA) via atmospheric chemical/physical processes (Chameides et al., 1988, Andreae and Crutzen, 1997; Fuentes et al., 2000; Jang et al., 2002; Goldstein and Galbally, 2007). Ozone and aerosol are important because they affect human health, plant health, regional air quality and Earth's climate. Anthropogenic sources of VOC mostly include fossil fuel combustion (e.g. car exhaust, direct release from power plants, petroleum operations, industry, airplanes, and ships), and their global emissions are estimated to be 142 Tg yr^{-1} (Singh, 1995). For biogenic sources, vegetation are the most important and emit a vast array of BVOC, including isoprene (C_5H_8), monoterpenes ($C_{10}H_{16}$), sesquiterpenes ($C_{15}H_{24}$), and oxygenated compounds (e.g. acetaldehyde; C_2H_4O, acetone; C_3H_6O). The global emissions of BVOC (1150 Tg C yr^{-1}) are known to be an order of magnitude larger than those of AVOC, thus about 90% of VOC are emitted naturally on the global scale (Guenther et al., 1995).

Once emitted into the atmosphere from plants, BVOCs start being oxidized by atmospheric oxidants such as ozone, hydroxyl (OH) and nitrate (NO_3) radicals, and they i) ultimately form carbon dioxide (CO_2) mainly through carbon monoxide (CO), ii) transform into SOA, or iii) are removed by dry or wet deposition (Goldstein and Galbally, 2007; Hallquist 2009). Through these processes, even more numerous species of VOC and their oxidized forms (OVOC) are animatedly produced and removed from the atmosphere, and their ambient concentrations range from less than a pptv to tens of ppbv.

1.2 Eddy covariance flux measurement of BVOC

Quantifying both emission and deposition rates of BVOC and their oxidation products are important to understand tropospheric chemistry. Over past few decades, the measurement methods for determining BVOC fluxes from plants, which include leaf cuvette, branch-enclosure, and flux-tower measurements, have been steadily improved. Particularly, up to date the eddy-covariance (EC) method is considered the most reliable and direct method to determine BVOC exchange between the atmosphere and biosphere, and is being widely used for measuring ecosystem scale fluxes for atmospheric trace gases such as carbon dioxide (CO_2), water (H_2O), and ozone (O_3) (Baldocchi et al., 1988; Dabberdt et al., 1993; Kurpius et al, 2002; Baldocchi, 2003). The EC method is a micrometeorologically-based method of measuring turbulent fluxes

in the internal boundary layer of the atmosphere. Turbulent flux may be considered as a superposition of eddies of different sizes (frequencies). Generally the vertical mass flux of a substance (F_c) is given as the time average of the product of the concurrent vertical wind speed (w) and concentration of the target trace gas (c). The instantaneous values of w and c can be decomposed into a mean and a variance component, so called Reynolds decomposition. The flux of the target trace gas is thus

$$F_c = \overline{w \cdot c} = \overline{(\overline{w} + w') \cdot (\overline{c} + c')} = \overline{w' \cdot c'} \qquad (1\text{-}1)$$

The over-bars denote the time average and the primes the variance part. Because a substantial part of the flux is transported by small eddies, the EC method requires a sensor which has very fast response (e.g., faster than 5 Hz) and high sensitivity.

The first BVOC EC flux measurement was conducted by Shaw et al. (1998) using a trace atmospheric gas analyzer (TAGA), and they measured acetone and formic acid fluxes over a fallow farm field near Columbus, Ohio. Guenther and Hills (1998) followed by measuring isoprene fluxes above an oak forest using a fast isoprene sensor based on chemiluminescence reaction between a primary alkene and ozone. Over the past decade, the development of the fast-response proton transfer reaction-mass spectrometer (PTR-MS) was a major advance in capability for EC flux measurements of a broader range of BVOC (Karl et al., 2002; Lee et al., 2005; Davison et al., 2009; Misztal et al., 2011). More recently, proton transfer reaction - time of flight - mass spectrometer (PTR-TOF-MS) allowed measuring an unprecedented number of BVOC simultaneously (Jordan et al., 2009; Graus et al., 2010; Ruuskanen et al., 2011)

1.3 Motivation for Current Research

Recent field studies have shown observational evidence that unmeasured and very reactive VOC species are chemically produced and/or directly emitted from tree ecosystems to the atmosphere. For example, Ciccioli et al. (1999) have shown substantial β-caryophyllene (a sesquiterpene, $C_{15}H_{24}$) emission from orange trees through branch enclosure experiments, but they were not able to detect above fluxes above the orchard canopy as much as it was emitted, suggesting β-caryophyllene is very reactive and oxidized before escaping the canopy. Kurpius and Goldstein (2003) showed that canopy scale O_3 deposition at Blodgett forest in summer was dominated by chemical loss rather than dry deposition and stomatal uptake, and inferred there must be emissions of highly reactive BVOC which had not yet been measured. At the same site, Holzinger et al. (2005) have revealed large emission of VOC oxidation products above the canopy adding up to 6-30 times total monoterpene emission. In addition, Di Carlo et al. (2004) observed higher OH reactivity than expected over a northern Michigan forest. All these studies indicate that many unknown or unidentified VOCs are still not accounted for in the BVOC inventory from forest canopy emissions.

Despite the improvement of measurement techniques, emission and deposition rates of BVOC and OVOC remain unknown for many potentially important plant species due to lack of measurements, and the number of compounds targeted have been limited to a few chemical species. For example, the EC fluxes of maximum up to 10 VOC species have been

simultaneously measured by PTR-MS systems in previous studies reported (Misztal et al., 2011) due to a limitation of the quadrupole mass filter which can only scan a few compounds discontinuously in a given time window (e.g. 1 scan of 5 compounds per 1 second with each dwell time of 0.2 second). This constrains our knowledge of VOC exchange between the atmosphere and biosphere for many unexplored VOCs and their oxidation products as described above. Therefore, this research is motivated by the need for new approaches to determine emission/deposition rates of a broader range of currently unmeasured VOC and OVOC at the ecosystem scale.

1.4 Overview of this research

In this dissertation, two field measurement campaigns were conducted for investigating ecosystem-scale VOC/OVOC emission and deposition fluxes at two different sites in California (Fig. 1.1);

i) Blodgett forest (ponderosa pine forest) on the western slope of the Sierra Nevada Mountains: Biosphere Effects on AeRosols and Photochemistry EXperiment during summer 2009 (BEARPEX 2009, June 15 – July 31).
ii) An orange orchard on the Central valley floor during summer 2010 (CITRUS 2010, June 25 – July 26), as part of a one-year continuous filed campaign (October 2009 – November 2010).

In both field campaigns, PTRMS was used to measure EC flux and vertical gradients simultaneously on an hourly basis. The EC flux measurement is to determine the ecosystem scale fluxes of specific BVOC (such as methylbutenol, methanol, monoterpenes, and other oxidized VOC), and the vertical gradient measurement is to understand BVOC emission characteristic and oxidation process within/above the plant canopy. Figure 1.2 shows a simple schematic of the experimental setup in both field sites. One inlet above the plant canopy (about 2 times canopy height for both campaigns) was used for measuring VOC fluxes with a three-dimensional sonic anemometer for 30 minutes of each hour, and four or five inlets at different heights were dedicated to observing vertical gradients of VOC with samples taken from each height sequentially over the other 30 minutes of each hour.

In Chapter 2, I focus on developing and using the flux-gradient relationship based on EC fluxes and vertical gradients of three BVOCs measured by a quadrupole PTR-MS in the Blodgett forest site, and using the eddy diffusivity estimated by this method to determine the fluxes of the other compounds for which only vertical gradients were measured. I then compare the measured fluxes to historical BVOC flux measurement results from the same site to investigate how fluxes have changed with time in this rapidly growing ponderosa pine plantation. The flux-gradient similarity method is shown to be useful, and I recommend its use in experimental conditions when fast BVOC measurement is not available for a broad range of VOCs.

In Chapter 3, I develop the methods for drastically expanding the range of VOC for which biosphere-atmosphere fluxes can be measured using a newly developed instrument (i.e. PTR-

TOF-MS) coupled to the EC method. Two PTR systems (i.e. PTR-TOF-MS and PTR-MS) were simultaneously deployed during CITRUS 2010 in the orange grove. PTR-TOF-MS EC flux data are carefully verified and thoroughly compared with EC flux and vertical gradients measured by PTR-MS, a relatively well established technique.

In Chapter 4, I present eddy covariance emission and deposition fluxes of the full range of VOCs including their oxidation products, which have never been previously observed, based on the data collected during CITRUS 2010. My findings from the observation using PTR-TOF-MS are 1) the vast majority of measured VOC are actively exchanged between the biosphere and atmosphere, 2) depositions of OVOC are significant, and 3) a large number of species having small fluxes and low concentrations need to be considered in current BVOC emission models.

In Chapter 5, I briefly summarize the results from two field campaigns conducted and propose future directions to answer key questions for the biosphere-atmosphere exchange of VOC and OVOC and their coupling with tropospheric chemistry.

1.5 References

Andreae, M. O., and Crutzen, P. J.: Atmospheric aerosols: Biogeochemical sources and role in atmospheric chemistry, Science, 276, 1052-1058, 1997.

Baldocchi, D. D., Hicks, B. B., and Meyers, T. P.: Measuring Biosphere-Atmosphere Exchanges of Biologically Related Gases with Micrometeorological Methods, Ecology, 69, 1331-1340, 1988.

Baldocchi, D. D.: Assessing the eddy covariance technique for evaluating carbon dioxide exchange rates of ecosystems: past, present and future, Global Change Biol, 9, 479-492, 2003.

Chameides, W. L., Lindsay, R. W., Richardson, J., and Kiang, C. S.: The Role of Biogenic Hydrocarbons in Urban Photochemical Smog - Atlanta as a Case-Study, Science, 241, 1473-1475, 1988.

Ciccioli, P., Brancaleoni, E., Frattoni, M., Di Palo, V., Valentini, R., Tirone, G., Seufert, G., Bertin, N., Hansen, U., Csiky, O., Lenz, R., and Sharma, M.: Emission of reactive terpene compounds from orange orchards and their removal by within-canopy processes, J Geophys Res-Atmos, 104, 8077-8094, 1999.

Dabberdt, W. F., Lenschow, D. H., Horst, T. W., Zimmerman, P. R., Oncley, S. P., and Delany, A. C.: Atmosphere-Surface Exchange Measurements, Science, 260, 1472-1481, 1993.

Davison, B., Taipale, R., Langford, B., Misztal, P., Fares, S., Matteucci, G., Loreto, F., Cape, J. N., Rinne, J., and Hewitt, C. N.: Concentrations and fluxes of biogenic volatile organic compounds above a Mediterranean macchia ecosystem in western Italy, Biogeosciences, 6, 1655-1670, doi:10.5194/bg-6-1655-2009, 2009.

Di Carlo, P., Brune, W. H., Martinez, M., Harder, H., Lesher, R., Ren, X. R., Thornberry, T., Carroll, M. A., Young, V., Shepson, P. B., Riemer, D., Apel, E., and Campbell, C.: Missing OH reactivity in a forest: Evidence for unknown reactive biogenic VOCs, Science, 304, 722-725, 2004.

Fuentes, J. D., Lerdau, M., Atkinson, R., Baldocchi, D., Bottenheim, J. W., Ciccioli, P., Lamb, B., Geron, C., Gu, L., Guenther, A., Sharkey, T. D., and Stockwell, W.: Biogenic hydrocarbons in the atmospheric boundary layer: A review, B Am Meteorol Soc, 81, 1537-1575, 2000.

Goldstein, A. H., and Galbally, I. E.: Known and unexplored organic constituents in the earth's atmosphere, Environ Sci Technol, 41, 1514-1521, 2007.

Graus, M., Muller, M., and Hansel, A.: High Resolution PTR-TOF: Quantification and Formula Confirmation of VOC in Real Time, J Am Soc Mass Spectr, 21, 1037-1044, doi:10.1016/j.jasms.2010.02.006, 2010.

Guenther, A., Hewitt, C. N., Erickson, D., Fall, R., Geron, C., Graedel, T., Harley, P., Klinger, L., Lerdau, M., Mckay, W. A., Pierce, T., Scholes, B., Steinbrecher, R., Tallamraju, R., Taylor, J., and Zimmerman, P.: A Global-Model of Natural Volatile Organic-Compound Emissions, J Geophys Res-Atmos, 100, 8873-8892, 1995.

Guenther, A. B., and Hills, A. J.: Eddy covariance measurement of isoprene fluxes, J Geophys Res-Atmos, 103, 13145-13152, 1998.

Hallquist, M., Wenger, J. C., Baltensperger, U., Rudich, Y., Simpson, D., Claeys, M., Dommen, J., Donahue, N. M., George, C., Goldstein, A. H., Hamilton, J. F., Herrmann, H., Hoffmann, T., Iinuma, Y., Jang, M., Jenkin, M. E., Jimenez, J. L., Kiendler-Scharr, A., Maenhaut, W., McFiggans, G., Mentel, T. F., Monod, A., Prevot, A. S. H., Seinfeld, J. H., Surratt, J. D., Szmigielski, R., and Wildt, J.: The formation, properties and impact of secondary organic aerosol: current and emerging issues, Atmos Chem Phys, 9, 5155-5236, 2009.

Holzinger, R., Lee, A., Paw, K. T., and Goldstein, A. H.: Observations of oxidation products above a forest imply biogenic emissions of very reactive compounds, Atmos Chem Phys, 5, 67-75, 2005.

Jang, M. S., Czoschke, N. M., Lee, S., and Kamens, R. M.: Heterogeneous atmospheric aerosol production by acid-catalyzed particle-phase reactions, Science, 298, 814-817, 2002.

Jordan, A., Haidacher, S., Hanel, G., Hartungen, E., Mark, L., Seehauser, H., Schottkowsky, R., Sulzer, P., and Mark, T. D.: A high resolution and high sensitivity proton-transfer-reaction time-of-flight mass spectrometer (PTR-TOF-MS), Int J Mass Spectrom, 286, 122-128, doi:10.1016/j.ijms.2009.07.005, 2009.

Karl, T. G., Spirig, C., Rinne, J., Stroud, C., Prevost, P., Greenberg, J., Fall, R., and Guenther, A.: Virtual disjunct eddy covariance measurements of organic compound fluxes from a subalpine forest using proton transfer reaction mass spectrometry, Atmos Chem Phys, 2, 279-291, 2002.

Kurpius, M. R., McKay, M., and Goldstein, A. H.: Annual ozone deposition to a Sierra Nevada ponderosa pine plantation, Atmos Environ, 36, 4503-4515, 2002.

Kurpius, M. R., and Goldstein, A. H.: Gas-phase chemistry dominates O_3 loss to a forest, implying a source of aerosols and hydroxyl radicals to the atmosphere, Geophys Res Lett, 30, 1371, doi:10.1029/2002gl016785, 2003.

Lee, A., Schade, G. W., Holzinger, R., and Goldstein, A. H.: A comparison of new measurements of total monoterpene flux with improved measurements of speciated monoterpene flux, Atmos Chem Phys, 5, 505-513, 2005.

Misztal, P. K., Nemitz, E., Langford, B., Di Marco, C. F., Phillips, G. J., Hewitt, C. N., MacKenzie, A. R., Owen, S. M., Fowler, D., Heal, M. R., and Cape, J. N.: Direct ecosystem fluxes of volatile organic compounds from oil palms in South-East Asia, Atmos Chem Phys, 11, 8995-9017, doi:10.5194/acp-11-8995-2011, 2011.

Ruuskanen, T. M., Mueller, M., Schnitzhofer, R., Karl, T., Graus, M., Bamberger, I., Hortnagl, L., Brilli, F., Wohlfahrt, G., and Hansel, A.: Eddy covariance VOC emission and deposition fluxes above grassland using PTR-TOF, Atmos Chem Phys, 11, 611-625, doi:10.5194/acp-11-611-2011, 2011.

Shaw, W. J., Spicer, C. W., and Kenny, D. V.: Eddy correlation fluxes of trace gases using a tandem mass spectrometer, Atmos Environ, 32, 2887-2898, 1998.

Singh, H. B.: Composition, chemistry, and climate of the atmosphere, Van Nostrand Reinhold, New York, xii, pp 88-119, 1995.

Figure 1.1. Google Earth image of two field sites for BEARPEX 2009 and CITRUS 2010 in California.

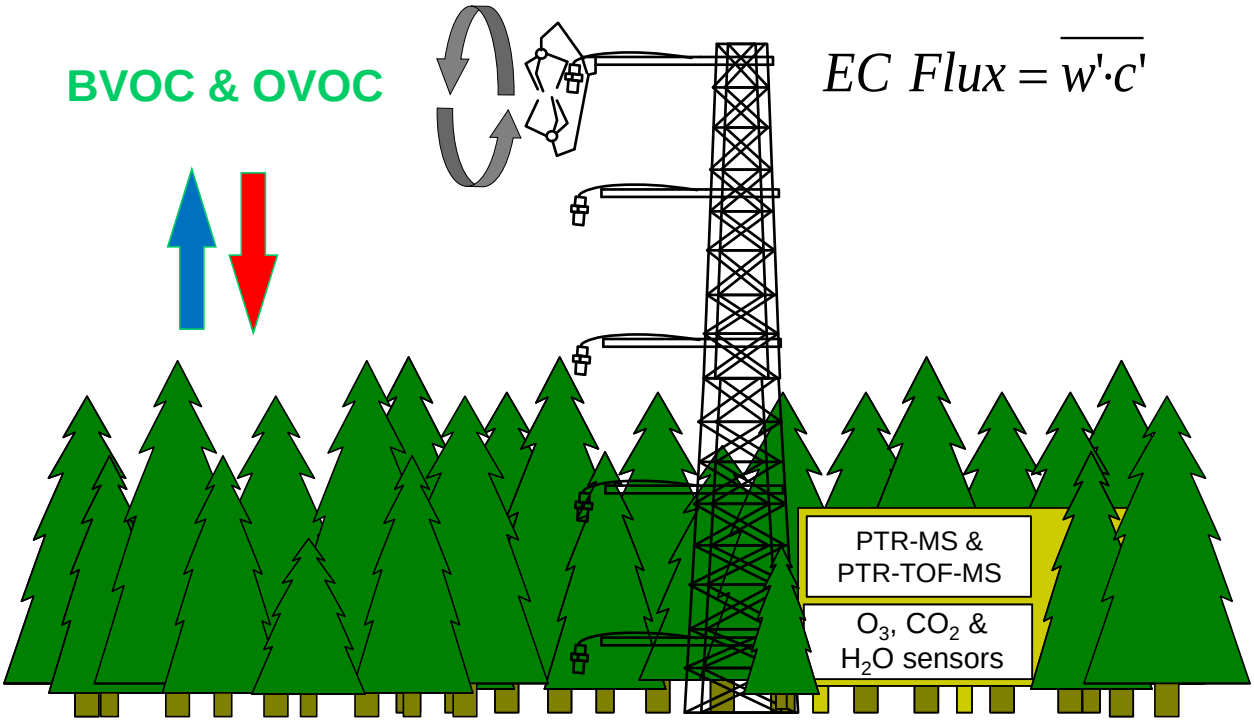

Figure 1.2. Simple schematic of the experiment setup for BEARPEX 2009 and CITRUS 2010. One inlet above the plant canopy was used to determine canopy scale fluxes of biogenic volatile organic compounds (BVOC) and their oxidation products (OVOC) by applying the Eddy Covariance (EC) method, and four or five inlets were installed to measure vertical gradients of BVOC/OVOC.

Chapter 2: Biogenic volatile organic compound emissions during BEARPEX 2009 measured by eddy covariance and flux-gradient similarity methods

Abstract

The Biosphere Effects on AeRosols and Photochemistry EXperiment (BEARPEX) took place in Blodgett Forest, a Ponderosa pine forest in the Sierra Nevada Mountains of California, during summer 2009. We deployed a Proton Transfer Reaction – Mass Spectrometer (PTR-MS) to measure fluxes and concentrations of biogenic volatile organic compounds (BVOCs). Eighteen ion species including the major BVOC expected at the site were measured sequentially at 5 heights to observe their vertical gradient from the forest floor to above the canopy. Fluxes of the 3 dominant BVOCs methanol, 2-Methyl-3-butene-2-ol (MBO), and monoterpenes, were measured above the canopy by the eddy covariance method. Canopy scale fluxes were also determined by the flux-gradient similarity method (K-theory). A universal K (K_{univ}) was determined as the mean of individual K's calculated from the measured fluxes divided by vertical gradients for methanol, MBO, and monoterpenes. This K_{univ} was then multiplied by the gradients of each observed ion species to compute their fluxes. The flux-gradient similarity method showed very good agreement with the Eddy Covariance method. Fluxes are presented for all measured species and compared to historical measurements from the same site, and used to test emission algorithms used to model fluxes at the regional scale. MBO was the dominant emission observed followed by methanol, monoterpenes, acetone, and acetaldehyde. The flux-gradient similarity method is shown to be a useful, and we recommend its use especially in experimental conditions when fast measurement of BVOC species is not available.

2.1 Introduction

Defining source strengths of biogenic volatile organic compounds (BVOC; e.g. isoprene and monoterpenes) and understanding their role in ozone (O_3) and secondary organic aerosol (SOA) formation are critical issues in atmospheric chemistry and climate science (Chameides et al., 1988; Andreae and Crutzen, 1997; Fuentes et al., 2000; Jang et al., 2002). On the global scale, VOC emissions from terrestrial vegetation are estimated to be an order of magnitude greater than those from fossil fuel combustion (Guenther et al, 1995). Additional unmeasured organics in the atmosphere are assumed to exist in both the gas and particle phases (Goldstein and Galbally, 2007). Substantial evidence has also been presented for the emissions of highly reactive BVOCs from forest ecosystems that have yet to be adequately quantified and included in BVOC emission models (Kurpius and Goldstein, 2003; De Carlo et al., 2004; Holzinger et al. 2005). More comprehensive observations are needed to better constrain the full range of BVOC emissions from ecosystems and their importance for atmospheric chemistry.

Landscape-scale BVOC flux measurement techniques (e.g. eddy covariance, relaxed eddy accumulation, flux-gradient similarity, and mixed boundary layer) have been increasingly implemented in recent years (Goldstein et al., 1996; Schade and Goldstein, 2001; Karl et al., 2002; Lee et al., 2005). The eddy covariance (EC) method using proton transfer reaction – mass spectrometry (PTR-MS) is currently the most direct and reliable measurement for measuring BVOC fluxes at the canopy scale (Karl et al., 2002, Lee et al., 2005). However, this instrument allows continuous EC measurement of fluxes for only a limited number of compounds because the EC method requires fast measurement response time (e.g. > 1 Hz data) to capture concentration changes in the eddies over the forest and the quadrupole mass filter in PTR-MS requires a dwell time of order 0.2 seconds per mass to obtain adequate signal. The flux-gradient similarity approach, generally called K-theory, can be used for measuring fluxes at the canopy scale. In this method, the flux is calculated by multiplying the atmospheric eddy diffusivity (K) by the vertical concentration gradient of trace gases (Goldstein et al., 1996). In past applications for measuring BVOC fluxes using this approach, K was determined from flux and vertical gradient measurements of H_2O, CO_2, or sensible heat and multiplied by a 30 minute average vertical BVOC gradient measured by in-situ GC (Goldstein et al., 1998, Schade et al., 2000). Disadvantage of this approach is that the vertical source and sink profiles of H_2O, CO_2, or sensible heat may differ significantly from those of BVOCs resulting in errors in the similarity assumption for K among these different tracers. Thus, more accurate determination of BVOC fluxes by this approach for a wide range of species should be possible using EC flux and vertical gradient measurements of a few dominant BVOCs to determine K, and then multiplying K by vertical gradients for each of the observed BVOCs.

The Biosphere Effects on Aerosols and Photochemistry Experiment (BEARPEX) 2009 was designed to study the emissions of BVOC and their role in SOA formation, oxidant, and ozone photochemistry. As part of BEARPEX 2009, we deployed a PTR-MS (Ionicon QMS) to measure EC fluxes and vertical gradients of BVOCs in a ponderosa pine plantation in the Sierra Nevada mountains of California with the goals to 1) determine fluxes of BVOCs (17 species) by a combination of direct EC flux measurements and the flux-gradient similarity approach, 2)

compare measured fluxes with historical measurements from the same site, in order to highlight vegetation change effects on emissions, and 3) test emission algorithm for the main BVOC species emitted by the vegetation and provide basal emission factors which could be used to model fluxes at regional scale.

2.2 Experiment

2.2.1 Measurement site

The BEARPEX 2009 intensive field campaign took place in Blodgett Forest from 15 June to 31 July 2009. This site is a Ponderosa pine forest located in the western foothills of the Sierra Nevada Mountains of California (38.90^{o}N, 120.63^{o}W, 1315m elevation), ~75 km downwind of Sacramento, and has been described in detail elsewhere (Goldstein et al., 2000; Lamanna and Goldstein, 1999; Schade and Goldstein, 2001; Dillon et al., 2002). Briefly, the land is owned and operated by Sierra Pacific Industries (SPI), and the plantation is dominated by ponderosa pine (Pinus ponderosa L.) trees with an average tree height of 8.7 m in 2009. The understory is dominated by manzanita (*Arctostaphylos* spp.) and whitethorn (*Ceanothus cordulatus*). In summertime, winds at this site are predominantly westerly to southwesterly (220 – 280^{o}) during the day and northeasterly at night (30-60^{o}). This daytime wind pattern transports polluted air from the Sacramento urban area to the pine forest site, along with isoprene and its oxidation products dominantly emitted from oak forests ~30 km southwest of the site (Dreyfus et al., 2002). The site is characterized by a Mediterranean type climate, with the majority of precipitation occurring between September and May, and almost no rain in the summer. Average daily temperature ranged from 12^{o} to 26^{o}C during the campaign period, with no rain recorded.

Two towers were set up at this site. One was a 15 m tall walk-up tower which was installed in 1997. Meteorological parameters such as air temperature, humidity, wind speed and direction, and photosynthetically active radiation (PAR) were measured continuously from this tower and stored in 30 min averaged data sets. Ecosystem-scale fluxes and mixing ratios of trace gases including CO_2, O_3 and VOCs have been measured at this original tower since its construction (Goldstein et al., 2000; Kurpius et al., 2002; Holzinger et al., 2005; Lee et al., 2005; Fares et al. 2010). A new 18 m tall scaffolding tower was built in 2007 and located ~10 m north from the original tower. During the 2007 and 2009 summer intensive campaigns (BEARPEX 2007 and BEARPEX 2009), a full range of atmospheric trace gases and aerosols were measured by researchers from more than 10 institutions (Bouvier-Brown et al., 2009a, Wolfe et al., 2009, Smeets et al.,2009, Ren et al., 2010). Observations of vertical gradients and fluxes of BVOCs by PTR-MS were made from 17 June (25 June for fluxes) to 29 July 2009 at the new tower. Electrical power was provided by a propane generator located approximately 125 m north of the new tower. Contamination from generator exhaust was observed occasionally at night when wind was slow and variable, but BVOC measurements were rarely affected.

2.2.2 PTR-MS BVOC measurement

Instrument setup

A PTR-MS (Ionicon Analytik, Innsbruck, Austria) was set up to measure BVOC mixing ratios at multiple heights for determination of fluxes and vertical gradients. All measured compounds are listed by mass to charge ratios (*m/z*) in Table 2.1. The principles of the PTR-MS have been described in detail elsewhere (Lindinger et al., 1998; de Gouw and Warneke, 2007). Briefly, the PTR-MS is a chemical ionization technique that uses hydronium ions (H_3O^+) to transfer a proton (H^+) from water to the VOC of interest, thus any VOC with a proton affinity higher than water is ionized in the instrument's drift tube, introduced into the quadrupole mass spectrometer and detected by the secondary electron multiplier (SEM). The same instrument has been employed for past measurements of fluxes and vertical gradients at Blodgett Forest (Holzinger et al., 2005; Lee et al., 2005), and also for a similar measurement set up in a citrus orchard (Fares et al., 2012).

Air sample inlet heights on the measurement tower are depicted in figure 2.1. During each hour, six gas sampling inlets were used. One sampling inlet and a 3-D sonic anemometer (Campbell CSAT-3) were co-located at the top of the tower (17.8m, about twice the canopy height) to measure flux by EC during the first 30 minutes of each hour. During second 30 minutes of every hour the other five inlets were sampled sequentially to measure vertical gradients above and within the forest canopy for 6 minutes at each height (17.8 m, 13.6 m, 9.5 m, 5.7 m, and 1.5 m). All inlets were protected by identical Teflon filters (PFA holder, PTFE membrane, pore size 2 μm) to avoid contamination by particles in the air sample. Each inlet was plumbed to the PTR-MS with identical 30 m lengths of PFA tubing (OD 6.35mm, ID 3.96 mm). A sample flow of 10L/min was maintained at all times through each sample tube to minimize residence time and any memory effects from previously sampled air, and to maintain a turbulent flow for the EC flux measurement. The Teflon filters were replaced every week and no signal differences for any measured compounds were observed after changing the filters. The PTR-MS sequentially sub-sampled ~0.6 L/min from each inlet, and was maintained at an E/N (electric field to buffer gas number density) ratio of 139 Td by adjusting drift tube pressure, temperature, and voltage to 200 Pa, 50 ^oC, and 604 V, respectively. The reaction time in the drift tube was 100 μs and the count rate of $H_3O^+H_2O$ ions (water clusters) was less than 3% of the count rate of H_3O^+ ions. The H_3O^+ reactant ion was kept in the range $8 \pm 2 \times 10^6$ counts s^{-1}.

Measurement calibration

Calibrations were performed by dynamic dilution of gravimetrically mixed gas-phase standards (Apel & Riemer, USA) including 2.2 – 5.1 ppmv of methanol, acetaldehyde, acetone, isoprene, methyl-vinyl-ketone, benzene, α-pinene, *d*-limonene, Δ-3-carene into zero air at ambient humidity levels. Zero air was created by passing sampled ambient air through a stainless steel tube filled with Platinum-coated quartz wool (Shimadzu) heated to 350^oC, catalytically removing VOCs from the sample. This zero air was directly measured to determine instrumental background counts twice daily (2:30-2:40 and 15:00-15:10 PST), and no significant difference between daytime and nighttime background was observed. Calibrations were also done twice a

day for 20 minutes each after background measurement by diluting with purified air to concentrations of 40 ppbv – 100 ppbv. In order to check linearity of calibration curves at different concentrations of standard gases and compare them to the twice daily calibrations, we also performed 5-level multipoint calibrations (e.g. 7, 12, 24, 35, 47 ppbv for d-limonene) before and after instrument and site maintenance activities during the campaign, such as optimizing the PTR-MS SEM voltage and shutting down the electrical generator for oil changes. Measured mixing ratios from before-and-after calibration curves were in very good agreement for all compounds, with maximum difference within 6%, and a minimum R-square of 0.98. To determine mixing ratios of masses for which standard gases were not available, we calculated normalized sensitivities (counts/concentration) based on calculated proton transfer reaction rate coefficients and the instrument-specific transmission curve (de Gouw and Warneke 2007). This curve was determined for *m/z* 33 to 219 using a gas standard mixture (methanol, acetonitrile, acetaldehyde, acetone, methacrolein, benzene, toluene, xylene, triflorobenzene, bromobenzene, trichlorobenzene, and iodotoluene) at concentrations of 100 ppb (Apel & Riemer, USA). The transmission test was conducted along with each multipoint calibration. PTR-MS signal at *m/z* 69 is the sum of a fragment of 2-methyl-3-butene-2-ol plus the parent mass of isoprene (MBO + isoprene). Calibration of the mixing ratio for this mass was achieved by scaling the PTR-MS measurement to equal the sum of MBO + ISOP measured simultaneously by gas chromatography-flame ionization detector (GC-FID) (C. Park and G. Schade group, Texas A&M university, correlation coefficient (slope 1, R^2 0.73). For monoterpenes (MTs), the parent ion is observed at *m/z* 137 and the most abundant fragment occurs at *m/z* 81. The signal intensity was higher at *m/z* 81 than *m/z* 137 because of higher transmission efficiency. Thus, *m/z* 81 was used for total monoterpene flux measurements and calibrated by using a mixed monoterpene (alpha-pinene, 3-carene, and d-limonene) standard gas. The sum of *m/z* 81 and 137 was used for vertical gradient measurement. Comparison between the monoterpene concentrations from the flux inlet determined on *m/z* 81 with the vertical gradient inlet at the same height (17.8 m) for the adjacent 30 minute period determined on the sum of *m/z* 81+137 showed good agreement (slope 0.95, R^2 0.84). Measurement accuracy for all compounds included in the calibration gas standard cylinder was better than ± 20%. For all other compounds the concentration has been estimated using the collision rate constant which should equal the reaction rate constant within ± 30% (Holzinger et al., 2005).

2.2.3 Eddy covariance flux measurements

Fluxes of four BVOC masses (*m/z* 33, 69, 81, and 113) were measured using the eddy covariance method. Mixing ratios were measured with dwell time of 0.2 s per mass (5 Hz measurement resolution, ~0.8 s per a cycle), resulting in 2120 measurement cycles per 30 min flux period. Wind speed and temperature signals from 3-D sonic anemometer were recorded on a datalogger (Campbell Scientific CR-23x) at 10Hz. For each 30 min flux measurement period, horizontal and vertical wind vectors were rotated according to a planar fit technique (Wilczack et al. 2001). Individual lag times for each 30-min flux period were determined by finding the time point with the maximum cross-correlation coefficient of vertical wind speed and BVOC mixing ratios in ± 60 seconds time windows. Lag times accounted for changes in clock synchronization between the PTR-MS computer and the data logger recording wind data, and for sampling flow

and instrument response times. In cases in which a clear covariance peak was not observed, particularly at night time when vertical turbulence was low, we interpolated lags between the two nearest points having strong covariance peaks. The lag time correction has been applied to these data, and we used the same lag time for all masses. After the lag time correction, figure 2.2 shows the cross correlations between vertical wind speed and each BVOC (*m/z* 33, 69, and 81) by time peak at 0 second, indicating all BVOCs measured have the same lag times in one flux period.

Fluxes for 4 mass to charge ratios of interest (*m/z* 33, 69, 81 and 113, but we do not report *m/z* 113 fluxes in this paper) were determined according to the virtual (continuous flow) disjunct eddy covariance method (Rinne et al., 2001; Karl et al., 2002), which can be regarded as a variant of the EC method. The vertical fluxes of BVOCs were calculated as the mean covariance between deviations of the vertical wind speed and each BVOC mixing ratio for a flux period (30 minutes), thus we used a subsample of the vertical wind speed (w) data after subtracting the lag time (Δt) due to slower data acquisition frequency for each measured BVOC (5 Hz) than the wind (10 Hz). Flux was determined according to the equation:

$$F_{EC} = \frac{\sigma}{N}\sum_{i=1}^{N} w' \cdot c'(i) \qquad (1)$$

where σ is the air density (mol m^{-3}), w' is the instantaneous deviation of the vertical wind speed from its average, c' is that of the BVOC mixing ratio (nmol mol^{-1}) (i.e. $w' = w - \overline{w}$, $c' = c - \overline{c}$), and N is the total number of data points in the measurement period.

The EC method requires that the estimated fluxes within an analyzed period are stationary. To test for sationarity, we divided each 30 min flux period into 5 segments (6 min data for each), calculated the EC flux for each segment, and compared the average to the EC flux for the full 30 min period. We rejected data if the tilt angle from rotating the vertical wind data exceeded 5^{o} or fluxes for any times when the segmental flux was not within ± 30% of the full 30 min flux (Lee et al., 2004; Foken and Wichura, 1996). More than 92 % of daytime (9:00 – 15:00 PST) and 86% of nighttime (21:00 – 3:00 PST) data passed these filtering criteria.

We tested for potential flux errors from several known sources. Spectral attenuation by sensor separation and inlet dampening effects were estimated using transfer functions described elsewhere in detail (Moore, 1986; Massman, 1991), and these had less than 1 % affect on our measured EC fluxes. Loss of flux signal can arise from inadequate sensor response time and can be estimated as;

$$\frac{F_{meas}}{F_{true}} = \frac{1}{1 + (2\pi \cdot f_m \cdot \tau_c)^{\alpha}} \qquad (2)$$

where F_{meas} is the measured flux, F_{true} is the true flux (non-attenuated flux), f_m is the frequency of the peak at which the frequency weighted cospectrum maximizes, τ_c is the first-order response time of the instrument, and α is 7/8 for neutral and unstable stratification within the surface layer

and 1 for stable condition (Horst, 1997). Based on this consideration, if we consider only daytime (9:00 to 17:00 PST) fluxes with τ_c of 1 second and f_m of ranges between 0.01 and 0.02 for day time, fluxes could be underestimated by 8-14 %. This is a similar range to what was estimated during a previous study at this site (Lee et al, 2005), and we did not correct flux data for this effect.

The storage of BVOC emission between the ground and the flux measurement height may be important during times when the air is in a stable stratified condition or turbulent mixing is weak, thus plant or soil emissions in such periods may not be well represented in the above canopy flux mesaurements. We incorporated this into our flux calculation using

$$F = F_{EC} + \frac{\partial}{\partial t}\int_0^h [BVOC](z)dz \qquad (3)$$

where, z and h is the height of vertical gradient and EC flux measurements, and [*BVOC*] is the mixing ratio of each compound. The storage term for methanol (*m/z* 33), MBO+isoprene (*m/z* 69), and monoterpenes (*m/z* 81) contributed 57%, 8%, and 65% respectively compared to EC flux in the morning hours 06:00 – 08:00 PST, and were extremely small during the daytime (less than 0.7%).

2.2.4 Vertical gradient measurements

Vertical gradients were measured for 18 masses as listed in Table 2.1. These masses were chosen to observe the most important compounds at this site based on previous BVOC observations performed by gas chromatography (GC) and PTR-MS from 1997 to 2007 (Lamanna and Goldstein, 1999; Schade et al., 2000; Holzinger et al., 2005; Bouvier-Brown et al., 2009a). Using multiple ion detection mode in the PTR-MS software (Balzer QS 422), these masses were scanned for 14 cycles over 6 minutes for each height with a dwell time on each mass of 1 second, except for *m/z* 205 for which we used a dwell of 5 seconds to improve detection limits for this mass. The first 4 cycles after switching inlet heights were discarded, and data for the last 10 cycles for each height were used to compute hourly averaged datasets.

2.3 Results

2.3.1 Concentration and vertical gradients

Figure 2.3 (a) – (c) shows the full time series of volume mixing ratios for methanol (*m/z* 33), MBO+isoprene (*m/z* 69), and the sum of monoterpenes (*m/z* 81 + *m/z* 137), with mixing ratios averaged from all measurement heights. All these compounds appear dependant on temperature

shown in figure 2.3(d). Methanol is most abundant, followed by MBO+isoprene, acetone, acetaldehyde, MVK+MACR, and total monoterpenes as summarized in Table 2.1. Figure 2.4 presents the average diurnal profile of vertical gradients for methanol, MBO+isoprene, and monoterpenes in addition to ozone. Mixing ratios of all these BVOCs decrease with increased inlet height indicating emission from the forest, and this higher mixing ratio at lower height within the canopy is due to more biomass near the surface. In contrast, the ozone gradient is inversed, suggesting active BVOC oxidation processes and/or stomatal uptake by plants exist within the canopy (Kurpius and Goldstein, 2003; Fares et al. 2010). Diurnal patterns of these 3 BVOCs regularly peak in the morning and evening. This is mainly due to breakup of the atmospheric boundary layer (ABL) in the morning, while the ABL lowers in the evening coupled with stomatal opening/closing by plant circadian cycle, with the peaks corresponding to the transition time of ABL height observed by Choi et al. (2011). After these morning peaks, mixing ratios decrease because of dilution of emissions into a larger mixing layer and faster oxidation of BVOCs during daytime from high daytime ozone mixing ratios, which were observed up to 100 ppbv. High mixing ratios and strong gradients for methanol and monoterpenes for nighttime reflect temperature-dependent emission, but MBO+isoprene emissions are known to be temperature and light dependent (Harley et al., 1998; Schade et al., 2000; Guenther et al., 2006). Distinctively higher methanol mixing ratio near the surface (1.5 m height) suggests that soil, leaf litter, or understory plant emission may significantly contribute to methanol emission at this site (Schade and Goldstein 2001). The same diurnal pattern has been shown previously at the site (Holzinger et al, 2005; Bouvier-Brown et al., 2009a). In addition to these compounds, figure 2.5 shows vertical gradients and diurnal cycles for MVK+MACR and sesquiterpenes. MVK and MACR are well known as major secondary products from the atmospheric oxidation of isoprene, but isoprene emission from this site is minor without strong vertical gradients observed during daytime, meaning that local isoprene emissions and MVK+MACR production are small. The maximum mixing ratio peak showed around hours 15:00 – 16:00 PST. This pattern is because the air parcel from oak forest, which is a high isoprene emitter, undergoes oxidation of isoprene and is transported to the site with isoprene oxidation products (i.e. MVK and MACR), this result being consistent with previous study (Dreyfus et al., 2002). Sesquiterpenes are not easy to measure in the ambient air because: 1) they exist at low concentration; 2) many of them have a very short lifetime; 3) their large molecule structure and low volatility makes them harder to sample through the Teflon tubing due to stickiness. However, we successfully measured sesquiterpenes by setting dwell time of mass scanning for 5 sec and having a fast and continuous sample flow in the tube (residence time of ~2.3 sec), yet the measurement of sequsquiterpenes are still highly uncertain due to their low transmission efficiency passing through PTR-MS qudrupole lens and losses in the sampling inlet and instrument's internal inlet surfaces. Nevertheless, vertical gradients of sequsquiterpenes showed a very similar pattern to monoterpenes, indicating emission patterns are similar.

An averaged daytime (10:00 – 17:00 PST) sesquiterpene mixing ratio of 84 ppt at 1.5 m above the ground was observed. This is about twice greater than GC measurement conducted in the similar season during BEARPEX 2007 (Bouvier-Brown et al., 2009a), but the GC data included only 6 speciated sesquiterpenes, suggesting that additional sesquiterpene species could be emitted in this ponderosa pine forest site.

2.3.2 Eddy covariance fluxes

The full time series of fluxes for methanol (*m/z* 33), MBO+isoprene (*m/z* 69) and monoterpenes (*m/z* 81) are depicted in figure 2.3(f), (g), and (h). Generally, fluxes of all 3 species show strong temperature dependent emission throughout the measurement period. For example, low emissions were observed around day 190 when temperature is relatively low, with high emissions observed during the high temperatures of day 200. Similar diurnal cycles between the three masses are also observed, with emission starting at sunrise, increasing as air temperature and light intensity increased during daytime, and stopping after sunset (Fig. 2.6.). Based on the vertical gradient for methanol and monoterpenes shown in figure 2.4(a) and (b), nighttime emissions seem to occur, but no significant fluxes were observed due to lower vertical turbulent mixing.

The sum of MBO and isoprene is quantified as *m/z* 69, however MBO is the main contributor to *m/z* 69 fluxes since isoprene emission at this site is minor, as described above. Therefore, MBO is the predominant emission from the site with a day average ~ 0.90 mg C m^{-2} h^{-1}, and is about 5 times greater than either methanol or monoterpene emissions (Fig. 2.6.).

2.4 Analysis and Discussion

2.4.1 Flux estimation by flux-gradient relationship (K-theory)

Fluxes of the other 14 species selected for vertical gradients were not measured, because the PTR-MS can measure EC fluxes only for a few compounds at a time due to limitations of the quadrupole mass filter. Instead, we used a flux-gradient similarity approach, also known as K-theory, for determining fluxes of all compounds not measured by the EC method (Goldstein et al., 1996; Goldstein et al., 1998). The trace gas flux (F) is assumed to be proportional to the time-averaged mixing ratio gradient (dC/dz) above the forest for intervals longer than the time scale of the slowest significant turbulence events:

$$F = K \frac{dC}{dz} \qquad (4)$$

where *K* is the eddy diffusivity and is determined for each hour of measurements. In previous studies which used K-theory for quantifying VOC fluxes, *K* was computed from flux and vertical gradient measurements of carbon dioxide (CO_2), water (H_2O), or sensible heat, and then multiplied by VOC vertical gradients (Goldstein et al., 1996; Goldstein et al., 1998; Schade et al., 2000). However, this approach may have uncertainties which arise from different sources and sinks for each scalar. In order to improve this, we derived *K* directly from BVOC fluxes and

gradients (K_{m33} for methanol, K_{m69} for MBO+isoprene, and K_{m81} for monoterpenes), and we further derived a universal K (K_{univ}) by averaging K computed from the three different BVOCs according to the equation:

$$K_{univ} = \frac{(K_{m33} + K_{m69} + K_{m81})}{3} \approx \frac{F_{m33}}{dC_{m33}/dz} \approx \frac{F_{m69}}{dC_{m69}/dz} \approx \frac{F_{m81}}{dC_{m81}/dz} \quad (5)$$

To calculate K for each *m/z*, we used gradient data from 17.8 m (mixing ratio data from flux measurements were used) and 9.5 m (gradient measurements) which were above the canopy. With one instrument it is not possible to simultaneously measure mixing ratios for different heights, and one also needs to consider the time difference between flux and gradient measurements. So, all gradient data were interpolated to match the same time period as the flux measurements. In addition, data were not used if the gradient for an hour was too small to be detected reliably (less than twice standard deviation of zero air signal) since those values induce a large uncertainty in K, or if the gradient was inverted, e.g. a higher mixing ratio at 17.5m than 9.5m with upward flux. Based on these criteria, 75 % for methanol, 51 % for MBO+isoprene, and 77 % for monoterpene data were used, with the vast majority of unused observations occurring at night. The three K values (K_{m33}, K_{m69}, and/or K_{m81}) were calculated for every hour, and averaged to a K_{univ} of which was then applied to estimate fluxes for all compounds with measured vertical gradients. Figure 2.7 presents the diurnal variation of K_{m33}, K_{m69}, K_{m81}, and K_{univ}. The pattern of K is similar to the flux diurnal profile for most species with maxima during the day when vertical turbulent mixing is strongest. The three K values (K_{m33}, K_{m69}, K_{m81}) agreed well with each other (within 8% by slope of scatter plots, not shown). This indicates that the two sampling heights have similar footprint characteristics in terms of underlying vegetation and soil, and the different time scales in photooxidation processes for these 3 compounds does not significantly affect the calculation of K at this site. To validate that K_{univ} can be properly used to calculate fluxes for the other compounds, we applied K_{univ} to vertical gradients of methanol, MBO+isoprene, and monoterpenes. Hourly fluxes computed by K_{univ} were compared to direct EC flux measurements, and on average these agreed within 4% with R-square of higher than 0.83 for all three species (Fig. 2.8).

Fluxes of the additional 14 measured BVOC species were determined by multiplying observed gradients with K_{univ}. Figure 2.9 shows the resultant diurnal flux cycles for 15 BVOC species, including methanol for reference. Daily average net fluxes are presented in Table 2.1. Among these 14 species, acetone (*m/z* 59) and acetaldehyde (*m/z* 45) fluxes showed the most significant emissions throughout the day with maximum around noon with 0.21 and 0.12 mg C m^{-2} h^{-1}, respectively. After the noon peak, emission rates of both compounds decreased at hours 13:00 – 14:00 PST, indicating that active photochemical production/loss processes of VOC above the canopy may suppress the measurable flux strength of these compounds. This phenomenon was also observed in summer 1999 at the same site using a GC-REA (Gas Chromatography-Relaxed Eddy Accumulation) system (Schade and Goldstein, 2001). Methyl chavicol (*m/z* 149) and sesquiterpene (*m/z* 205) emissions were also apparent with daytime maxima of 0.06 and 0.08 mg C m^{-2} h^{-1}, respectively. Low level emissions of acetonitrile (*m/z* 42), hexanal and hexenols (*m/z* 83), hexenal (*m/z* 99), and *m/z* 111 (unidentified OVOCs) were observed with daytime maxima each below 0.05 mg C m^{-2} h^{-1}. Interestingly, some oxygenated

BVOCs produced by photooxidation of terpenes or isoprene such as MVK+MACR (*m/z* 71), *m/z* 113 (unidentified OVOCs), *m/z* 151 (pinonaldehyde), and *m/z* 155 (linalool + unidentified OVOCs) were both emitted and deposited throughout the day, though the flux magnitudes were relatively small. This observation implies those compounds were produced by photooxidation within/above the canopy and were also deposited from the atmosphere to the ecosystem. We observed emission of nopinone (*m/z* 139) in the afternoon during hours 13:00 – 15:00 PST. Nopinone is a main β-pinene plus OH oxidation product, and β-pinene is one of the most abundant monoterpene species at this site (Lee et al., 2005; Bouvier-Brown et al., 2009a). This observation of nopinone emission from the canopy with maximum in the afternoon is consistent with the daily maximum combination of light and temperatures driving both the β-pinene emissions, and its oxidation by OH radicals. Hourly total and fractional BVOC fluxes for all measured species are presented in figure 2.10. A 24 hour mean net total emission of 1.5 mg C m^{-2} h^{-1} was estimated with a daytime (10:00 – 14:00 PST) average of 4.0 mg C m^{-2} h^{-1}. Emissions were dominated by MBO+isoprene (61 % to the total, and almost exclusively MBO due to minimal isoprene emission at this site by, as shown by Schade and Goldstein, 2001), followed by monoterpenes (13 %) and methanol (12%). For the other compounds which were estimated by K-theory, acetone and acetaldehyde emissions were 4.9 % and 2.6 % of the total emission, followed by sesquiterpenes (1.9 %), methyl chavicol (1.0 %) , with low levels of emissions for the others (less than 1 % for each). Though we did not observe substantial deposition fluxes, the maximum total deposition (-0.015 mg C m^{-2} h^{-1}) by 2 OVOCs (*m/z* 151 and 155) occurred at noontime.

2.4.2 BVOC emission model

To parameterize measured emissions with commonly used BVOC emission models, we categorized the observed emissions into species that are dependent on temperature versus dependent on both light and temperature. The emission of monoterpenes from this site is known from past observations to be mainly dependent on temperature (e.g. Schade and Goldstein, 2003), with a relationship that can be expressed as (Tingey 1980; Guenther et al., 1993);

$$E_T = F_{30}\, e^{\beta(T_{air}-30)} \qquad (6)$$

where F_{30} is the basal emission rate at 30 ^oC, β ($^oC^{-1}$) is a temperature dependence coefficient, and T_{air} (^oC) represents the within-canopy air temperature. From our EC flux data, F_{30} (0.6 ± 0.14 mg C m^{-2} h^{-1}, mean ± standard deviation) was determined as the mean of data collected at the within-canopy air temperature range of 29 ^oC – 31 ^oC, and β (0.12 ± 0.01 $^\circ C^{-1}$) was computed by inverting Eq (6). Canopy scale flux measurements previously reported from this site using PTR-MS EC and GC-FID REA systems had ranges of 0.47 – 1.2 mg C m^{-2} h^{-1} for F_{30} and 0.06 – 0.15 $^oC^{-1}$ for β (Schade and Goldstein, 2003; Lee et al., 2005; Holzinger et al., 2006; Bouvier-Brown et al., 2012), in good agreement with the results reported here.

In contrast to monoterpenes, MBO emissions are driven by both temperature and light intensity as described here (Harley et al., 1998; Schade and Goldstein, 2001):

$$E_{T+L} = BER \cdot \gamma_P \cdot \gamma_T \quad (7)$$

where *BER* represents the basal emission rate at standard condition (PAR of 1000 µmol m^{-2} s^{-1} and within-canopy air temperature of 30 ^{o}C), and γ_P and γ_T are temperature emission activity factor and light emission activity factor, as follows,

$$\gamma_P = \alpha \cdot c \cdot \left(\frac{PAR}{\sqrt{1+\alpha^2 \cdot PAR^2}} \right) \quad (8)$$

$$\gamma_T = E_{opt} \left(\frac{C_{T2} \cdot e^{\frac{(1/T_{opt} - 1/T)}{R} \cdot C_{T1}}}{C_{T2} - C_{T1} \cdot (1 - e^{\frac{(1/T_{opt} - 1/T)}{R} \cdot C_{T2}})} \right) \quad (9)$$

where α (=0.0011) and c (=1.37) are empirical coefficients, E_{opt} (=1.45) is the maximum normalized emission capacity, T_{opt} (=312 K by default) is the temperature at which E_{opt} occurs, T is air temperature (K), R is the ideal gas constant (=0.00831 kJ mol^{-1} K^{-1}), and C_{T1} (131 kJ mol^{-1}) and C_{T2} (154 kJ mol^{-1}) are the energies of deactivation and activation, respectively. All constants used were taken from Schade and Goldstein (2001). Based on this model, *BER* (3.8 ± 0.7 mg C m^{-2} h^{-1}) was derived from our MBO EC flux data. Applying this *BER* with PAR and temperature, the model showed good agreement with our EC flux measurement data (slope: 0.93, R^2: 0.89, n=388), with the model slightly underestimating observations on average by 7 %. This basal emission rate is at least 1.2 times larger than previously reported in summer 1999 and the daytime emission also increased from summer 1998 and 1999 but not linearly (Baker et al., 1999; Schade and Goldstein, 2001; Bouvier-Brown et al., 2012 in press). Daytime maxima of 1.2, 1.7, and 2.6 mg C m^{-2} h^{-1} were observed for years 1998, 1999, and 2009, respectively. The shaded area below the canopy has increased as the forest matured, so lower emission capacity in lower canopy is expected while an overall increase is expected due to the increase in emitting biomass at the site. Based on tree survey, the biomass of the site in summer 2009 (1005 g m^{-2}) has increased at least 5 times more from summer 1998 (184 g m^{-2}).

Methanol emission is also known to be correlated with light and temperature (Nemecek-Marshall et al., 1995; Schade and Goldstein, 2001). Interestingly, our vertical gradients for methanol shown in figure 2.4 strongly indicate nighttime gradients and this is similar with monoterpene suggesting the main emission driver is temperature. In contrast, the daytime mixing ratio pattern is similar to that of MBO, not like monoterpenes, indicating temperature and light dependent emission is important during the day. In addition, the flux pattern is similar to that of monoterpenes in the morning when upward flux starts to increase but similar to that of MBO in the afternoon when the flux decreases. This suggests methanol emission is possibly less dependent on light, and this may be due to methanol emission from the soil. Soil methanol emission has been reported by Schade and Goldstein (2001) and Schade and Custer, (2004). Based on our analysis of both emission model algorithms, the model of light + temperature for methanol (*BER*: 0.71 ± 0.21 mg C m^{-2} h^{-1}) resulted in better correlation with EC flux measurements (slope: 0.91, R^2: 0.74, n=351). Our 2009 measurements had at least 2 times lower emission for daytime fluxes than summer 1999. This is possibly due to understory shrub removal

performed in spring 1999 which may have induced an unusually large emission due to decay of plant debris during summer 1999 (Warneke et al. 1999). Methanol emission is also associated with pectin demethylation when cell walls elongate during leaf/needle expansion and plant growth is recognized as the primary global source of methanol to the atmosphere (Fall and Benson, 1996; Galbally and Kirstine, 2002). Methanol bursts from expanding needles is a phenomenon that may have been occurring at higher rates in summer 1999 when pine trees were younger and growing more rapidly as compared to the pine trees in 2009. Moreover, a limited understory biomass in 1999 represented a minor sink for methanol, while in 2009 dense understory vegetation may represent a sink for this OVOC.

In addition to these three dominant BVOCs, acetone, acetaldehyde, sesquiterpenes, and methyl chavicol have been reported as significant emissions from this site (Schade and Goldstein, 2001; Bouvier-Brown et al., 2009c), and our estimations of flux via K-theory are also consistent with these reports. Diurnal cycles of emissions for these compounds correlated better with that of monoterpenes than MBO, suggesting mainly temperature dependent emission. By assuming temperature as the main emission driver, we determined F_{30} and β as summarized in Table 2.2 for these 4 compounds. For acetone and acetaldehyde, we found slightly smaller F_{30} and β than those reported by Schade and Goldstein (2001), but within the uncertainty range. The daytime fluxes and concentrations showed similar magnitude to summer 1999, which is interesting since the biomass of the site has increased substantially over this 10 year period.

Leaf-scale emission rates of monoterpenes, sesquiterpenes and methyl chavicol were previously reported from this site (Bouvier-Brown et al., 2009c), but canopy-scale fluxes of sesquiterpenes and methyl chavicol have not been previously reported. We estimated the canopy-scale basal emission rate by multiplying the ecosystem foliar density (1005 g [dry weight] m^{-2} for BEARPEX 2009) to leaf-scale basal emission rate and applied the emission model using the scaled F_{30} with β. Figure 2.11 presents temperature dependent emissions for monoterpenes and sesquiterpenes from leaf-scale emissions, canopy-scale fluxes, and temperature-algorithm basal emission model results optimized for this study. For monoterpenes, the canopy level emissions are in the middle of the range of leaf scale emissions, and this indicates little or no loss before escaping the canopy. In contrast, sesquiterpenes are known to be oxidized rapidly in the tree canopy due to their high reactivity (Ciccioli et al., 1999; Bouvier-Brown et al., 2009c), this can justify the lower emissions measured at the canopy level as compared to up-scaled emission from leaf-level measurements. For methyl chavicol, we derived a lower F_{30} (0.08 ± 0.06 mg C m^{-2} h^{-1}) from the canopy scale flux data than was reported for leaf-scale measurements (range 0.16 – 1.1 mg C m^{-2} h^{-1}, scaled for canopy-scale) by Bouvier-Brown et al. (2009c), but we observed a higher β (0.2 ± 0.06 $^{o}C^{-1}$ for this study, and the range of 0.12 – 0.2 $^{o}C^{-1}$ for leaf-scale). Bouvier-Brown et al. (2009b) reported that methyl chavicol emission accounted for 4 – 24% of carbon mass emitted as MBO. Our methyl chavicol to MBO ratios were in the range 0.8 – 7.8 % during hours 13:00 – 15:00 when methyl chavicol and MBO emission were maximum, consistent with the lower end of the range previously reported.

2.5 Summary

Proton transfer reaction-mass spectrometry (PTR-MS) using quadrupole mass spectrometry has been applied to BVOC EC flux measurements, but only allows measurement of fluxes for a few compounds (e.g. 4 ion species applied for this study). To quantify fluxes of a broader range of BVOCs, we simultaneously measured EC fluxes and vertical gradients of BVOCs during BEARPEX 2009. Using a flux-gradient relationship ('K-theory'), we successfully determined fluxes of 14 BVOC species in addition to MBO, monoterpenes, and methanol by EC. Comparison of fluxes measured by the eddy covariance method with fluxes estimated by K-theory for MBO, methanol, and monoterpenes showed excellent agreement. MBO (*m/z* 69) was the dominant BVOC emission observed (0.90 mg C m-2 h-1 in a 24 hour mean), followed by monoterpenes (*m/z* 81) and methanol (*m/z* 33) which were similar (0.20 and 0.18 mg C m-2 h-1, respectively). Fluxes of the other 14 BVOC species all showed net emission, with 24 hour mean total emission of 0.2 mg C m^{-2} h^{-1}, equivalent to monoterpene or methanol emissions. Of these 14, acetone (*m/z* 59) and acetaldehyde (*m/z* 45) emissions were largest at 0.07 and 0.04 mg C m^{-2} h^{-1}, respectively, followed by sesquiterpene (*m/z* 205, 0.03 mg C m^{-2} h^{-1}), methyl chavicol (*m/z* 149, 0.02 mg C m^{-2} h^{-1}), with a lower level of emission for all the others (less than 0.01 mg C m^{-2} h^{-1} for each). By comparing with leaf-scale emission of monoterpenes and sesquiterpenes previously studied at the site, we found there was significant chemical loss of sesquiterpenes before they could escape the forest canopy, but not for monoterpenes, consistent with previous studies (Ciccioli et al., 1999; Bouvier-Brown et al., 2009a). Overall, estimating BVOC emissions using the flux-gradient relationship applied to direct measurements proved to be a useful method for investigation of ecosystem scale BVOC fluxes.

2.6 References

Andreae, M. O., and Crutzen, P. J.: Atmospheric aerosols: Biogeochemical sources and role in atmospheric chemistry, Science, 276, 1052-1058, 1997.

Baker, B., Guenther, A., Greenberg, J., Goldstein, A., and Fall, R.: Canopy fluxes of 2-methyl-3-buten-2-ol over a ponderosa pine forest by relaxed eddy accumulation: Field data and model comparison, J Geophys Res-Atmos, 104, 26107-26114, 1999.

Bouvier-Brown, N. C., Goldstein, A. H., Gilman, J. B., Kuster, W. C., and de Gouw, J. A.: In-situ ambient quantification of monoterpenes, sesquiterpenes, and related oxygenated compounds during BEARPEX 2007: implications for gas- and particle-phase chemistry, Atmos Chem Phys, 9, 5505-5518, 2009a.

Bouvier-Brown, N. C., Goldstein, A. H., Worton, D. R., Matross, D. M., Gilman, J. B., Kuster, W. C., Welsh-Bon, D., Warneke, C., de Gouw, J. A., Cahill, T. M., and Holzinger, R.: Methyl chavicol: characterization of its biogenic emission rate, abundance, and oxidation products in the atmosphere, Atmos Chem Phys, 9, 2061-2074, 2009b.

Bouvier-Brown, N. C., Holzinger, R., Palitzsch, K., and Goldstein, A. H.: Large emissions of sesquiterpenes and methyl chavicol quantified from branch enclosure measurements, Atmos Environ, 43, 389-401, doi:10.1016/j.atmosenv.2008.08.039, 2009c.

Bouvier-Brown, N. C., Schade, G. W., Misson, L., Lee, A., McKay, M., and Goldstein, A. H.: Contributions of biogenic volatile organic compounds to net ecosystem carbon flux in a ponderosa pine plantation, Atmos Environ, 60, 527-533, doi:10.1016/j.atmosenv.2012.06.070, 2012.

Chameides, W. L., Lindsay, R. W., Richardson, J., and Kiang, C. S.: The Role of Biogenic Hydrocarbons in Urban Photochemical Smog - Atlanta as a Case-Study, Science, 241, 1473-1475, 1988.

Choi, W., Faloona, I. C., McKay, M., Goldstein, A. H., and Baker, B.: Estimating the atmospheric boundary layer height over sloped, forested terrain from surface spectral analysis during BEARPEX, Atmos Chem Phys, 11, 6837-6853, doi:10.5194/acp-11-6837-2011, 2011.

Ciccioli, P., Brancaleoni, E., Frattoni, M., Di Palo, V., Valentini, R., Tirone, G., Seufert, G., Bertin, N., Hansen, U., Csiky, O., Lenz, R., and Sharma, M.: Emission of reactive terpene compounds from orange orchards and their removal by within-canopy processes, J Geophys Res-Atmos, 104, 8077-8094, 1999.

de Gouw, J., and Warneke, C.: Measurements of volatile organic compounds in the earth's atmosphere using proton-transfer-reaction mass spectrometry, Mass Spectrom Rev, 26, 223-257, doi:10.1002/Mas.20119, 2007.

Di Carlo, P., Brune, W. H., Martinez, M., Harder, H., Lesher, R., Ren, X. R., Thornberry, T., Carroll, M. A., Young, V., Shepson, P. B., Riemer, D., Apel, E., and Campbell, C.: Missing OH reactivity in a forest: Evidence for unknown reactive biogenic VOCs, Science, 304, 722-725, 2004.

Dillon, M. B., Lamanna, M. S., Schade, G. W., Goldstein, A. H., and Cohen, R. C.: Chemical evolution of the Sacramento urban plume: Transport and oxidation, J Geophys Res-Atmos, 107, 4045, doi:10.1029/2001jd000969, 2002.

Dreyfus, G. B., Schade, G. W., and Goldstein, A. H.: Observational constraints on the contribution of isoprene oxidation to ozone production on the western slope of the Sierra Nevada, California, J Geophys Res-Atmos, 107, 4365, doi:10.1029/2001jd001490, 2002.

Fall, R., and Benson, A. A.: Leaf methanol - The simplest natural product from plants, Trends Plant Sci, 1, 296-301, 1996.

Fares, S., Goldstein, A., and Loreto, F.: Determinants of ozone fluxes and metrics for ozone risk assessment in plants, J Exp Bot, 61, 629-633, doi:10.1093/Jxb/Erp336, 2010.

Fares, S., Park, J.-H., Gentner, D. R., Weber, R., Ormeno, E., Karlik, J., and Goldstein, A. H.: Seasonal cycles of biogenic volatile organic compound fluxes and concentrations in a California citrus orchard, Atmos. Chem. Phys. Discuss., 12, 17987-18027, doi:10.5194/acpd-12-17987-2012, 2012.

Foken, T., and Wichura, B.: Tools for quality assessment of surface-based flux measurements, Agr Forest Meteorol, 78, 83-105, 1996.

Fuentes, J. D., Lerdau, M., Atkinson, R., Baldocchi, D., Bottenheim, J. W., Ciccioli, P., Lamb, B., Geron, C., Gu, L., Guenther, A., Sharkey, T. D., and Stockwell, W.: Biogenic hydrocarbons in the atmospheric boundary layer: A review, B Am Meteorol Soc, 81, 1537-1575, 2000.

Galbally, I. E., and Kirstine, W.: The production of methanol by flowering plants and the global cycle of methanol, J Atmos Chem, 43, 195-229, 2002.

Goldstein, A. H., Fan, S. M., Goulden, M. L., Munger, J. W., and Wofsy, S. C.: Emissions of ethene, propene, and 1-butene by a midlatitude forest, J Geophys Res-Atmos, 101, 9149-9157, 1996.

Goldstein, A. H., Goulden, M. L., Munger, J. W., Wofsy, S. C., and Geron, C. D.: Seasonal course of isoprene emissions from a midlatitude deciduous forest, J Geophys Res-Atmos, 103, 31045-31056, 1998.

Goldstein, A. H., Hultman, N. E., Fracheboud, J. M., Bauer, M. R., Panek, J. A., Xu, M., Qi, Y., Guenther, A. B., and Baugh, W.: Effects of climate variability on the carbon dioxide, water, and sensible heat fluxes above a ponderosa pine plantation in the Sierra Nevada (CA), Agr Forest Meteorol, 101, 113-129, 2000.

Goldstein, A. H., and Galbally, I. E.: Known and unexplored organic constituents in the earth's atmosphere, Environ Sci Technol, 41, 1514-1521, 2007.

Guenther, A., Hewitt, C. N., Erickson, D., Fall, R., Geron, C., Graedel, T., Harley, P., Klinger, L., Lerdau, M., Mckay, W. A., Pierce, T., Scholes, B., Steinbrecher, R., Tallamraju, R., Taylor, J., and Zimmerman, P.: A Global-Model of Natural Volatile Organic-Compound Emissions, J Geophys Res-Atmos, 100, 8873-8892, 1995.

Guenther, A., Karl, T., Harley, P., Wiedinmyer, C., Palmer, P. I., and Geron, C.: Estimates of global terrestrial isoprene emissions using MEGAN (Model of Emissions of Gases and Aerosols from Nature), Atmos Chem Phys, 6, 3181-3210, 2006.

Guenther, A. B., Zimmerman, P. R., Harley, P. C., Monson, R. K., and Fall, R.: Isoprene and Monoterpene Emission Rate Variability - Model Evaluations and Sensitivity Analyses, J Geophys Res-Atmos, 98, 12609-12617, 1993.

Harley, P., Fridd-Stroud, V., Greenberg, J., Guenther, A., and Vasconcellos, P.: Emission of 2-methyl-3-buten-2-ol by pines: A potentially large natural source of reactive carbon to the atmosphere, J Geophys Res-Atmos, 103, 25479-25486, 1998.

Holzinger, R., Lee, A., Paw, K. T., and Goldstein, A. H.: Observations of oxidation products above a forest imply biogenic emissions of very reactive compounds, Atmos Chem Phys, 5, 67-75, 2005.

Horst, T. W.: A simple formula for attenuation of eddy fluxes measured with first-order-response scalar sensors, Bound-Lay Meteorol, 82, 219-233, 1997.

Holzinger, R., Lee, A., McKay, M., and Goldstein, A. H.: Seasonal variability of monoterpene emission factors for a Ponderosa pine plantation in California, Atmos Chem Phys, 6, 1267-1274, 2006.

Jang, M. S., Czoschke, N. M., Lee, S., and Kamens, R. M.: Heterogeneous atmospheric aerosol production by acid-catalyzed particle-phase reactions, Science, 298, 814-817, 2002.

Karl, T. G., Spirig, C., Rinne, J., Stroud, C., Prevost, P., Greenberg, J., Fall, R., and Guenther, A.: Virtual disjunct eddy covariance measurements of organic compound fluxes from a subalpine forest using proton transfer reaction mass spectrometry, Atmos Chem Phys, 2, 279-291, 2002.

Kurpius, M. R., McKay, M., and Goldstein, A. H.: Annual ozone deposition to a Sierra Nevada ponderosa pine plantation, Atmos Environ, 36, 4503-4515, 2002.

Kurpius, M. R., and Goldstein, A. H.: Gas-phase chemistry dominates O-3 loss to a forest, implying a source of aerosols and hydroxyl radicals to the atmosphere, Geophys Res Lett, 30, 1371, doi:10.1029/2002gl016785, 2003.

Lamanna, M. S., and Goldstein, A. H.: In situ measurements of C-2-C-10 volatile organic compounds above a Sierra Nevada ponderosa pine plantation, J Geophys Res-Atmos, 104, 21247-21262, 1999.

Lee, A., Schade, G. W., Holzinger, R., and Goldstein, A. H.: A comparison of new measurements of total monoterpene flux with improved measurements of speciated monoterpene flux, Atmos Chem Phys, 5, 505-513, 2005.

Lee, X., Massman, W. J., and Law, B. E.: Handbook of micrometeorology : a guide for surface flux measurement and analysis, Atmospheric and oceanographic sciences library, 29, Kluwer Academic, Dordrecht ; Boston ; London, xiv, 250 p. pp., 2004.

Lindinger, W., Hansel, A., and Jordan, A.: On-line monitoring of volatile organic compounds at pptv levels by means of proton-transfer-reaction mass spectrometry (PTR-MS) - Medical applications, food control and environmental research, Int J Mass Spectrom, 173, 191-241, 1998.

Massman, W. J.: The Attenuation of Concentration Fluctuations in Turbulent-Flow through a Tube, J Geophys Res-Atmos, 96, 15269-15273, 1991.

Moore, C. J.: Frequency-Response Corrections for Eddy-Correlation Systems, Bound-Lay Meteorol, 37, 17-35, 1986.

Nemecekmarshall, M., Macdonald, R. C., Franzen, F. J., Wojciechowski, C. L., and Fall, R.: Methanol Emission from Leaves - Enzymatic Detection of Gas-Phase Methanol and Relation of Methanol Fluxes to Stomatal Conductance and Leaf Development, Plant Physiol, 108, 1359-1368, 1995.

Ren, X., Gao, H., Zhou, X., Crounse, J. D., Wennberg, P. O., Browne, E. C., LaFranchi, B. W., Cohen, R. C., Mckay, M., Goldstein, A. H., and Mao, J.: Measurement of atmospheric nitrous acid at Blodgett Forest during BEARPEX2007, Atmos Chem Phys, 10, 6283-6294, doi:10.5194/acp-10-6283-2010, 2010.

Rinne, H. J. I., Guenther, A. B., Warneke, C., de Gouw, J. A., and Luxembourg, S. L.: Disjunct eddy covariance technique for trace gas flux measurements, Geophys Res Lett, 28, 3139-3142, 2001.

Schade, G. W., Goldstein, A. H., Gray, D. W., and Lerdau, M. T.: Canopy and leaf level 2-methyl-3-buten-2-ol fluxes from a ponderosa pine plantation, Atmos Environ, 34, 3535-3544, 2000.

Schade, G. W., and Goldstein, A. H.: Fluxes of oxygenated volatile organic compounds from a ponderosa pine plantation, J Geophys Res-Atmos, 106, 3111-3123, 2001.

Schade, G. W., and Goldstein, A. H.: Increase of monoterpene emissions from a pine plantation as a result of mechanical disturbances, Geophys Res Lett, 30, 1380, doi:10.1029/2002gl016138, 2003.

Schade, G. W., and Custer, T. G.: OVOC emissions from agricultural soil in northern Germany during the 2003 European heat wave, Atmos Environ, 38, 6105-6114, doi:10.1016/j.atmosenv.2004.08.017, 2004.

Smeets, C. J. P. P., Holzinger, R., Vigano, I., Goldstein, A. H., and Rockmann, T.: Eddy covariance methane measurements at a Ponderosa pine plantation in California, Atmos Chem Phys, 9, 8365-8375, 2009.

Tingey, D. T., Manning, M., Grothaus, L. C., and Burns, W. F.: Influence of Light and Temperature on Monoterpene Emission Rates from Slash Pine, Plant Physiol, 65, 797-801, 1980.

Warneke, C., Karl, T., Judmaier, H., Hansel, A., Jordan, A., Lindinger, W., and Crutzen, P. J.: Acetone, methanol, and other partially oxidized volatile organic emissions from dead plant matter by abiological processes: Significance for atmospheric HOx chemistry, Global Biogeochem Cy, 13, 9-17, 1999.

Wilczak, J. M., Oncley, S. P., and Stage, S. A.: Sonic anemometer tilt correction algorithms, Bound-Lay Meteorol, 99, 127-150, 2001.

Wolfe, G. M., Thornton, J. A., Yatavelli, R. L. N., Mckay, M., Goldstein, A. H., LaFranchi, B., Min, K. E., and Cohen, R. C.: Eddy covariance fluxes of acyl peroxy nitrates (PAN, PPN and MPAN) above a Ponderosa pine forest, Atmos Chem Phys, 9, 615-634, 2009.

Table 2.1. Mixing ratio and flux information for 18 selected ion species.

Compounds	Mass / charge (m/z)	Empirical molecular formulae (protonated mass)	Mixing ratio 24h-mean (day/night)[a] [nmol mol^{-1}]	Flux 24h-mean (day)[a] [mg C m^{-2} h^{-1}]
Methanol	33	CH_3OHH^+	16 (13 / 16)	0.18 (0.48)
Acetonitrile	42	$C_2H_3NH^+$	0.15 (0.16 / 0.15)	0.003 (0.008)
Acetaldehyde	45	$C_2H_4OH^+$	1.9 (1.6 / 2.4)	0.038 (0.104)
Acetone	59	$C_3H_6OH^+$	3.6 (3.5 / 4)	0.073 (0.18)
MBO[b] + isoprene	69	$C_5H_8H^+$ ($C_5H_{10}OH^+$)[c]	4.2 (5.6 / 2.1)	0.90 (2.51)
MVK + MACR[d]	71	$C_4H_6OH^+$	1.2 (1.5 / 1.3)	0.013 (0.019)
Benzene	79	$C_6H_6H^+$	0.071 (0.059 / 0.083)	0.001 (0.003)
Monoterpenes	81, 137	$C_6H_8H^+$, $C_{10}H_{16}H^+$	1.1 (0.6 / 1.3)	0.2 (0.46)
Hexanal, hexenols	83	$C_6H_{10}H^+$	0.14 (0.12 / 0.16)	0.010 (0.023)
Hexenals	99	$C_6H_{10}OH^+$	0.16 (0.15 / 0.18)	0.012 (0.031)
Unknown OVOCs	111	$C_8H_{14}H^+$, $C_6H_6O_2H^+$, $C_7H_{10}OH^+$	0.026 (0.02 / 0.029)	0.003 (0.006)
Unknown OVOCs	113	$C_8H_{16}H^+$, $C_7H_{12}OH^+$, $C_6H_8O_2H^+$, $C_5H_4O_3H^+$	0.15 (0.18 / 0.15)	0.0001 (-0.0001)
Nopinone	139	$C_9H_{14}OH^+$	0.056 (0.046 / 0.071)	0.006 (0.016)
Methyl chavicol	149	$C_{10}H_{12}OH^+$	0.099 (0.064 / 0.084)	0.015 (0.038)
Pinonaldehyde	151	$C_{10}H_{14}OH^+$	0.021 (0.017 / 0.023)	0.002 (0.004)
Linalool, Unknown OVOCs	155	$C_{10}H_{18}OH^+$, $C_9H_{14}O_2H^+$	0.015 (0.016 / 0.017)	0.0007 (0.003)
Sesquiterpenes	205	$C_{15}H_{24}H^+$	0.095 (0.072 / 0.098)	0.028 (0.06)

[a] Daytime and nighttime means are for hours 10:00 – 14:00 and 22:00 – 02:00 PST, respectively.
[b] 2-Methyl-3-butene-2-ol
[c] Parent MBO ion in parenthesis. MBO main fragment ion is the same as isoprene parent ion.
[d] Sum of methylvinylketone and methacrolein

Table 2.2. Modeled values for basal mission rate (BER and F_{30}) and temperature-dependence factor (β)

Compound	Basal emission rate at 30°C, F_{30} [mg C m^{-2} h^{-1}]	β [$^oC^{-1}$]
MBO+isoprene (m/z 69)	(3.8 ± 0.70)*	(N.A.)**
Monoterpenes (m/z 81)	0.60 ± 0.14	0.12 ± 0.01
Methanol (m/z 33)	0.54 ± 0.17 (0.71 ± 0.21)*	0.08 ± 0.01 (N.A.)**
Acetone (m/z 59)	0.24 ± 0.14	0.09 ± 0.04
Acetaldehyde (m/z 45)	0.13 ± 0.07	0.07 ± 0.05
Sesquiterpenes (m/z 205)	0.11 ± 0.10	0.07 ± 0.09
Methyl chavicol (m/z 149)	0.08 ± 0.06	0.20 ± 0.06

* Basal emission rate at PAR of 1000 µmol m^{-2} s^{-1} and air temperature of 30 °C for light+temperature algorithm.
** Not available for light+temperature algorithm. Detailed equations are described in Eq (7)-(9).

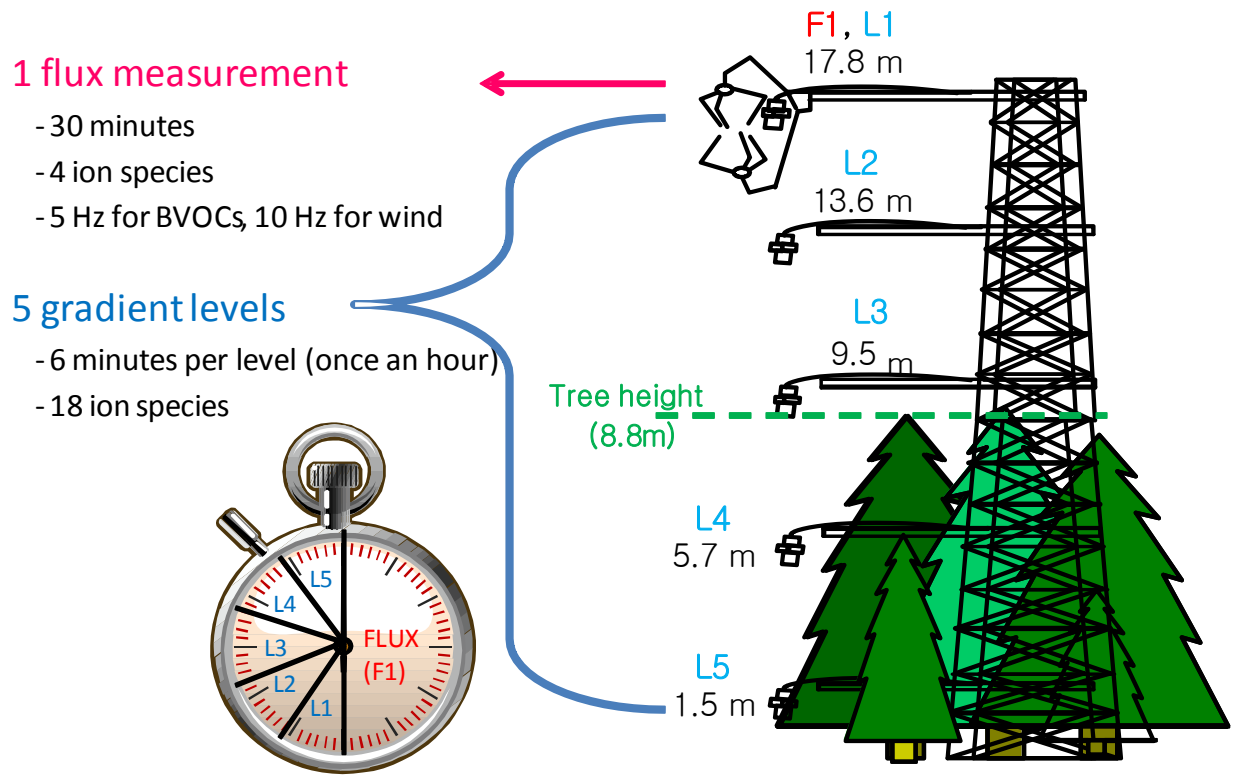

Figure 2. 1. Inlet configuration and sampling schedule on the 18 m tall tower during BEARPEX 2009. The PTR-MS sampled from an inlet (F1) at 17.8 m co-located with a 3-dimensional sonic anemometer during the first 30 min of each hour for eddy covariance flux measurements, then sampled sequentially from five inlets (L1 – L5) positioned at 17.8, 13.6, 9.5, 5.7, and 1.5 m above ground during the next 30 min to measure vertical gradients. Mean tree height was 8.8 m.

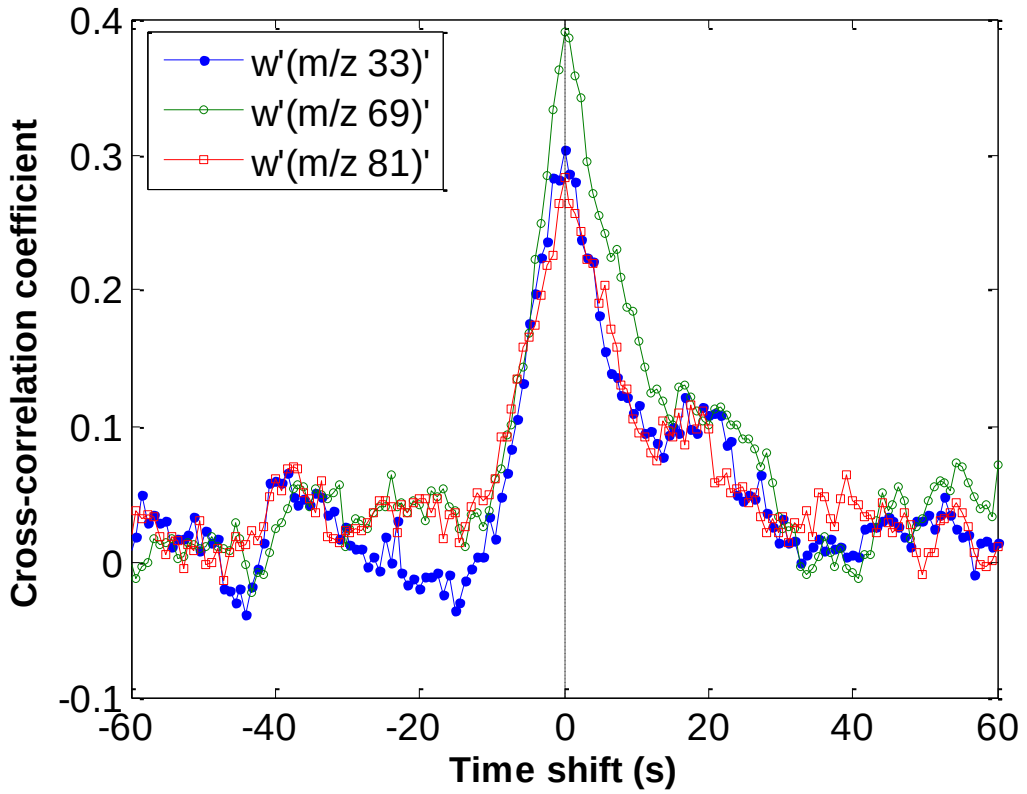

Figure 2. 2. Cross-correlation of vertical wind speed (w) and volume mixing ratios for 3 ion species (m/z 33, 69, and 81) at 14:00 – 14:30 PST on 18 July, 2009. Lag time corrections between vertical wind speed and volume mixing ratio of X seconds have been applied to these data.

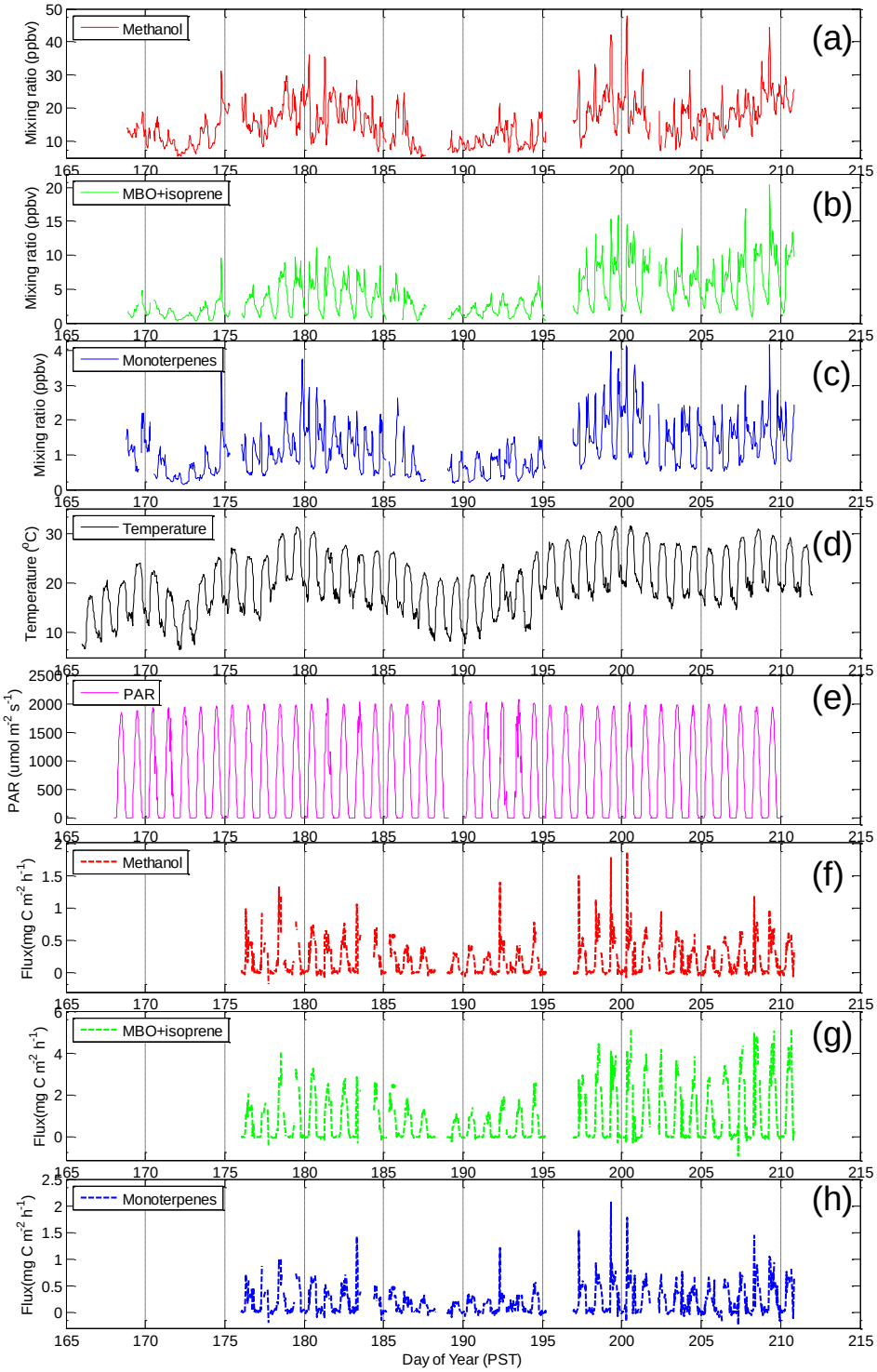

Figure 2. 3. Volume mixing ratio time-series of (a) methanol, (b) MBO+isoprene and (c) monoterpenes, (d) air temperature, (e) photosynthetically active radiation (PAR), and fluxes of (f) methanol, (g) MBO+isoprene and (h) monoterpenes. All data are averaged on an hourly basis.

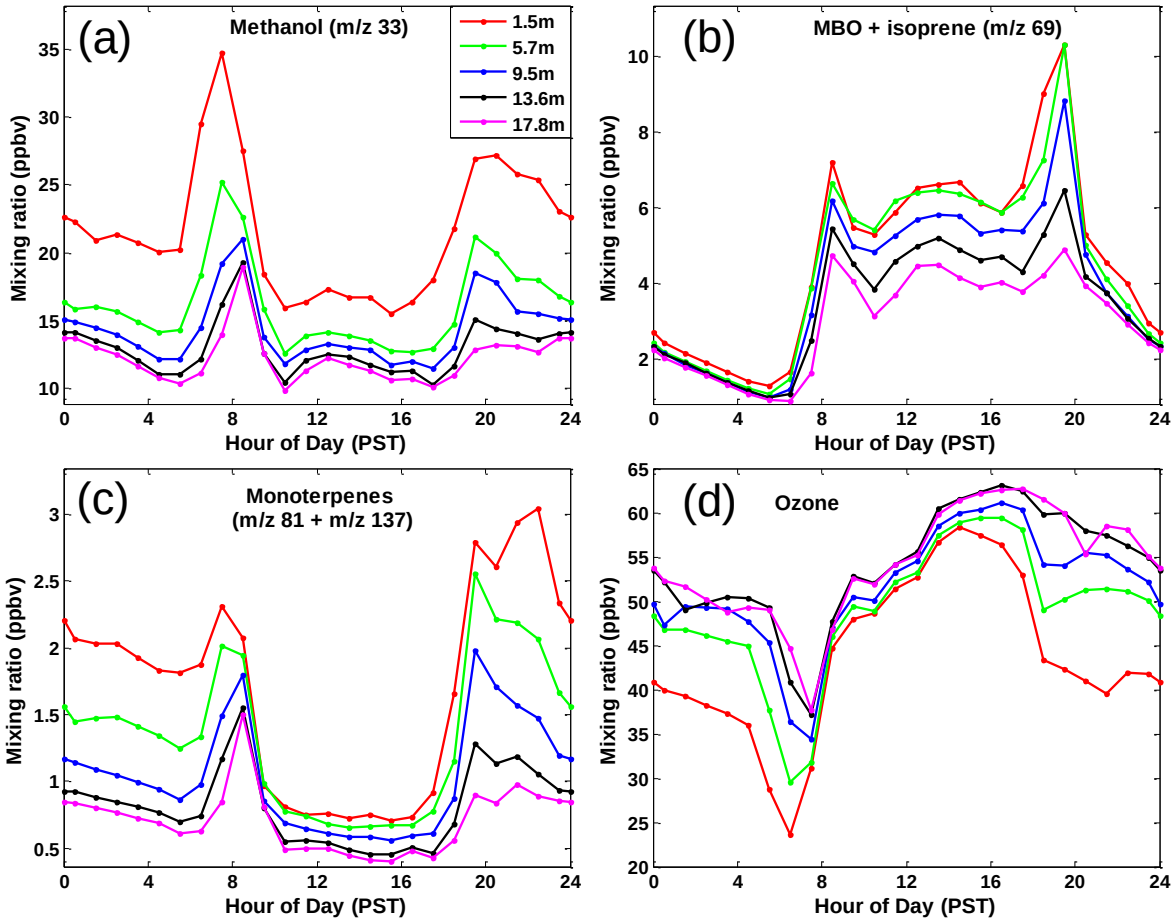

Figure 2. 4. Averaged diurnal cycles of vertical gradients for (a) methanol, (b) MBO+isoprene, (c) monoterpenes, and (d) ozone. Measurement heights are indicated in the legend (a).

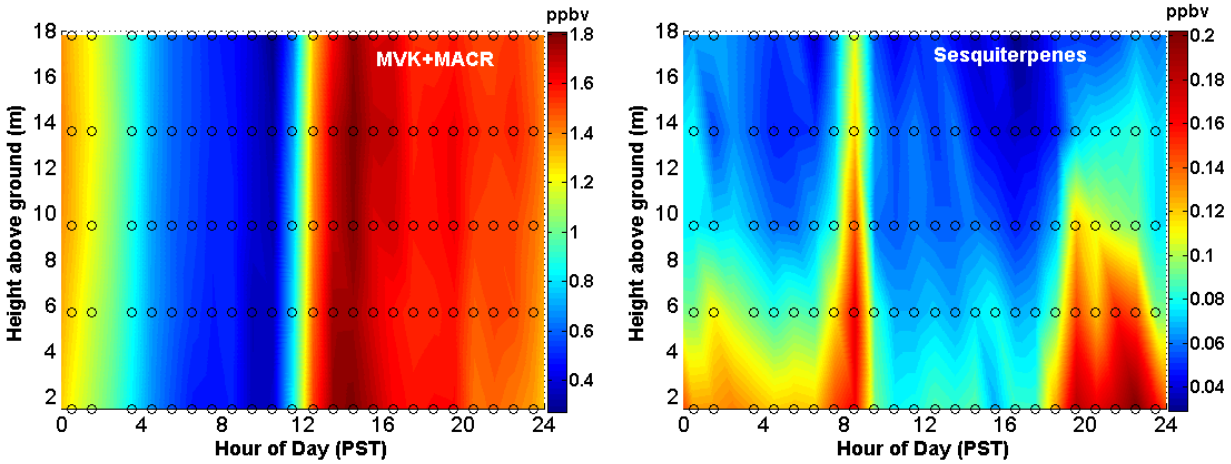

Figure 2. 5. Mean vertical gradient diurnal patterns for MVK+MACR (left) and sesquiterpenes (right). Color represents interpolated concentration gradients with actual measurement timing and vertical positions indicated by open circles.

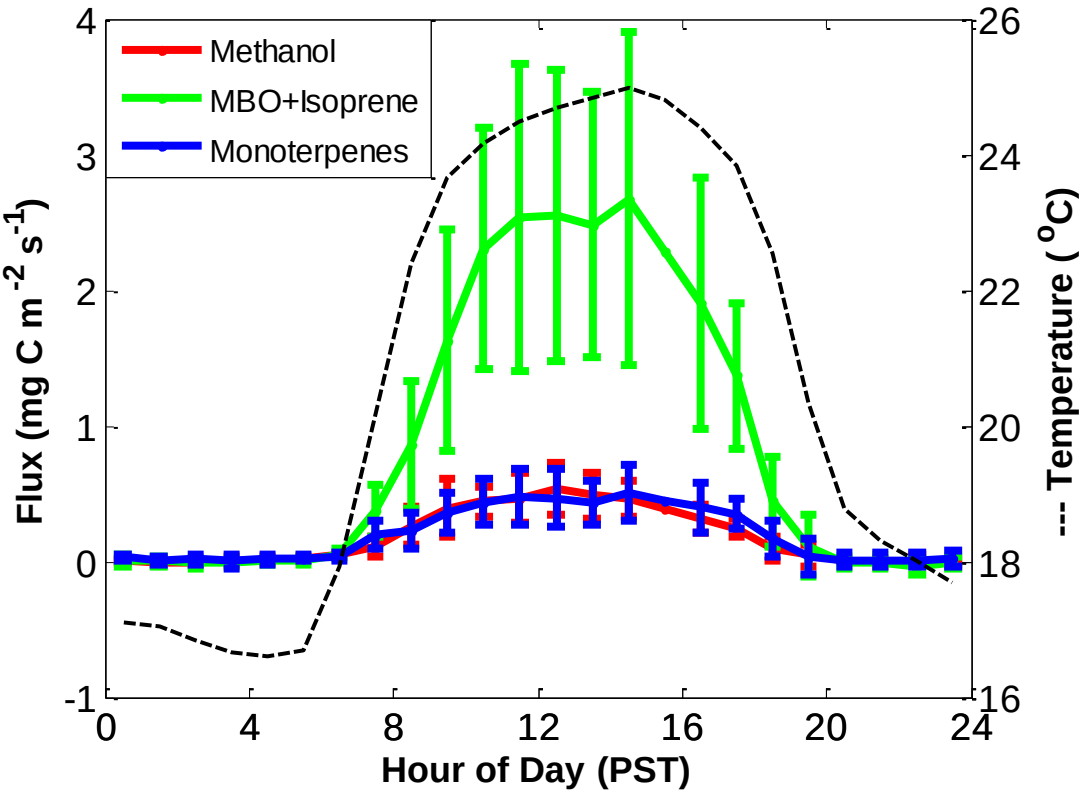

Figure 2. 6. Mean diurnal variation of air temperature (dashed black line) and fluxes for methanol (red line), MBO+isoprene (green line), and monoterpenes (blue line). Error bars denote standard deviations of all measurements at the respective hour of the day.

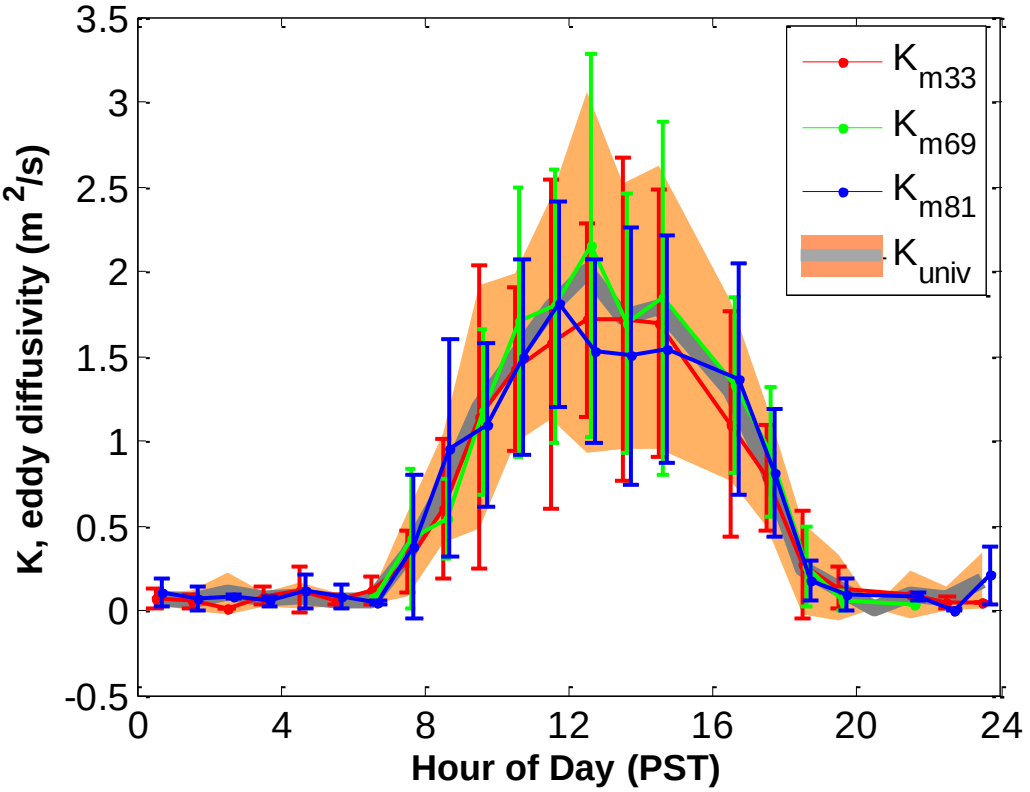

Figure 2. 7. Mean eddy diffusivity diurnal patterns calculated from measured fluxes and vertical gradients of methanol (K_{m33}), MBO+isoprene (K_{m69}), monoterpene (K_{m81}) and the universal K (K_{univ}) calculated according to Eq. (5). Error bars and shaded area denote standard deviations from the mean.

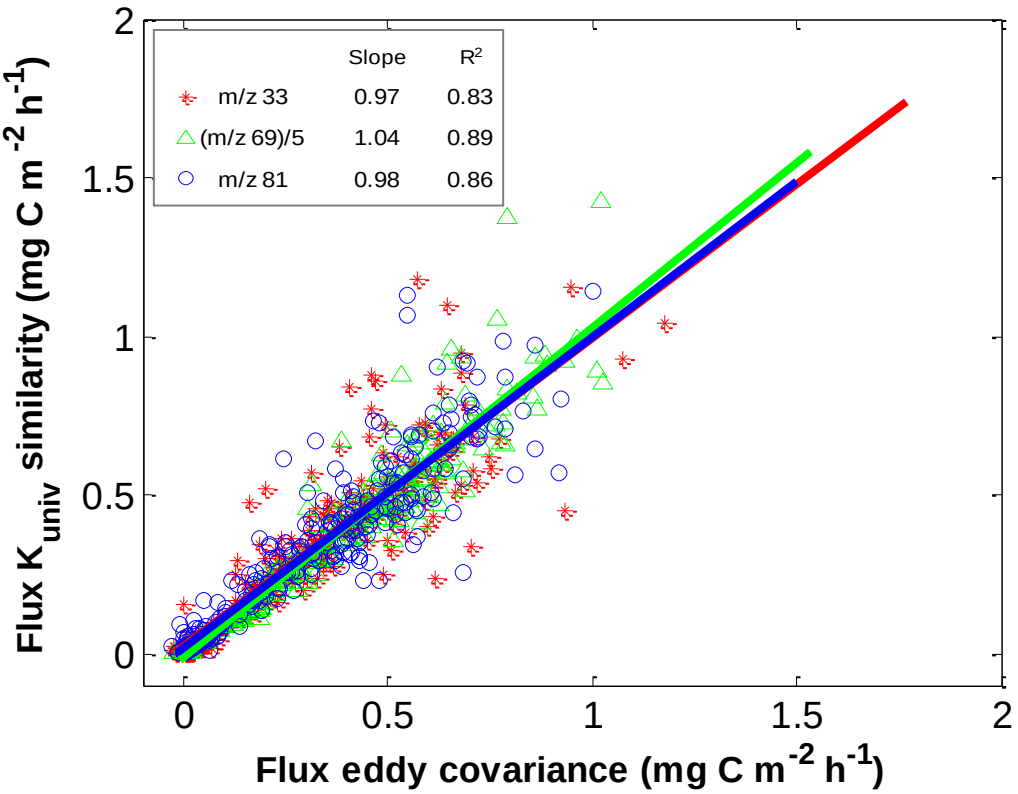

Figure 2. 8. Comparison between flux determined by the eddy covariance method and flux determined by the flux-gradient similarity method using the universal K (K_{univ}) for methanol (m/z 33, red star), MBO+isoprene (m/z 69, green triangle), and monoterpenes (m/z 81, blue circle). The red, green, and blue lines are the best linear fit for methanol, MBO+isoprene, and monoterpenes, respectively.

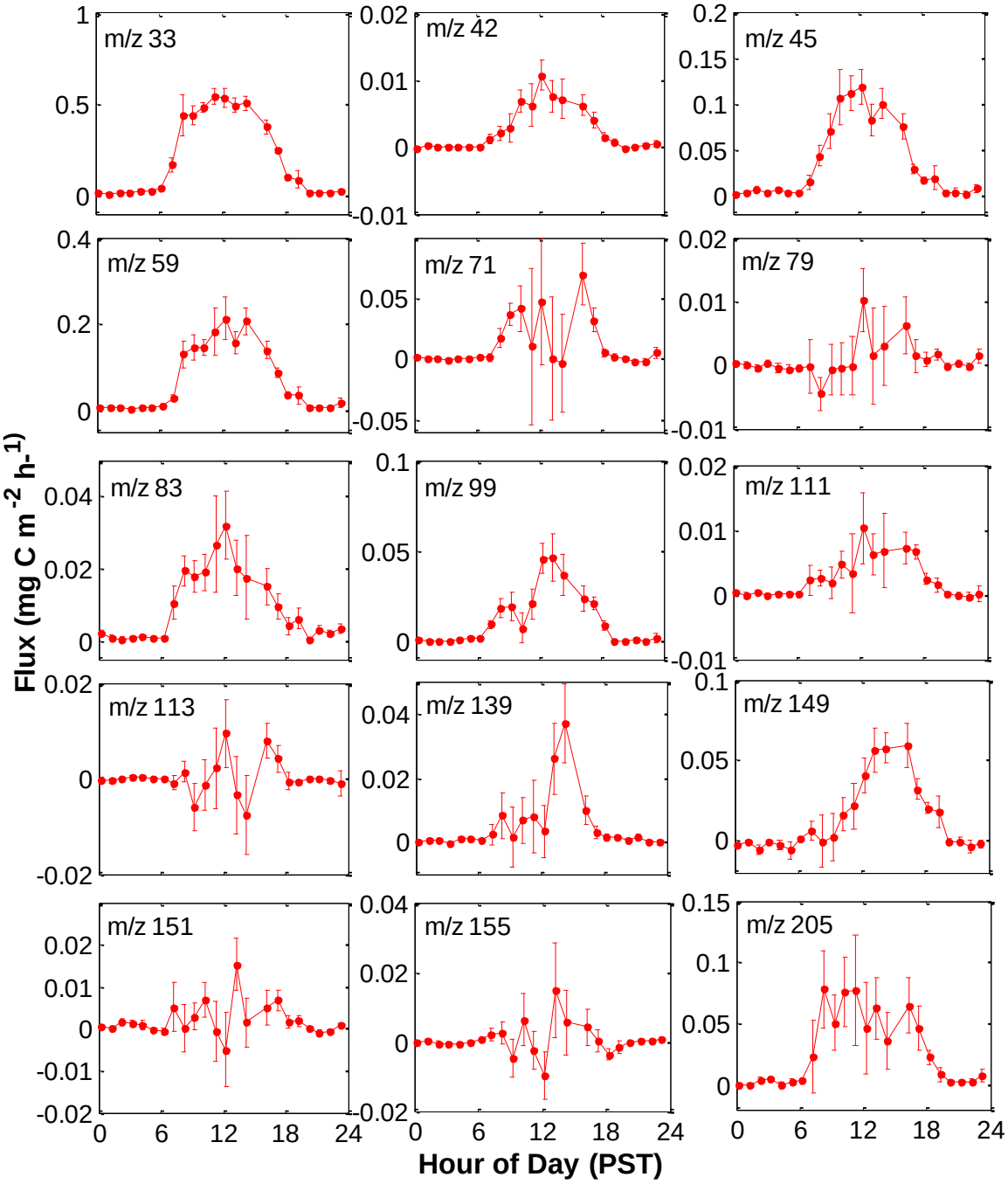

Figure 2. 9. Mean diurnal cycles of fluxes determined by the similarity method using the universal K for 15 ion species observed. Vertical bars denote standard errors from the mean.

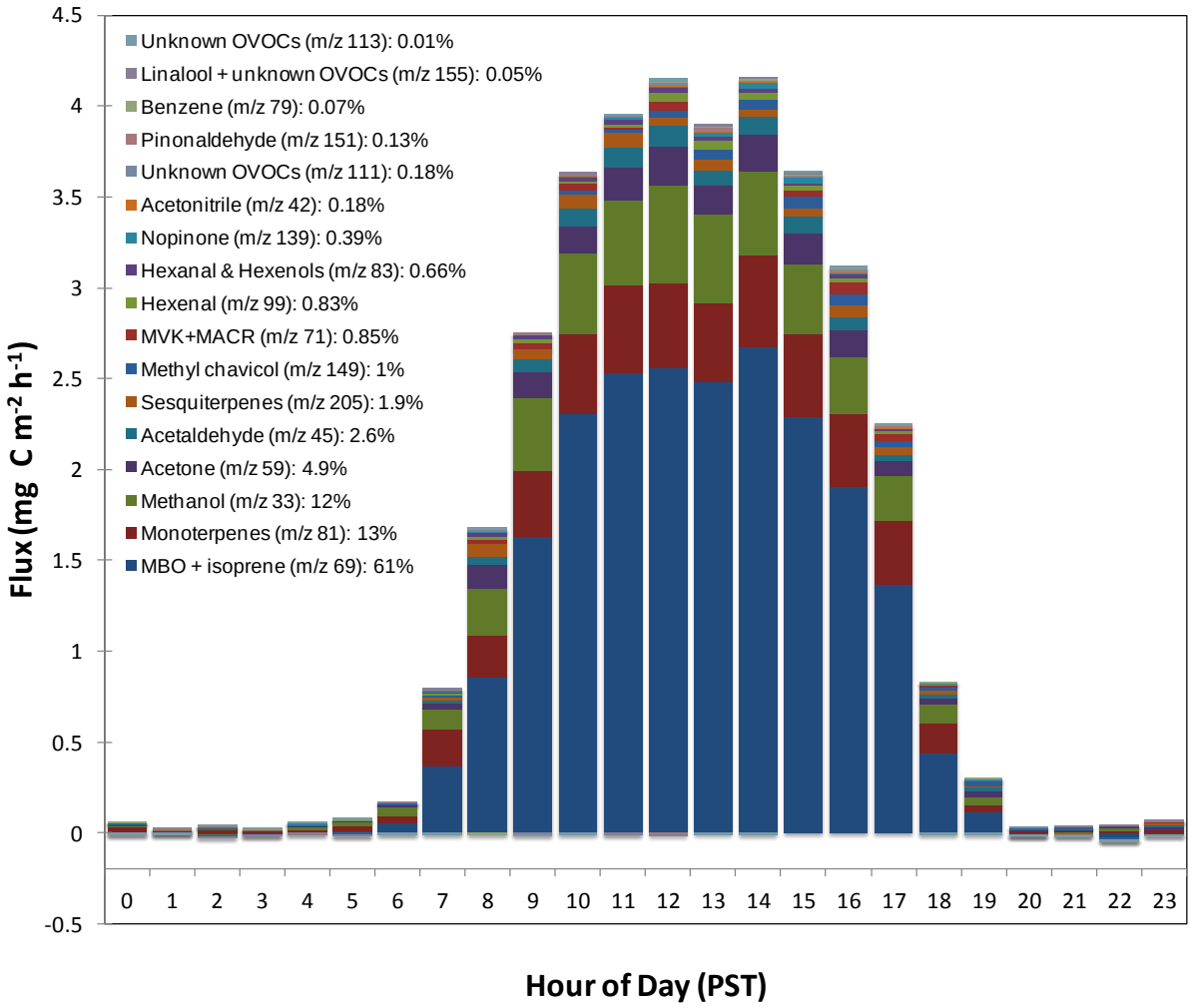

Figure 2. 10. Total hourly mean BVOC diurnal flux on a carbon mass basis shown as staged bar plots with contributions indicated for each of the 17 masses measured. Largest fluxes are at the bottom. The percentages in the legend indicate contributions of individual compounds to the daily total emission.

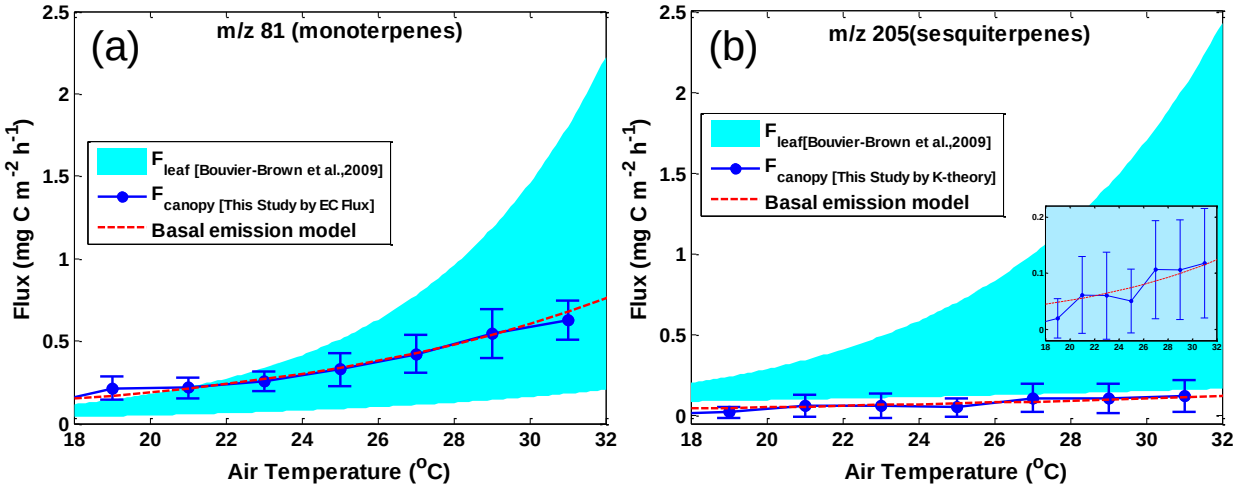

Figure 2. 11. Comparisons between leaf scale emissions and canopy scale emissions of (a) monoterpenes and (b) sesquiterpenes as a function of temperature. Shaded area indicates the range of expected canopy level emissions from leaf scale emissions reported previously by Bouvier-Brown et al. (2009). Blue dots represent canopy scale (a) eddy covariance flux for monoterpenes and (b) flux determined by the similarity method using the universal K for sesquiterpenes. All fluxes were aggregated into 2°C temperature bins, and error bars denote standard deviations. Red dotted line represents basal emission model optimized for this study based on the canopy scale fluxes, and the inset in (b) enlarges the vertical scale, showing the exponential relationship between temperature and sesquiterpene flux.

Chapter 3: Eddy covariance emission and deposition flux measurements using proton transfer reaction – time of flight – mass spectrometry (PTR-TOF-MS): comparison with PTR-MS measured vertical gradients and fluxes

Abstract

During summer 2010, a proton transfer reaction – time of flight – mass spectrometer (PTR-TOF-MS) and a standard proton transfer reaction mass spectrometer (PTR-MS) were deployed simultaneously for one month in an orange orchard in the Central Valley of California to collect continuous data suitable for eddy covariance (EC) flux calculations. The high time resolution (5 Hz) and high mass resolution (up to 5000 m/Δm) data from the PTR-TOF-MS provided the basis for calculating the concentration and flux for a wide range of volatile organic compounds (VOC). Throughout the campaign, 664 mass peaks were detected in mass-to-charge ratios between 10 and 1278. Here we present PTR-TOF-MS EC fluxes of the 27 ion species for which the vertical gradient was simultaneously measured by PTR-MS. These EC flux data were validated through spectral analysis (i.e., co-spectrum, normalized co-spectrum, and ogive). Based on inter-comparison of the two PTR instruments, no significant instrumental biases were found in either mixing ratios or fluxes, and the data showed agreement within 5% on average for methanol and acetone. For the measured biogenic volatile organic compounds (BVOC), the EC fluxes from PTR-TOF-MS were in agreement with the qualitatively inferred flux directions from vertical gradient measurements by PTR-MS. For the 27 selected ion species reported here, the PTR-TOF-MS measured total (24h) mean net flux of 299 µg C m^{-2} h^{-1}. The dominant BVOC emissions from this site were monoterpenes (*m/z* 81.070 + *m/z* 137.131 + *m/z* 95.086, 34%, 102 µg C m^{-2} h^{-1}) and methanol (*m/z* 33.032, 18%, 72 µg C m^{-2} h^{-1}). The next largest fluxes were detected at the following masses (attribution in parenthesis): *m/z* 59.048 (mostly acetone, 12.2%, 36.5 µg C m^{-2} h^{-1}), *m/z* 61.027 (mostly acetic acid, 11.9%, 35.7 µg C m^{-2} h^{-1}), *m/z* 93.069 (para-cymene + toluene, 4.1%, 12.2 µg C m^{-2} h^{-1}), *m/z* 45.033 (acetaldehyde, 3.8%, 11.5 µg C m^{-2} h^{-1}), *m/z* 71.048 (methylvinylketone + methacrolein, 2.4%, 7.1 µg C m^{-2} h^{-1}), and *m/z* 69.071 (isoprene + 2-methyl-3-butene-2-ol, 1.8%, 5.3 µg C m^{-2} h^{-1}). Low levels of emission and/or deposition (< 1.6% for each, 5.8% in total flux) were observed for the additional reported masses. Overall, our results show that EC flux measurements using PTR-TOF-MS is a powerful new tool for characterizing the biosphere-atmosphere exchange including both emission and deposition for a large range of BVOC and their oxidation products.

3.1 Introduction

Quantifying both emission and deposition of atmospheric volatile organic compounds (VOC) and their oxidation products is critical in understanding their roles in tropospheric chemistry, particularly their contributions to photochemical production of ozone (O_3) and secondary organic aerosol (SOA) (Chameides et al., 1988; Andreae and Crutzen, 1997; Fuentes et al., 2000; Jang et al., 2002; Goldstein and Galbally, 2007). Ozone and aerosols affect human health, plant health, regional air quality and Earth's climate. On the global scale, biogenic volatile organic compounds (BVOC) emissions from vegetation are estimated to be an order of magnitude larger than those from fossil fuel combustion, so BVOC emissions constitute approximately 90% of global VOC emissions (Guenther et al, 1995). Emission rates of BVOC remain unknown for many potentially important plant species due to lack of measurements, and agricultural crops represent an area of significant uncertainty (Ormeño et al., 2010). The full range of BVOC emitted from any plant or ecosystem may also be poorly constrained due to instrumental limitations in existing data sets. Moreover, in present BVOC emission models such as the Biogenic Emission Inventory System (BEIS, Pierce et al., 1998) and the Model of Emissions of Gases and Aerosols from Nature (MEGAN, Guenther et al., 2006), there are additional uncertainties for example in estimating the VOC fluxes by up-scaling from leaf-level measurements to the ecosystem or landscape scale. A few studies have shown discrepancies between branch enclosure and canopy scale BVOC measurements. For example, Bouvier-Brown et al. (2009) and Ciccioli et al. (1999) detected much less emission of sesquiterpenes above plant canopies compared to the amount measured from branch enclosure tests, revealing significant losses of the sesquiterpenes before they escape the plant canopy due to their high reactivity.

Even larger uncertainties exist in the ultimate fate of atmospheric VOC, which must be oxidized until they form CO, CO_2, or secondary aerosol, or are removed from the atmosphere by wet or dry deposition (Goldstein and Galbally, 2007). Understanding of VOC deposition is particularly uncertain due to a lack of direct flux measurements, yet this loss process has been inferred to dominate the removal of VOC from the atmosphere (Hallquist et al., 2009). Recently, Karl et al. (2010) and Tani et al. (2010) have reported that some oxygenated VOC (OVOC), either directly emitted or formed from VOC oxidation in the atmosphere, are measurably deposited to plant ecosystems.

The eddy-covariance method is widely considered the most reliable and direct method to determine ecosystem scale fluxes for trace gases and is being widely applied to determine CO_2 and H_2O exchange between the atmosphere and biosphere (Baldocchi et al., 1988; Dabberdt et al., 1993; Baldocchi, 2003). The method requires a sensor which has very fast response (e.g., 5-20 Hz) and high sensitivity. For BVOC flux measurements using the EC method, the first field experiment was conducted by Shaw et al. (1998) and Guenther and Hills (1998); respectively, they measured acetone and formic acid fluxes over grassland using a trace atmospheric gas analyzer (TAGA) and isoprene fluxes over an oak forest using a chemiluminescence sensor. The development of the fast-response proton transfer reaction-mass spectrometer (PTR-MS) was a major advance in capability for BVOC EC flux measurements, but this instrument allowed flux

measurements simultaneously for relatively few compounds because of limitations of the quadrupole mass filter (Karl et al., 2002).

Recently, a proton transfer reaction – time of flight – mass spectrometer (PTR-TOF-MS) has been developed which can measure an unprecedented number of BVOC simultaneously with very high time resolution, breaking through instrumental and technical limitations (Jordan et al., 2009; Graus et al., 2010). The new instrument allows simultaneous measurement of an unprecedented range of BVOC emissions to the atmosphere while also observing their oxidation products and deposition. The first EC measurements of BVOC using PTR-TOF-MS were previously reported over a grassland. This work was focused on comparing methanol (Muller et al., 2010) and monoterpenes (Bamberger et al., 2011) measured with PTR-MS, and analyzing the EC flux data from PTR-TOF-MS (Ruuskanen et al., 2011).

In this study, we report the first PTR-TOF-MS eddy covariance flux measurements above a tree ecosystem and intensively validate the appropriateness of EC flux measurements using PTR-TOF-MS by comparing with EC fluxes and vertical gradient measurements from PTR-MS. To do that, a PTR-TOF-MS and a conventional PTR-MS were deployed simultaneously to collect continuous BVOC data for one month over an orange orchard in the Central Valley of California. The high time resolution (5 Hz) and high mass resolution (up to 5000 m/Δm) data from the PTR-TOF-MS provided the basis for determining concentrations and fluxes for the full range of VOC. We validate BVOC fluxes from the PTR-TOF-MS for select species (27 masses) by comparing them with data from the conventional PTR-MS (EC flux for five species and vertical gradient measurements for 21 species), and then discuss total VOC fluxes for the selected species.

3.2 Experiment

3.2.1 Measurement site

BVOC concentration and flux measurements by PTR-TOF-MS and PTR-MS were made from 25 June to 26 July in 2010 as part of a one-year continuous field campaign (October 2009 – November 2010) in an orange orchard in the Central Valley of California. The measurement site was a private orchard located 3 km west of the University of California Lindcove Research and Extension Center in Exeter (36° 21′ 23. 68″N and 119 ° 5′32.14″W, 131m above sea level). A detailed site description is given by Fares et al. (2012b). Briefly, this area features a Mediterranean-type climate with warm and dry summers; no rain was observed during the measurement period and the temperature remained within the range of 16 – 40 °C. Winds were predominantly westerly during the day and easterly at night. During the daytime (10:00 – 14:00 PST; Pacific Standard Time) footprints were mostly (> 90%) within the orchard of 'Valencia' orange trees (mean tree height ~3.7 m). A 9.8 m telescoping tower was erected on the site holding meteorological sensors and gas sample inlets for measuring vertical gradients and fluxes

of trace gases (e.g., O_3, CO, CO_2, H_2O, and VOC). All the trace gas measurement instrumentation was housed in a temperature-controlled field laboratory.

3.2.2 Instrumentation

The PTR-TOF-MS and the standard PTR-MS were deployed simultaneously to collect VOC mixing ratio data suitable for applying eddy covariance flux calculations and for investigating vertical gradients. The basic principle of both instruments has been described elsewhere in detail (for PTR-MS: Lindinger et al., 1998; de Gouw and Warneke, 2007; for PTR-TOF-MS: Jordan et al., 2009, Graus et al., 2010). Specifics of instrumental setup for this field experiment are given below. In addition, two 3-D sonic anemometers (Applied Technologies, Inc., Boulder, CO) were mounted on the tower at 7.1 m and 9.2 m above ground level to measure wind speed and temperature; the 10 Hz data were recorded by a data logger (CR3000, Campbell Scientific Inc., Logan, UT).

VOC mixing ratios were measured by PTR-TOF-MS through 2 individual gas sample inlets at 7.1 m (Fig. 3.1). For the first half (0-30 min) of each hour, a 15 m PFA tube (I.D. ~4 mm) was used to sample the ambient air from the tower. The tube was heated to ~50^{o}C, and a sample flow of 10 L min^{-1} was maintained by a mass flow controller (MKS Instruments). This inlet was located next to the 3-D sonic anemometer and shared with the standard PTR-MS. During the second half (30-60 min) of each hour, the air was sampled through a 10 m coated stainless steel tube (I.D. ~1 mm, Restek sulfinert coating) heated ~150 ^{o}C to prevent wall loss of VOCs. Both inlets were protected by particle filters (Teflon filter with PFA holder, PTFE membrane, pore size 2 µm), which were replaced every 2 weeks. In this paper, we will focus on flux data from the first half hour for PTR-TOF-MS. During the whole campaign period, the drift tube of the PTR-TOF-MS was operated at a temperature of 120 ^{o}C, a drift voltage of 600 V, and a pressure of 2.2 – 2.4 hPa. These conditions correspond to an E/N (electric field to number density of air ratio) value of ~150 Td. To apply the eddy covariance method, high time resolution data (e.g 5-20 Hz) are required. Therefore, ions were pulsed every 60 µs into the time-of-flight region, and detected by the Multi Channel Plate (MCP) at 0.2 ns resolution (5 GHz) resulting in 299,499 bins per spectrum, allowing detection of an *m/z* (mass-to-charge ratio) range from 10 to 1278 Da. By co-adding 3333 initial mass spectra, collection of 5 Hz data (1 cycle per 0.2 second) was achieved and 900 cycle data were stored every 3 min in the compressed HDF5 format. Data processing to determine mass peaks was done by the IDL routine which has been developed and described in detail by Holzinger et al. (2010a). In total, 664 mass peaks with significant signal above the background noise were identified during this campaign.

For PTR-MS VOC measurements, the first half of each hour (0-30 min) was used to measure fluxes of 5 masses (*m/z* 33, 59, 69, 81, and 113) by sharing the same inlet with PTR-TOF-MS at 7.1 m. The dwell time on each mass was 0.2 sec; thus, one cycle of measurements including the primary ion signal (*m/z* 21 and 37) and several analog input channels were completed in ~1.1 sec (Fig. 3.2). An additional 4 inlets were used sequentially for 6 min each during the second half (30-60 min) of each hour (Fig. 3.2). These inlets, within (1.0 m and 3.76 m) and above (4.85 m and 9.18 m) the canopy, were used to sample vertical gradients of 21 species (*m/z*) including the

masses selected for the flux measurements (Fares et al., 2012a). The gradient inlets were identically designed (~20 m PFA tubing, ID ~4 mm, sample flow of 10 L min^{-1}) and continuously flushed at all times. The gradient measurement dwell times were one second per *m/z*, and 13 cycles per height level were averaged to form hourly values. The PTR-MS instrument was maintained at an E/N ratio of ~128 Td (drift tube temperature: 45 ^{o}C, voltage: 600 V, pressure: 2.0 – 2.2 hPa).

Instrumental background and calibration measurements were performed automatically two times per day (02:30 – 03:00 and 15:30 – 16:00 PST). The instrumental background was determined by measuring zero air produced from ambient air purified by passing through a catalytic converter (stainless steel tube filled with platinum-coated quartz wool) at 350 ^{o}C. Dilutions (10-50 ppb) of gravimetrically mixed gas-standards of methanol, acetaldehyde, acetone, isoprene, methyl-vinyl-ketone, benzene, hexenal, hexanal, and d-limonene (Apel & Riemer) were regularly measured to provide calibration in both instruments. Concentrations for compounds which were not calibrated with gas standards were calculated using default reaction rate constants (3×10^{-9} cm^3 s^{-1} $molecule^{-1}$), measured transmission efficiencies, and calculated reaction times. The transmission efficiency of both mass spectrometers were measured from *m/z* 33 to *m/z* 219 using a gas standard mixture of methanol, acetonitrile, acetaldehyde, acetone, methyl-vinyl-ketone, benzene, toluene, xylene, trifluorobenzene, bromobenzene, trichlorobenzene, and iodotoluene at concentrations of ~100 ppb each (Apel & Riemer). Calculating VOC volume mixing ratios by transmission factors and reaction rate constants has been described in Holzinger et al. (2010b).

3.2.3 Flux calculation using the eddy covariance (EC) method

Flux calculation for the PTR-MS was based on the continuous flow disjunct eddy covariance method following Davison et al. (2009) and described elsewhere in detail (Fares et al., 2012a).

For PTR-TOF-MS, we applied the following method to calculate EC fluxes for all identified mass peaks:

1) *Data preparation:* 8000 cycles of the 5 Hz VOC data (corresponding to minutes 3.3-30 of each hour) were used for EC calculations. Even though the evaluated period was thus ~26.7 minutes, for readability we refer to these periods as 30 minutes fluxes. The 10 Hz wind data from minute 0-30 of each hour were reduced to 5 Hz data that matched the VOC sampling time.

2) *Data de-spiking and gap-filling:* The VOC and wind data files contained spikes (typically 0-15 per 30 minutes) which were due to electronic noise and/or unidentified software malfunctions. These spikes were removed by deleting data points exceeding 10 times the standard deviation of the 8000 point dataset. In addition, saving of the 3 min data files on the hard disk caused gaps of durations up to one second. All these gaps were filled with mean values of the 20 neighboring data points (before & after).

3) *Wind data rotation:* Horizontal and vertical wind data for all flux periods were rotated according to a planar fit technique which forces the mean vertical wind speed to equal 0 (Wilczack et al. 2001).

4) *Lag time correction between 3-D sonic anemometer and PTR-TOF-MS:* The lag times were determined by checking the cross-correlation of vertical wind speed with VOC data by shifting wind data in steps of 0.2 seconds (data time resolution). The lag time was determined as the time shift which maximized the cross-correlation coefficient. All 30 min flux data between 10:00 and 16:00 PST were evaluated. Because the internal clocks of the PTR-TOF-MS computer and the data logger differed slightly, the lag times varied between 9.2 sec and 17.8 sec during the course of the campaign. However, no abrupt shifts were observed during periods of continuous operation. The following lag times were applied (for continuous measurement periods): 9.2 s (06/26 – 06/29), 14.6 s (07/02 – 07/10), 17.8 s (07/11 – 07/13), 16.6 s (07/14 – 07/21), and 17.4 s (07/22 – 07/26). Figure 3.3 shows average daytime cross correlations for five lag time corrected compounds.

5) *EC flux calculation:* Fluxes of BVOC (F_{wc}, nmol m^{-2} s^{-1}) were calculated using the EC method in which the vertical fluxes of BVOC are determined by the mean covariance between deviations of the vertical wind speed and each BVOC mixing ratio for each 30 min period,

$$F_{wc} = \frac{\sigma}{N}\sum_{i=1}^{N}(w_i - \overline{w})\cdot(c_i - \overline{c}) = \frac{\sigma}{N}\sum_{i=1}^{N} w_i' \cdot c_i' \qquad (1)$$

where σ is the air density (mol m^{-3}), N is the total number of data points in each 30 min measurement period, and $w_i - \overline{w}$ or w_i' is the instantaneous deviation of the vertical wind speed from its average, and $c_i - \overline{c}$ or c' is the instantaneous deviation of the BVOC mixing ratio from its average (nmol mol^{-1} or ppbv). We did not apply de-trending procedures since linear or non-linear de-trending can remove real fluxes; therefore, we used only block averaging for each flux period.

6) *Flux data filtering:* We discarded data to insure more robust results if (i) the tilt angle from rotating the vertical wind data exceeded 5^o or (ii) the flux data did not comply with our stationarity criterion. To evaluate the stationarity, we divided each 30 min flux period into 5 segments, calculating the EC flux for each segment, and comparing the average of the five segments to the EC flux for the full 30 min period. The measurement was discarded if the difference between these two quantities was larger than 30% (Lee et al., 2004; Foken and Wichura, 1996). For all the BVOCs observed, 55 – 85 % of daytime and 30 – 65 % of nighttime data complied with these criteria.

7) *Flux error estimation:*

The potential errors in flux estimation are summarized in Table 3.1. Briefly, uncertainties in EC flux may include systematic errors due to (i) sensor separation, (ii) inlet dampening, (iii)

insufficient instrument time response, (iv) uncertainties in concentration determinations, or (v) random noise in the EC flux.

Sensor separation errors are caused by different sampling positions for the sonic anemometer and ambient sample inlet of the PTR-TOF-MS resulting in a flux underestimation which can be estimated using a transfer function (Moore, 1986):

$$T_s(f) = e^{-9.9\left(\frac{f \cdot s}{U}\right)^{1.5}} \quad (2)$$

where f is the cospectral frequency (Hz), s is the sensor separation distance (m) and U is mean horizontal wind speed (m s^{-1}). During the campaign, the inlet was located laterally 0.1 m away from the sonic anemometer, so for the observed range of wind speeds (0.5-3.5 m/s), this error should be less than 2% of the flux.

Inlet dampening errors are due to attenuation of small mixing ratio fluctuations when sampling through a tube. Flux underestimation from inlet dampening is typically evaluated using a transfer function (Massman, 1991):

$$T_s(f) = e^{-\frac{4\pi^2 \Lambda a L f^2}{u^2}} \quad (3)$$

where Λ is the attenuation parameter (assuming ~4.2 at Re ~3400 for CH_4) , L and a are length (15 m) and inner radius (0.002 m) of the sampling tube and u is mean tube flow velocity (14.7 m s^{-1}). We estimate a negligible (<0.15 %) error due to this effect. However, this error estimate was developed for CH_4 which is probably not representative for most VOCs. Especially some condensable and/or sticky compounds such as acetic acid may suffer from much larger dampening errors. For better estimates we would need to characterize the attenuation parameters for all individual compounds. Inlet dampening of fluctuations for condensable or sticky species causes a systematic underestimate of the flux as discussed further in section 3.2 for acetic acid (*m/z* 61.027).

Flux errors also can be caused by insufficient instrument time response to small fluctuations contributing to the flux, and this error can be approximated by a transfer function (Horst, 1997):

$$T_s(f) = \frac{1}{1 + (2\pi f \tau)^2} \quad (4)$$

where, τ is the time response (0.1 s) of the instrument, and we estimate this error is ~ 0.25% for our measurements.

In addition, flux estimation errors arise from instrument noise which may correlate with vertical wind speed and is estimated by (Lenschow and Kristensen, 1985; Ritter et al., 1990; Farmer et al., 2006):

$$\sigma_{inst}^2 = \frac{\sigma_w^2 \sigma_n^2 \Delta t}{T} \quad (5)$$

where T is the time length of a sample (30 min), σ_w and σ_n are the variance of the vertical wind speed and the instrument noise, and Δt is the sampling interval (0.2 s). For the PTR-TOF-MS, instrument noise is described by a Poisson distribution: the 1σ error in a measurement that is derived from counting a total of N ions is $\sqrt{N}$ (de Gouw and Warneke, 2007), so σ_n can be calculated in concentration units using the instrument sensitivity for each flux period. Daytime (10:00 – 14:00 PST) flux uncertainty based on this random error varied by compound from 0.1% to 16%.

Uncertainties in the flux also can arise from systematic errors in concentration determination. The accuracy for compounds calibration using known gas standards is better than 20%. For all other compounds the concentration has been estimated using calculated values for the collision rate constant which should equal the reaction rate constant within ± 30% (Holzinger et al., 2010a).

The possible error due to air density fluctuation related to H_2O concentration change (so called WPL correction) is also estimated (Lee et al., 2004). Here, we only considered H_2O effects since the PTR-TOF-MS is a closed-path sensor and the sampling line temperature and instrument temperature were controlled. Ignoring this correction could potentially cause overestimations (< 5 %) in deposition fluxes and underestimations (< 4 %) in emission fluxes under the assumption that all species are non-soluble. However, we did not correct for H_2O effects in our estimated fluxes because we consider this potential error to be minor, it would not affect the direction of the fluxes, and each compound may be subject to different additional H_2O effects that vary with solubility (e.g. desorption from the wall). Further investigations into the hygroscopic properties of each compound would be needed to elucidate possible additional errors.

For compounds with bi-directional fluxes, defining a flux detection limit is challenging. In order to detect bi-directional fluxes, we examined the absolute value of the cross correlation. We considered the flux detectable for compounds with an absolute value cross correlation (around zero time shift) at least three times the standard deviation of the noise of the absolute value cross correlation over time shifts of +/- 20 seconds. For compounds that had both deposition and emission, fluxes measured by PTR-TOF-MS, and vertical gradients by PTR-MS, we were also able to independently confirm that measured deposition occurred simultaneously with gradients that also indicated deposition, as demonstrated for methanol in figure 3.8a and c.

3.3 Results and Discussion

3.3.1 Flux and mixing ratio

A total of 664 mass peaks with significant signal above the noise were identified by IDL routines according to Holzinger et al. (2010a). These include major primary ions (e.g. $(H_2O)H^+$, $(H_2O)_2H^+$, $(H_2O)_3H^+$), impurities such as O_2^+, NO^+, N_2H^+, and ammonium ions (e.g. NH_3^+,

$NH_3NH_3H^+$). We applied the described flux routines to 555 peaks above *m/z* 31 (this includes protonated formaldehyde), excluding all above mentioned peaks. In this paper, we focus on 27 ion species including all those selected for PTR-MS flux and vertical gradient measurement, acetic acid (*m/z* 61.027), and a major fragment of terpenes (*m/z* 95.086) which showed significant flux.

In Table 3.2, the 27 selected ion species are listed by 24-hour (day/night) averaged mixing ratios and fluxes. Figure 3.4 shows the full time series and diurnal profiles of mixing ratios and fluxes measured by PTR-TOF-MS for methanol and acetone (monitored at *m/z* 33.032 and 59.048, respectively) which were the compounds with the highest mixing ratios measured at this site. The fluxes of BVOC directly emitted by plants reached maxima in the afternoon when the temperature and light levels were highest and vertical turbulent mixing was fastest. However, mixing ratios were lower during daytime compared to nighttime for most BVOC including methanol, acetone, acetaldehyde, acetic acid, and monoterpenes. This was mainly due to the dilution of the emissions into a larger mixing layer and faster oxidation of BVOC during daytime. A detailed discussion of diurnal boundary layer dynamics in this area and season can be found in Bianco et al. (2011).

3.3.2 Spectral analysis

Spectral analysis provides a useful tool to validate the instrument's performance in both high and low frequency regimes. Here, we analyze fluxes of the 5 ion species (*m/z* 33.032: CH_3OHH^+, *m/z* 59.048: $C_3H_6OH^+$, *m/z* 61.027: $C_2H_4O_2H^+$, *m/z* 81.070: $C_6H_8H^+$, *m/z* 93.069: $C_7H_8H^+$) showing the most significant fluxes at this site. The co-spectra in Fig. 3.5a and b present the frequency distribution for vertical wind speed (*w*) with sensible heat (*T*) and 5 dominant BVOC. The data represent average daytime conditions (10:00 – 14:00 PST) for the entire measurement period. Generally, the fall-off slopes for the five compounds in the inertial sub-range (above 0.03 Hz) follow a -5/3 slope similar to the sensible heat flux ($w'T'$) (Fig. 3.5a and b) and demonstrates that the PTR-TOF-MS system provides adequate time response to measure EC flux. Co-spectra of w' (*m/z* 59.048)$'$, w' (*m/z* 61.027)$'$, w' (*m/z* 81.070)$'$, and w' (*m/z* 93.069)$'$ show some negative values (closed symbols) at high frequency above 0.3 Hz, and this may indicate complex processes within and/or above the canopy such as fast photochemical loss/production oxidizing BVOCs with wake turbulence production. A similar phenomenon was observed in other studies for peroxyacetyl nitrate and formaldehyde (Wolfe et al., 2009; DiGangi et al., 2011). For the co-spectrum of w'(*m/z* 61.027)$'$, loss of flux signal is apparent as successive fall-off of signal at frequencies around ~0.06 Hz. This loss of signal may be explained by dampening of fast fluctuations in the sample tube due to stickiness of acetic acid, and is consistent with cross-correlations with vertical wind speed compared to those of other compounds that are less sticky (Fig. 3.3).

Figure 3.5c and d show normalized co-spectra demonstrating that the dominant frequencies transporting flux are in the range 0.03-0.1 Hz for these 5 ion species, similar to the normalized co-spectrum of $w'T'$. The co-spectra of individual compounds exhibit slightly different patterns. For example, the frequency of maximum flux for *m/z* 61.027 is similar to other compounds, but

it has a unique second maximum at low frequencies (around 0.003 Hz) and a significant dip between 0.06 and 0.5 Hz. In contrast, normalized co-spectra for *m/z* 33.032 and *m/z* 59.048 show small peaks at high frequency around 1 Hz. It is apparent from these comparisons that individual compounds have different eddy features that must result from differences in sources and sinks such as leaf/soil emission, photochemical production or loss at different time scales, or surface removal by degree of stickiness/solubility. These different features could potentially result from uncharacterized instrument noise, but most eddy features are reproducible so we consider noise an unlikely source. For example, for acetone these features (peaks at 0.03-0.1Hz and 1 Hz) typically show up in the normalized co-spectrum of individual 30 min periods (Fig. 3.7a). Therefore, we think this difference is a real characteristic of individual compounds, not instrument noise.

Normalized cumulative distributions of the co-spectra, commonly referred to as ogives, are shown in Fig. 3.5e and f. Comparing to the ogive of sensible heat flux provides an analytical approach to check for potential loss due to spectral attenuation or other factors (Oncely et al, 1996). When the data converge to 1 at low frequencies, this implies that all relevant eddies are well captured in one sampling period and no significant flux is transported by eddies beyond the duration of the sampling period. The ogives of all ions shown in the figure asymptotically approach 1 at low frequency, indicating that the sampling period of 27 min was sufficiently long. However, ogives of $w'(m/z\ 61.027)'$, $w'(m/z\ 81.070)'$, and $w'(m/z\ 93.069)'$ are shifted to lower frequency compared to those of $w'(m/z\ 33.032)'$ and $w'(m/z\ 59.048)'$ which are very similar to the $w'T'$ ogive. This indicates that there exist potential loss processes for these 3 compounds. In the case of acetic acid (*m/z* 61.027) inlet dampening of high frequency variations may explain the shift; for the other compounds the reason for the shift towards lower frequencies is currently not well understood.

Overall, the spectral analysis presented here demonstrates that fluxes of BVOC are well measured by PTR-MS-TOF-EC, except for some potential loss of flux for sticky compounds such as acetic acid. The analysis also demonstrates that BVOC fluxes at this site are likely controlled by different and sometimes even competing processes. In combination with canopy transport models the spectral information may prove useful for constraining the strength of individual sources/sinks such as biogenic emission, chemical production/loss, and dry deposition, and we recommend further research on this issue.

3.3.3 Intercomparison between PTR-TOF and PTR-MS

Mixing ratios and fluxes

We compare measurements of methanol (monitored at *m/z* 33.032 for PTR-TOF-MS and *m/z* 33 for PTR-MS) and acetone (monitored at *m/z* 59.048 for PTR-TOF-MS and *m/z* 59 for PTR-MS) to validate the performance of both PTR-MS and PTR-TOF-MS for measuring ambient mixing ratios and fluxes. These two compounds exhibited high and variable mixing ratios and fluxes, were measured by both instruments through the same sampling inlet simultaneously, and

were reliably calibrated using standard gases two times per day. For the other species commonly measured, *m/z* 69 and 113 showed relatively low mixing ratios and fluxes. Two distinct mass peaks on *m/z* 113 were identified by PTR-TOF-MS measurement (Table 3.2). Monoterpene fluxes by PTR-MS were measured at only *m/z* 81 (a main fragment of monoterpenes), but we found that monoterpene fluxes were dominated by 3 different masses (*m/z* 81.070, 95.086, 137.131). Fragmentation patterns of monoterpenes are highly dependent on E/N ratio and the specific monoterpene mix. Therefore, we focus on comparison of methanol and acetone in this section.

Inter-comparison results (Fig. 3.6) are presented with linear fits based on the Williamson-York method reviewed by Cantrell (2008) considering uncertainties in both the x and y variables with all the same weights. Half-hour mean mixing ratios and fluxes are included from 14 July through 26 July when both instruments continuously operated without any critical maintenance issues. Mixing ratio measurements of methanol and acetone over the 12-day period generally agree well with slopes of 0.99 (R^2 = 0.89) for methanol, and 0.99 (R^2 = 0.97) for acetone. Methanol and acetone fluxes (Fig. 3.6c and d) also agree well between the two instruments with slopes of 1.05 (R^2 = 0.75), and 1.00 (R^2=0.51), respectively. However, the correlation coefficient for acetone is lower than for methanol owing to a few data points where PTR-TOF-MS measured higher fluxes than PTR-MS. This difference is likely attributed to loss of high frequency eddies in the PTR-MS measurement due to both the lower time resolution and the specificity of the disjunct data acquisition for each chemical compound. To investigate this further, we inspected the normalized co-spectra for acetone fluxes from both measurements checking which frequencies were carrying significant flux, and found that a large acetone upward flux at high frequency measured by PTR-TOF-MS might be not properly detected by PTR-MS, contributing to this discrepancy. Figure 3.7 shows an example for time 14:00 PST on July 22, 2010. Each line presents the normalized co-spectra of sensible heat flux (broken black line) and acetone flux; original 5 Hz data from PTR-TOF-MS (red line with open circle), 1 Hz reduced data from PTR-TOF-MS (solid cyan line), 1 Hz disjunct sub-sampled (similarly to PTR-MS data acquisition) from PTR-TOF-MS (dotted green line), and ~ 1 Hz disjunct data from PTR-MS (solid blue line with plus). This comparison demonstrates that a significant portion of acetone flux occurred at high frequencies (> ~0.9 Hz) during this 30 min period, and PTR-MS was not able to capture this feature due to lower time resolution. Of interest, disjunct data acquisition also affected the reliability of turbulent transport information. Figure 3.7b shows co-spectra of 1 Hz disjunct data from both instruments, and maximum peaks are located at higher frequency than that of continuous data shown in figure 3.7a, in spite of good agreement between the co-spectra, indicating non-continuous data may lose real flux information. This phenomenon occurred similarly for methanol, but the portion of high frequency flux was lower than for acetone and had much less effect on the 30 min average flux. In addition, slightly different time windows used for EC flux calculations from the 2 different instruments could contribute to this imperfect correlation. Overall, even though there are occasional discrepancies in flux between the two instruments, the differences were minor, and we conclude there were no significant instrumental biases in either mixing ratio or flux measurements.

Fluxes by PTR-TOF-MS and vertical gradients by PTR-MS

To check whether the observed vertical gradients were qualitatively in agreement with the observed direction of fluxes, we compare EC fluxes measured by PTR-TOF-MS and vertical gradients measured by PTR-MS. Lower (or higher) average mixing ratios with increasing height above the canopy normally indicate that there is emission (or deposition), respectively. PTR-TOF-MS EC flux data from the first 0 – 30 min and consecutive 6-min averaged PTR-MS data at 4 different heights from the second 30 – 60 min are used to represent each hour. Average diurnal profiles of fluxes and vertical gradients measured by PTR-TOF-MS and PTR-MS (respectively) are shown in figures 3.8 – 3.10 for the 6 species with the highest fluxes and/or mixing ratios which were measured by both instruments. In addition, we show the average diurnal flux of acetic acid detected by PTR-TOF-MS, because it was one of the species emitted in highest quantity, however its vertical gradients were not measured by PTR-MS.

Methanol is the most abundant non-methane VOC in the troposphere with mixing ratios often exceeding 10 ppbv in the boundary layer in vegetated regions during summer (Goldan et al., 1995; Lamanna and Goldstein, 1999; Holzinger et al. 2001; Schade and Goldstein, 2006), and it is known to be either directly emitted from plants or deposited to wet surfaces such as leaves and soil (Schade et al., 2011; Karl et al., 2004). Consistently, methanol mixing ratios at this site were the highest of all the VOC observed with a range from 7.3 – 43.6 ppbv. Previous branch enclosure experiments for citrus species have demonstrated that methanol is the dominant VOC emitted on a molar basis (Fares et al., 2011). The diurnal cycle of vertical gradients (Fig. 3.8a) showed higher concentrations and stronger vertical gradients at nighttime than during daytime, while fluxes (Fig. 3.8c) were maximum during daytime around 15:00 PST, and small but measurable at night. The observed higher concentrations and larger vertical gradients at night are typical for species with temperature dependent emissions due to much faster vertical mixing during the day and stable atmospheric stratification during the night. Bi-directional fluxes for methanol, with emission in late evening and deposition in early morning, were clearly apparent in both the flux and vertical gradient directions, with the vertical gradients providing clear confirmation that the flux measurements of deposition were real.

Acetone is ubiquitous in the troposphere, and it has a variety of sources including terrestrial vegetation, biomass burning, anthropogenic emissions, and photochemical production (Pöschl et al., 2001; Jacob et al., 2002; Schade and Goldstein, 2006). With a daytime average around 4 ppbv, our results were well within the range of previous studies. Vertical gradients of acetone (Fig. 3.8b) were very weak in the early morning (02:00 – 07:00 PST) and more clearly visible for the rest of the day. This pattern was consistent with the PTR-TOF-MS EC measurements of high fluxes during the day, significant fluxes in the evening, and near zero fluxes in the early morning (Fig. 3.8d).

Acetaldehyde (Fig. 3.9a and d, monitored at *m/z* 45.033 for PTR-TOF-MS and *m/z* 45 for PTR-MS) is emitted by live leaves, and has similar sources as acetone (Kesselmeier and Staudt, 1999; Schade and Goldstein, 2001). Ciccioli et al. (1999) observed comparable fluxes of acetone and acetaldehyde from an orange orchard in Spain. We measured a mean diurnal flux of up to 1.1 nmol m^{-2} s^{-1} for acetone and 0.7 nmol m^{-2} s^{-1} for acetaldehyde, so our results were in general agreement with Ciccioli et al. (1999). The directions of observed vertical gradient and EC flux of acetaldehyde were generally in agreement.

Methyl vinyl ketone and methacrolein (MVK+MACR; monitored at *m/z* 71.048 for PTR-TOF-MS and *m/z* 71 for PTR-MS) are well known as major secondary products from the atmospheric oxidation of isoprene. Recently, Karl et al. (2010) and Tani et al. (2010) have reported MVK+MACR can be taken up by plants during daytime, but Jardine et al. (2012) found these compounds can be directly emitted due to within plant isoprene oxidation. Our observations of both flux and vertical gradient in the orange grove indicate emission occurred through most of the day and night, with a short period of deposition in the early morning from 04:00 – 06:00 PST (Fig. 3.9b and e), and an overall net emission. Vertical gradients (Fig. 3.9b) suggested some deposition occurring between 02:00 and 04:00 PST, yet the mixing ratios at that time were highest at 5 m, so the observed emission fluxes at 7.1 m were still consistent with the overall vertical gradient pattern. Our results for MVK+MACR clearly show bi-directional exchange but with a net emission from the orange orchard. This result contrasts with results of Karl et al. (2010) showing deposition dominating in multiple different ecosystems.

Toluene and a fragmentation product of para-cymene ($C_{10}H_{14}H^+$, monitored at *m/z* 135.116 in PTR-TOF) were detected at *m/z* 93 in PTR-MS and at *m/z* 93.069 in PTR-TOF-MS. The fragment ion from para-cymene accounts for about 80% of total ions from para-cymene based on our E/N ratios for both instruments (Tani et al., 2003; Ambrose et al., 2010). A few studies have claimed that toluene can be directly emitted from plants (Heiden et al., 1999; White et al., 2009), and also para-cymene emissions have been observed from orange trees (Ciccioli et al., 1999). Our observation of *m/z* 93 flux and vertical gradient showed upward flux throughout the day (Fig. 3.9c and f). In-situ gas chromatography (GC) measurements conducted during August, 2010, (data do not overlap with this time period) recorded para-cymene concentrations between 0.04 ppbv and 0.84 ppbv, and toluene concentrations were half of that concentration or less, making the toluene concentrations often below the detection limit for PTR-MS and PTR-TOF-MS. Therefore, we infer para-cymene was probably the main contributor to fluxes and vertical gradients of *m/z* 93.

Monoterpenes are BVOCs with chemical composition $C_{10}H_{16}$, and citrus trees emit various monoterpenes including limonene, ocimene, and sabinene (Fares et al., 2011; Ormeno et al., 2010; Ciccioli et al., 1999). PTR-MS or PTR-TOF-MS systems monitor the sum of monoterpenes mainly at *m/z* 137 (or 137.131) ($C_{10}H_{16}H^+$), with a main fragment at *m/z* 81 (or 81.070) ($C_6H_8H^+$) and several minor fragments including *m/z* 95 (or 95.086) ($C_7H_{10}H^+$). Fragments from sesquiterpenes (Kim et al., 2009) may also contribute to signals at the same masses, but their contribution should be minor because of very low concentrations. The fragmentation patterns are dependent on both the instrument operating conditions and the different monoterpene species present. Tani et al. (2003) reported fragmentation of d-limonene to *m/z* 81, 137, and 95 with yields of ~50%, ~30%, and ~10%, respectively, based on our E/N ratio condition (~150 Td). Misztal et al. (2012) showed the ratio of *m/z* 81 to *m/z* 137 for d-limonene increases at higher E/N ratio (e.g., ~6.5 at 140 Td). Both Tani et al. (2003) and Misztal et al. (2012) showed different fragmentation patterns for several specific monoterpenes when changing the instrumental conditions. Our GC data at this site in August showed d-limonene contributed 89 % to the sum of speciated monoterpene mixing ratios (Fares et al., 2012a). Therefore, *m/z* 81.070 fluxes measured by our PTR-TOF-MS should be higher than *m/z* 137.131 and *m/z* 95.086, consistent with our results (Fig. 3.10b). All three of these masses showed emissions over the full day, consistent with vertical gradients observed by PTR-MS (Fig. 3.10a).

Different ions of monoterpenes from the PTR-TOF-MS show different diurnal patterns which may indicate the existence of different emission mechanisms as sources for different monoterpenes.

In addition to the compounds measured by both instruments, acetic acid ($C_2H_4O_2H^+$; detected at *m/z* 61.027 in PTR-TOF-MS but not measured by PTR-MS) was among the top 5 emitted species with mixing ratios between 2 - 12 ppbv and a daytime flux about 1 nmol m^{-2} s^{-1} (Fig. 3.11). Acetic acid is known to be produced or consumed in plants by metabolism processes, the central respiratory/biosynthetic intermediate acetyl-CoA. A few branch enclosure and field experiments showed emission from trees and deposition to surfaces of plants or wet soil surfaces (Kesselmeier and Staudt, 1999; Kesselmeier, 2001; Jardine et al., 2011). However the biosphere-atmosphere exchange of acetic acid has not been extensively studied. Moreover, we did not have an authentic standard for acetic acid during the field campaign and more work is necessary to validate its concentration in PTR-TOF-MS measurements. Acetic acid is highly condensable and sticky, so some of it is likely lost to the walls of sampling tubes as discussed in section 3.2. Nevertheless, our data showed clear acetic acid emission from this site, and but we think these measured fluxes might underestimate the actual flux.

For other OVOC (Table 3.2), we observed bi-directional fluxes with relatively small magnitudes (daytime average up to 0.016 nmol m^{-2} s^{-1} for emission and -0.004 nmol m^{-2} s^{-1} for deposition) compared to the compounds described above. The emissions of these OVOC may be a result of oxidation processes within the canopy or direct emission from plants/soil. The observed depositions possibly suggest that parent hydrocarbon compounds either emitted from the site or advected from upwind sources are photochemically oxidized to form secondary compounds containing oxygen which are then removed from the atmosphere by dry deposition. In addition, we found at least 2 significant distinct mass peaks at each of the nominal *m/z* 107, 111, 113, and 139, indicating PTR-TOF-MS can efficiently separate among isobaric compounds and provide their empirical molecular formulae.

3.3.4 Total BVOC fluxes

Total BVOC fluxes are shown for the whole measurement period (Fig. 3.12). The fluxes shown include the 27 masses evaluated and are expressed in units µg C m^{-2} h^{-1}. The carbon numbers were inferred from the ion species detected by PTR-TOF-MS, but 10 carbons were applied for *m/z* 81.070 and *m/z* 95.086 because these masses are known to mainly be due to fragmentation of monoterpenes ($C_{10}H_{16}H^+$).

Measured BVOC fluxes (Fig. 3.12) showed emissions at all times of day reaching a maximum of 765 µg C m^{-2} h^{-1} (emissions of 25 masses) around hour 13:00 – 14:00 PST. During the night smaller but still positive fluxes were observed with a minimum of 79 µg C m^{-2} h^{-1} (emissions of 15 masses) around hour 00:00 – 01:00 PST. About half of the species (12 ions) were observed to downward flux (-57 µg C m^{-2} h^{-1}) during hour 03:00 – 04:00 PST. Sudden increases and decreases of fluxes at hour 07:00 – 08:00 and 19:00 – 20:00 PST were observed, respectively. This is likely due to transitions in boundary layer depth and atmospheric stability

occurring at those times, so high concentrations at night are flushed out in the morning with high fluxes, and in the evening biogenic emissions start to accumulate in the in the surface layer canopy resulting in low fluxes. Bi-directional fluxes (either emission or deposition) for OVOC were observed, but we did not find any compounds which were uniformly deposited throughout the day.

By adding up all contributions to the total net flux over a day, a 24 hour mean emission flux of 299 µg C m^{-2} h^{-1} was measured for the reported masses (Fig. 3.13). Terpene (*m/z* 81.070, 95.086, and 137.131) emissions contributed ~34 % to total net carbon flux for selected masses, and this might be slightly underestimated since sesquiterpene ($C_{15}H_{24}H^+$) fragments, for which 15 carbons should be assumed, are also distributed on these *m/z*. However, fluxes measured for sesquiterpenes should be minor due to low concentration and fast photochemical destruction below our measurement height. Methanol (*m/z* 33.032) was the second largest emission at 24% of the total by mass, but represented the largest emission on a molar basis. Acetone (*m/z* 59.048) and acetic acid (*m/z* 61.027) fluxes were similar magnitude (~12%), followed by para-cymene + toluene (*m/z* 93.069), acetaldehyde (*m/z* 45.033), MVK+MACR (*m/z* 71.048), and isoprene+MBO (*m/z* 69.071) with 4.1, 3.8, 2.4, and 1.8 % contributions, respectively (Fig. 3.13). For the other 17 masses the net emission flux only contributed 5% to the total fluxes.

3.4 Summary

We successfully measured and evaluated eddy covariance emission and deposition fluxes for 27 *m/z* ratios using a high resolution PTR-TOF-MS instrument over an orange orchard in California's Central Valley. EC flux data by PTR-TOF-MS were validated through spectral analysis, were quantitatively inter-compared with PTR-MS measurement results for the mixing ratios and fluxes, and were qualitatively compared with vertical gradients from PTR-MS for commonly measured compounds. Most of the observed compounds showed emissions from the surface. In addition, we found a significant emission of acetic acid which was only observed by PTR-TOF-MS measurement. Fluxes of terpenes, methanol, acetone, acetic acid, para-cymene + toluene, and acetaldehyde contributed about 90 % of the total flux of 27 masses observed by the PTR-TOF-MS on a carbon mass basis. The dominant BVOC emissions from this site were monoterpenes (*m/z* 81.070 + *m/z* 137.131 + *m/z* 95.086, 34%, 102 µg C m^{-2} h^{-1}) and methanol (*m/z* 33.032, 23.9 %, 72 µg C m^{-2} h^{-1}) followed by acetone (*m/z* 59.048, 12.2 %, 36.5 µg C m^{-2} h^{-1}), acetic acid (*m/z* 61.027, 11.9%, 35.7 µg C m^{-2} h^{-1}), para-cymene (*m/z* 93.069, 4.1%, 12.2 µg C m^{-2} h^{-1}), acetaldehyde (*m/z* 45.033, 3.8 %, 11.5 µg C m^{-2} h^{-1}), MVK+MACR (*m/z* 71.048, 2.4%, 7.1 µg C m^{-2} h^{-1}), and isoprene+MBO (*m/z* 69.071, 1.8%, 5.3 µg C m^{-2} h^{-1}). In addition, low levels (<1.6 % for each, 5.8 % in total flux) of emission/deposition for 17 masses were observed. We have demonstrated that EC flux measurement using PTR-TOF-MS provide a very powerful tool to investigate landscape scale exchanges of VOC and/or OVOC fluxes, observing both emissions and deposition simultaneously for a wide range of compounds.

3.5 References

Ambrose, J. L., Haase, K., Russo, R. S., Zhou, Y., White, M. L., Frinak, E. K., Jordan, C., Mayne, H. R., Talbot, R., and Sive, B. C.: A comparison of GC-FID and PTR-MS toluene measurements in ambient air under conditions of enhanced monoterpene loading, Atmos Meas Tech, 3, 959-980, doi: 10.5194/amt-3-959-2010, 2010.

Andreae, M. O., and Crutzen, P. J.: Atmospheric aerosols: Biogeochemical sources and role in atmospheric chemistry, Science, 276, 1052-1058, 1997.

Baldocchi, D. D., Hicks, B. B., and Meyers, T. P.: Measuring Biosphere-Atmosphere Exchanges of Biologically Related Gases with Micrometeorological Methods, Ecology, 69, 1331-1340, 1988.

Baldocchi, D. D.: Assessing the eddy covariance technique for evaluating carbon dioxide exchange rates of ecosystems: past, present and future, Global Change Biol, 9, 479-492, 2003.

Bamberger, I., Hortnagl, L., Ruuskanen, T. M., Schnitzhofer, R., Muller, M., Graus, M., Karl, T., Wohlfahrt, G., and Hansel, A.: Deposition fluxes of terpenes over grassland, J Geophys Res-Atmos, 116, D14305, doi: 10.1029/2010jd015457, 2011.

Bianco, L., Djalalova, I. V., King, C. W., and Wilczak, J. M.: Diurnal Evolution and Annual Variability of Boundary-Layer Height and Its Correlation to Other Meteorological Variables in California's Central Valley, Bound-Lay Meteorol, 140, 491-511, doi: 10.1007/s10546-011-9622-4, 2011.

Bouvier-Brown, N. C., Goldstein, A. H., Gilman, J. B., Kuster, W. C., and de Gouw, J. A.: In-situ ambient quantification of monoterpenes, sesquiterpenes, and related oxygenated compounds during BEARPEX 2007: implications for gas- and particle-phase chemistry, Atmos Chem Phys, 9, 5505-5518, 2009.

Cantrell, C. A.: Technical Note: Review of methods for linear least-squares fitting of data and application to atmospheric chemistry problems, Atmos Chem Phys, 8, 5477-5487, 2008.

Chameides, W. L., Lindsay, R. W., Richardson, J., and Kiang, C. S.: The Role of Biogenic Hydrocarbons in Urban Photochemical Smog - Atlanta as a Case-Study, Science, 241, 1473-1475, 1988.

Ciccioli, P., Brancaleoni, E., Frattoni, M., Di Palo, V., Valentini, R., Tirone, G., Seufert, G., Bertin, N., Hansen, U., Csiky, O., Lenz, R., and Sharma, M.: Emission of reactive terpene compounds from orange orchards and their removal by within-canopy processes, J Geophys Res-Atmos, 104, 8077-8094, 1999.

Dabberdt, W. F., Lenschow, D. H., Horst, T. W., Zimmerman, P. R., Oncley, S. P., and Delany, A. C.: Atmosphere-Surface Exchange Measurements, Science, 260, 1472-1481, 1993.

Davison, B., Taipale, R., Langford, B., Misztal, P., Fares, S., Matteucci, G., Loreto, F., Cape, J. N., Rinne, J., and Hewitt, C. N.: Concentrations and fluxes of biogenic volatile organic compounds above a Mediterranean macchia ecosystem in western Italy, Biogeosciences, 6, 1655-1670, doi:10.5194/bg-6-1655-2009, 2009.

de Gouw, J., and Warneke, C.: Measurements of volatile organic compounds in the earth's atmosphere using proton-transfer-reaction mass spectrometry, Mass Spectrom Rev, 26, 223-257, doi: 10.1002/Mas.20119, 2007.

DiGangi, J. P., Boyle, E. S., Karl, T., Harley, P., Turnipseed, A., Kim, S., Cantrell, C., Maudlin, R. L., Zheng, W., Flocke, F., Hall, S. R., Ullmann, K., Nakashima, Y., Paul, J. B., Wolfe, G. M., Desai, A. R., Kajii, Y., Guenther, A., and Keutsch, F. N.: First direct measurements of formaldehyde flux via eddy covariance: implications for missing in-canopy formaldehyde sources, Atmos Chem Phys, 11, 10565-10578, doi:10.5194/acp-11-10565-2011, 2011.

Fares, S., Gentner, D. R., Park, J. H., Ormeno, E., Karlik, J., and Goldstein, A. H.: Biogenic emissions from Citrus species in California, Atmos Environ, 45, 4557-4568, doi: 10.1016/j.atmosenv.2011.05.066, 2011.

Fares, S., Park, J. H., Gentner, D. R., Weber, R., Ormeno, E., Karlik, J., and Goldstein, A. H.: Seasonal cycles of biogenic volatile organic compound fluxes and concentrations in a California citrus orchard, Atmos. Chem. Phys. Discuss., 12, 17987-18027, doi:10.5194/acpd-12-17987-2012, 2012a.

Fares, S., Weber, R., Park, J.-H., Gentner, D., Karlik, J., and Goldstein, A. H.: Ozone deposition to an orange orchard: Partitioning between stomatal and non-stomatal sinks, Environmental Pollution, 169, 258-266, doi:10.1016/j.envpol.2012.01.030, 2012b.

Farmer, D. K., Wooldridge, P. J., and Cohen, R. C.: Application of thermal-dissociation laser induced fluorescence (TD-LIF) to measurement of HNO_3, Sigma alkyl nitrates, Sigma peroxy nitrates, and NO_2 fluxes using eddy covariance, Atmos Chem Phys, 6, 3471-3486, 2006.

Foken, T., and Wichura, B.: Tools for quality assessment of surface-based flux measurements, Agr Forest Meteorol, 78, 83-105, 1996.

Fuentes, J. D., Lerdau, M., Atkinson, R., Baldocchi, D., Bottenheim, J. W., Ciccioli, P., Lamb, B., Geron, C., Gu, L., Guenther, A., Sharkey, T. D., and Stockwell, W.: Biogenic hydrocarbons in the atmospheric boundary layer: A review, B Am Meteorol Soc, 81, 1537-1575, 2000.

Goldan, P. D., Kuster, W. C., Fehsenfeld, F. C., and Montzka, S. A.: Hydrocarbon measurements in the southeastern United States: The Rural Oxidants in the Southern Environment (ROSE) program 1990, J Geophys Res-Atmos, 100, 25945-25963, 1995.

Goldstein, A. H., and Galbally, I. E.: Known and unexplored organic constituents in the earth's atmosphere, Environ Sci Technol, 41, 1514-1521, 2007.

Graus, M., Muller, M., and Hansel, A.: High Resolution PTR-TOF: Quantification and Formula Confirmation of VOC in Real Time, J Am Soc Mass Spectr, 21, 1037-1044, doi: 10.1016/j.jasms.2010.02.006, 2010.

Guenther, A., Hewitt, C. N., Erickson, D., Fall, R., Geron, C., Graedel, T., Harley, P., Klinger, L., Lerdau, M., Mckay, W. A., Pierce, T., Scholes, B., Steinbrecher, R., Tallamraju, R., Taylor, J., and Zimmerman, P.: A Global-Model of Natural Volatile Organic-Compound Emissions, J Geophys Res-Atmos, 100, 8873-8892, 1995.

Guenther, A., Karl, T., Harley, P., Wiedinmyer, C., Palmer, P. I., and Geron, C.: Estimates of global terrestrial isoprene emissions using MEGAN (Model of Emissions of Gases and Aerosols from Nature), Atmos Chem Phys, 6, 3181-3210, 2006.

Guenther, A. B., and Hills, A. J.: Eddy covariance measurement of isoprene fluxes, J Geophys Res-Atmos, 103, 13145-13152, 1998.

Hallquist, M., Wenger, J. C., Baltensperger, U., Rudich, Y., Simpson, D., Claeys, M., Dommen, J., Donahue, N. M., George, C., Goldstein, A. H., Hamilton, J. F., Herrmann, H., Hoffmann, T., Iinuma, Y., Jang, M., Jenkin, M. E., Jimenez, J. L., Kiendler-Scharr, A., Maenhaut, W., McFiggans, G., Mentel, T. F., Monod, A., Prevot, A. S. H., Seinfeld, J. H., Surratt, J. D.,

Szmigielski, R., and Wildt, J.: The formation, properties and impact of secondary organic aerosol: current and emerging issues, Atmos Chem Phys, 9, 5155-5236, 2009.
Heiden, A. C., Kobel, K., Komenda, M., Koppmann, R., Shao, M., and Wildt, J.: Toluene emissions from plants, Geophys Res Lett, 26, 1283-1286, 1999.
Holzinger, R., Jordan, A., Hansel, A., and Lindinger, W.: Methanol measurements in the lower troposphere near Innsbruck (047 degrees 16 ' N; 011 degrees 24 ' E), Austria, Atmos Environ, 35, 2525-2532, 2001.
Holzinger, R., Kasper-Giebl, A., Staudinger, M., Schauer, G., and Rockmann, T.: Analysis of the chemical composition of organic aerosol at the Mt. Sonnblick observatory using a novel high mass resolution thermal-desorption proton-transfer-reaction mass-spectrometer (hr-TD-PTR-MS), Atmos Chem Phys, 10, 10111-10128, doi: 10.5194/acp-10-10111-2010, 2010a.
Holzinger, R., Williams, J., Herrmann, F., Lelieveld, J., Donahue, N. M., and Rockmann, T.: Aerosol analysis using a Thermal-Desorption Proton-Transfer-Reaction Mass Spectrometer (TD-PTR-MS): a new approach to study processing of organic aerosols, Atmos Chem Phys, 10, 2257-2267, 2010b.
Horst, T. W.: A simple formula for attenuation of eddy fluxes measured with first-order-response scalar sensors, Bound-Lay Meteorol, 82, 219-233, 1997.
Jacob, D. J., Field, B. D., Jin, E. M., Bey, I., Li, Q. B., Logan, J. A., Yantosca, R. M., and Singh, H. B.: Atmospheric budget of acetone, J Geophys Res-Atmos, 107, 4100, doi: 10.1029/2001jd000694, 2002.
Jang, M. S., Czoschke, N. M., Lee, S., and Kamens, R. M.: Heterogeneous atmospheric aerosol production by acid-catalyzed particle-phase reactions, Science, 298, 814-817, 2002.
Jardine, K., Serrano, A. Y., Arneth, A., Abrell, L., Jardine, A., Artaxo, P., Alves, E., Kesselmeier, J., Taylor, T., Saleska, S., and Huxman, T.: Ecosystem-scale compensation points of formic and acetic acid in the central Amazon, Biogeosciences, 8, 3709-3720, doi: 10.5194/bg-8-3709-2011, 2011.
Jardine, K. J., Monson, R. K., Abrell, L., Saleska, S. R., Arneth, A., Jardine, A., Ishida, F. Y., Serrano, A. M. Y., Artaxo, P., Karl, T., Fares, S., Goldstein, A., Loreto, F., and Huxman, T.: Within-plant isoprene oxidation confirmed by direct emissions of oxidation products methyl vinyl ketone and methacrolein, Global Change Biol, 18, 973-984, doi: 10.1111/j.1365-2486.2011.02610.x, 2012.
Jordan, A., Haidacher, S., Hanel, G., Hartungen, E., Mark, L., Seehauser, H., Schottkowsky, R., Sulzer, P., and Mark, T. D.: A high resolution and high sensitivity proton-transfer-reaction time-of-flight mass spectrometer (PTR-TOF-MS), Int J Mass Spectrom, 286, 122-128, doi: 10.1016/j.ijms.2009.07.005, 2009.
Karl, T., Potosnak, M., Guenther, A., Clark, D., Walker, J., Herrick, J. D., and Geron, C.: Exchange processes of volatile organic compounds above a tropical rain forest: Implications for modeling tropospheric chemistry above dense vegetation, J Geophys Res-Atmos, 109, D18306, doi: 10.1029/2004jd004738, 2004.
Karl, T., Harley, P., Emmons, L., Thornton, B., Guenther, A., Basu, C., Turnipseed, A., and Jardine, K.: Efficient Atmospheric Cleansing of Oxidized Organic Trace Gases by Vegetation, Science, 330, 816-819, doi: 10.1126/science.1192534, 2010.
Karl, T. G., Spirig, C., Rinne, J., Stroud, C., Prevost, P., Greenberg, J., Fall, R., and Guenther, A.: Virtual disjunct eddy covariance measurements of organic compound fluxes from a subalpine forest using proton transfer reaction mass spectrometry, Atmos Chem Phys, 2, 279-291, 2002.

Kesselmeier, J., and Staudt, M.: Biogenic volatile organic compounds (VOC): An overview on emission, physiology and ecology, J Atmos Chem, 33, 23-88, 1999.
Kesselmeier, J.: Exchange of short-chain oxygenated volatile organic compounds (VOCs) between plants and the atmosphere: A compilation of field and laboratory studies, J Atmos Chem, 39, 219-233, 2001.
Kim, S., Karl, T., Helmig, D., Daly, R., Rasmussen, R., and Guenther, A.: Measurement of atmospheric sesquiterpenes by proton transfer reaction-mass spectrometry (PTR-MS), Atmos Meas Tech, 2, 99-112, 2009.
Lamanna, M. S., and Goldstein, A. H.: In situ measurements of C-2-C-10 volatile organic compounds above a Sierra Nevada ponderosa pine plantation, J Geophys Res-Atmos, 104, 21247-21262, 1999.
Lee, X., Massman, W. J., and Law, B. E.: Handbook of micrometeorology : a guide for surface flux measurement and analysis, Atmospheric and oceanographic sciences library, 29, Kluwer Academic, Dordrecht ; Boston ; London, xiv, 250 p. pp., 2004.
Lenschow, D. H., and Kristensen, L.: Uncorrelated noise in turbulence measurements, J Atmos Ocean Technol, 2, 68-81, 1985.
Lindinger, W., Hansel, A., and Jordan, A.: On-line monitoring of volatile organic compounds at pptv levels by means of proton-transfer-reaction mass spectrometry (PTR-MS) - Medical applications, food control and environmental research, Int J Mass Spectrom, 173, 191-241, 1998.
Massman, W. J.: The Attenuation of Concentration Fluctuations in Turbulent-Flow through a Tube, J Geophys Res-Atmos, 96, 15269-15273, 1991.
Misztal, P. K., Heal, M. R., Nemitz, E., and Cape, J. N.: Development of PTR-MS selectivity for structural isomers: Monoterpenes as a case study, Int J Mass Spectrom, 310, 10-19, 2012.
Moore, C. J.: Frequency-Response Corrections for Eddy-Correlation Systems, Bound-Lay Meteorol, 37, 17-35, 1986.
Muller, M., Graus, M., Ruuskanen, T. M., Schnitzhofer, R., Bamberger, I., Kaser, L., Titzmann, T., Hortnagl, L., Wohlfahrt, G., Karl, T., and Hansel, A.: First eddy covariance flux measurements by PTR-TOF, Atmos Meas Tech, 3, 387-395, 2010.
Oncley, S. P., Friehe, C. A., Larue, J. C., Businger, J. A., Itsweire, E. C., and Chang, S. S.: Surface-layer fluxes, profiles, and turbulence measurements over uniform terrain under near-neutral conditions, J Atmos Sci, 53, 1029-1044, 1996.
Ormeño, E., Gentner, D. R., Fares, S., Karlik, J., Park, J. H., and Goldstein, A. H.: Sesquiterpenoid Emissions from Agricultural Crops: Correlations to Monoterpenoid Emissions and Leaf Terpene Content, Environ Sci Technol, 44, 3758-3764, doi: 10.1021/Es903674m, 2010.
Pierce, T., Geron, C., Bender, L., Dennis, R., Tonnesen, G., and Guenther, A.: Influence of increased isoprene emissions on regional ozone modeling, J Geophys Res-Atmos, 103, 25611-25629, 1998.
Pöschl, U., Williams, J., Hoor, P., Fischer, H., Crutzen, P. J., Warneke, C., Holzinger, R., Hansel, A., Jordan, A., Lindinger, W., Scheeren, H. A., Peters, W., and Lelieveld, J.: High acetone concentrations throughout the 0-12 km altitude range over the tropical rainforest in Surinam, J Atmos Chem, 38, 115-132, 2001.
Ritter, J. A., Lenschow, D. H., Barrick, J. D. W., Gregory, G. L., Sachse, G. W., Hill, G. F., and Woerner, M. A.: Airborne Flux Measurements and Budget Estimates of Trace Species over

the Amazon Basin during the Gte Able-2b Expedition, J Geophys Res-Atmos, 95, 16875-16886, 1990.

Ruuskanen, T. M., Mueller, M., Schnitzhofer, R., Karl, T., Graus, M., Bamberger, I., Hortnagl, L., Brilli, F., Wohlfahrt, G., and Hansel, A.: Eddy covariance VOC emission and deposition fluxes above grassland using PTR-TOF, Atmos Chem Phys, 11, 611-625, doi: 10.5194/acp-11-611-2011, 2011.

Schade, G. W., and Goldstein, A. H.: Fluxes of oxygenated volatile organic compounds from a ponderosa pine plantation, J Geophys Res-Atmos, 106, 3111-3123, 2001.

Schade, G. W., and Goldstein, A. H.: Seasonal measurements of acetone and methanol: Abundances and implications for atmospheric budgets, Global Biogeochem Cy, 20, Gb1011, doi: 10.1029/2005gb002566, 2006.

Schade, G. W., Solomon, S. J., Dellwik, E., Pilegaard, K., and Ladstatter-Weissenmayer, A.: Methanol and other VOC fluxes from a Danish beech forest during late springtime, Biogeochemistry, 106, 337-355, doi: 10.1007/s10533-010-9515-5, 2011.

Shaw, W. J., Spicer, C. W., and Kenny, D. V.: Eddy correlation fluxes of trace gases using a tandem mass spectrometer, Atmos Environ, 32, 2887-2898, 1998.

Tani, A., Hayward, S., and Hewitta, C. N.: Measurement of monoterpenes and related compounds by proton transfer reaction-mass spectrometry (PTR-MS), Int J Mass Spectrom, 223, 561-578, 2003.

Tani, A., Tobe, S., and Shimizu, S.: Uptake of Methacrolein and Methyl Vinyl Ketone by Tree Saplings and Implications for Forest Atmosphere, Environ Sci Technol, 44, 7096-7101, doi: 10.1021/Es1017569, 2010.

White, M. L., Russo, R. S., Zhou, Y., Ambrose, J. L., Haase, K., Frinak, E. K., Varner, R. K., Wingenter, O. W., Mao, H., Talbot, R., and Sive, B. C.: Are biogenic emissions a significant source of summertime atmospheric toluene in the rural Northeastern United States?, Atmos Chem Phys, 9, 81-92, 2009.

Wilczak, J. M., Oncley, S. P., and Stage, S. A.: Sonic anemometer tilt correction algorithms, Bound-Lay Meteorol, 99, 127-150, 2001.

Wolfe, G. M., Thornton, J. A., Yatavelli, R. L. N., Mckay, M., Goldstein, A. H., LaFranchi, B., Min, K. E., and Cohen, R. C.: Eddy covariance fluxes of acyl peroxy nitrates (PAN, PPN and MPAN) above a Ponderosa pine forest, Atmos Chem Phys, 9, 615-634, 2009.

Table 3. 1. Possible source specific flux estimation errors.

Source of error	Bias	Estimated error
Sensor separation	Underestimation	< 2 %
High frequency damping	Underestimation	< 0.15 %
Instrumental response time	Underestimation	0.25 %
Random noise	None	0.1 – 16 % *
Concentration estimation	None	<30 % (or <20 % **)
H_2O and density fluctuation	Underestimation for deposition flux	< 5 %
	Overestimation for emission flux	< 4 %

* Based on daytime (10:00-14:00 PST) species specific errors.
** The error of the species calibrated with a standard gas is less than 20%.

Table 3. 2. Mixing ratio and flux information for 27 selected ion species.

Mass to charge ratio(m/z)		Possible empirical formulae and dominant compound[a]	Typical Mixing Ratio [nmol mol^{-1}] 24h-mean(day/night) [b]	EC Flux[c] [µg C m^{-2} h^{-1}] 24h-mean(day/night) [b]
PTR-MS	PTR-TOF-MS			
33	33.032	CH_3OHH^+ (-1.4) Methanol	19.89 (16.85 / 24.55)	71.5 (182.44 / 9.46)
42	42.033	$C_2H_3NH^+$ (-1.0) Acetonitrile	0.3 (0.3 / 0.3)	0 (3.1 / 0.7)
45	45.033	$C_2H_4OH^+$ (-0.9) Acetaldehyde	2.91 (2.68 / 3.28)	11.5 (38.6 / 3.4)
59	59.048	$C_3H_6OH^+$ (-0.9) Acetone	4.52 (3.73 / 5.35)	36.5 (98.6 / 11.7)
61[d]	61.027	$C_2H_4O_2H^+$ (-1.2) Acetic acid	4.91 (5 / 5.51)	35.7 (79.9 / 0.8)
69	69.071	$C_5H_8H^+$ (0.8) Isoprene + MBO[e]	0.28 (0.18 / 0.35)	5.31 (8.07 / 1.88)
71	71.048	$C_4H_6OH^+$ (-0.8) MVK+MACR[f]	0.3 (0.2 / 0.36)	7.05 (14.8 / 2.31)
79	79.054	$C_6H_6H^+$ (0.4) Benzene	0.1 (0.05 / 0.14)	4.14 (4.29 / 0.18)
81	81.070	$C_6H_8H^+$ (0.1) Monoterpenes	0.5 (0.22 / 0.74)	65.6 (90.8 / 40.2)
83	83.086	$C_6H_{10}H^+$ (0.6) Hexanal, Hexenols	0.13 (0.07 / 0.17)	1.72 (2.8 / 0.14)
87	87.077	$C_5H_{10}OH^+$ (-3.7) MBO[e]	0.07 (0.04 / 0.09)	1.4 (-1.3 / 0.2)
93	93.069	$C_7H_8H^+$ (-0.8) Toluene + Para-cymene	0.14 (0.04 / 0.22)	12.2 (25.5 / 4.4)
95[d]	95.086	$C_7H_{10}H^+$ (0.5) Monoterpenes	0.25 (0.16 / 0.33)	20.1 (32.6 / 15.0)
99	99.078	$C_6H_{10}OH^+$ (-2.6) Hexenals	0.04 (0.02 / 0.05)	1.42 (3.29 / 0.01)
107	107.049	$C_7H_6OH^+$ (-0.1) Benzaldehyde	0.05 (0.01 / 0.09)	1.65 (5.78 / 0.29)
	107.085	$C_8H_{10}H^+$ (-0.5) Xylene	0.08 (0.01 / 0.12)	5.6 (8.95 / 3.03)
111	111.080	$C_7H_{10}OH^+$ (-0.4) Unknown	0.06 (0.03 / 0.07)	0.72 (3.73 / -0.91)
	111.118	$C_8H_{14}H^+$ (1.2) Unknown	0.03 (0.02 / 0.04)	-1.24 (-1.53 / -0.83)
113	113.024	$C_5H_4O_3H^+$ (0.7) Unknown	0.06 (0.06 / 0.07)	-0.01 (-0.21 / -0.18)
	113.058	$C_6H_8O_2H^+$ (-1.7) Unknown	0.05 (0.03 / 0.06)	-0.19 (-3.18 / -0.52)
137	137.131	$C_{10}H_{16}H^+$ (-1.5) Monoterpenes	0.12 (0.05 / 0.18)	15.9 (18.8 / 9.95)
139	139.039	$C_7H_6O_3H^+$ (0) Unknown	0.02 (0.01 / 0.03)	0.75 (-0.96 / 0.66)
	139.110	$C_9H_{14}OH^+$ (-1.7) Nopinone	0.03 (0 / 0.05)	-0.15 (1.71 / -0.88)
149	149.094	$C_{10}H_{12}OH^+$ (-2.1) Methyl-chavicol	0.02 (0.01 / 0.04)	-0.5 (0.5 / 0.2)
151	151.109	$C_{10}H_{14}OH^+$ (-2.7)	0.02 (0.01 / 0.02)	1.04 (4.93 / -0.16)

		Pinonaldehyde		
155	155.137	$C_{10}H_{18}OH^+$ (-6.0) Linalool	0.01 (0.01 / 0.01)	0.1 (1.1 / 0.09)
205	205.195	$C_{15}H_{24}H^+$ (-0.1) Sesquiterpenes	0.02 (0.02 / 0.02)	0.8 (1.28 / 0.32)

[a] The difference between the measured mass and the exact ion mass in mDa is given in parenthesis.
[b] Daytime and nighttime average is taken by each data during hour 10:00 – 14:00 and 22:00 – 02:00 PST, respectively.
[c] Positive numbers represent emission from the surface, and negatives are deposition to the surface.
[d] No measurement by the PTR-MS.
[e] 2-methyl-3-butene-2-ol
[f] sum of methylvinylketone and methacrolein.

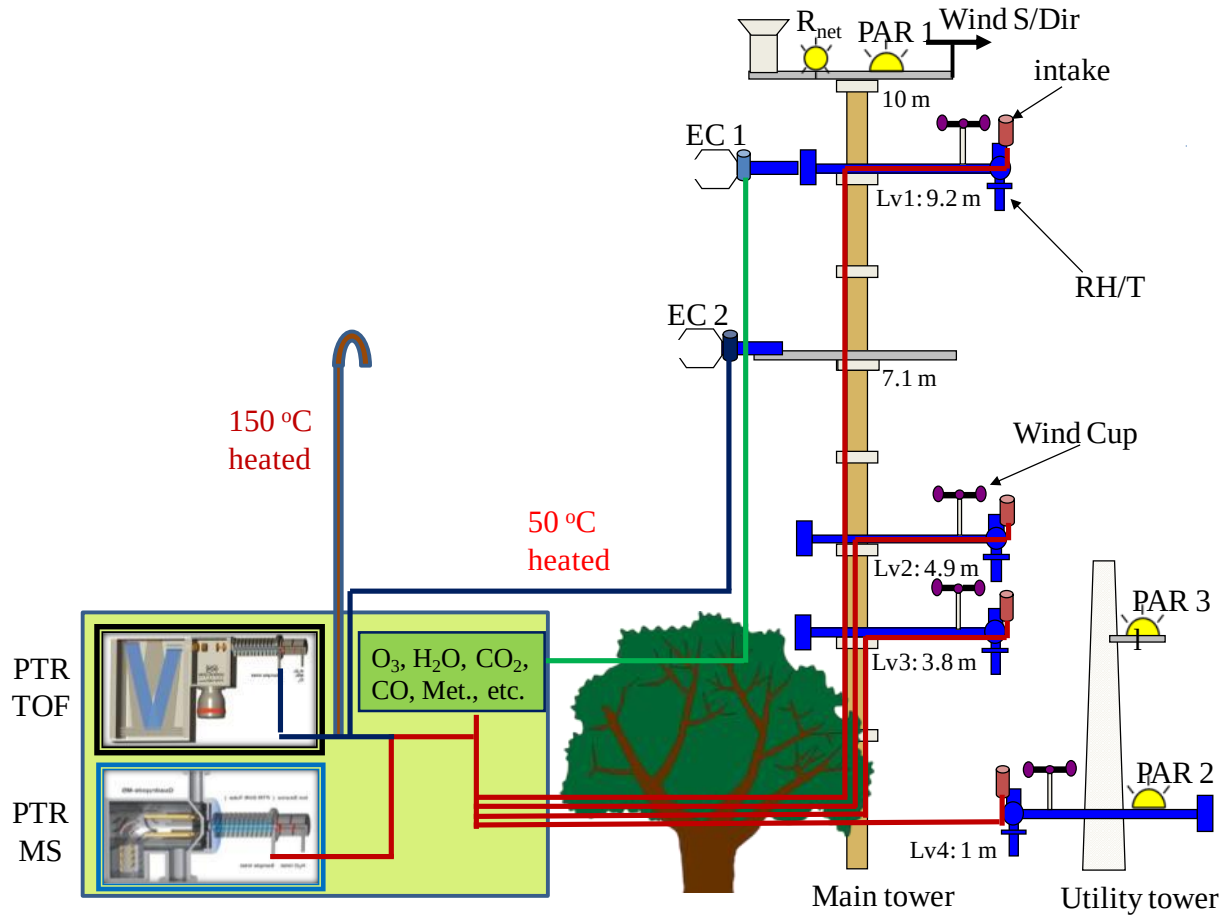

Figure 3. 1. Schematic diagram of PTR-TOF-MS and PTR-MS flux and vertical gradient measurement setup. The inlet at 7.1 m (EC 2) was shared by PTR-TOF-MS and PTR-MS for flux measurements during the first 30 min of each hour. Vertical gradients were measured with the PTR-MS for the second 30 minutes of each hour sequentially at four heights (Lv 1-4) while the PTR-TOF-MS sampled from the 150°C heated inlet located at 7.1m.

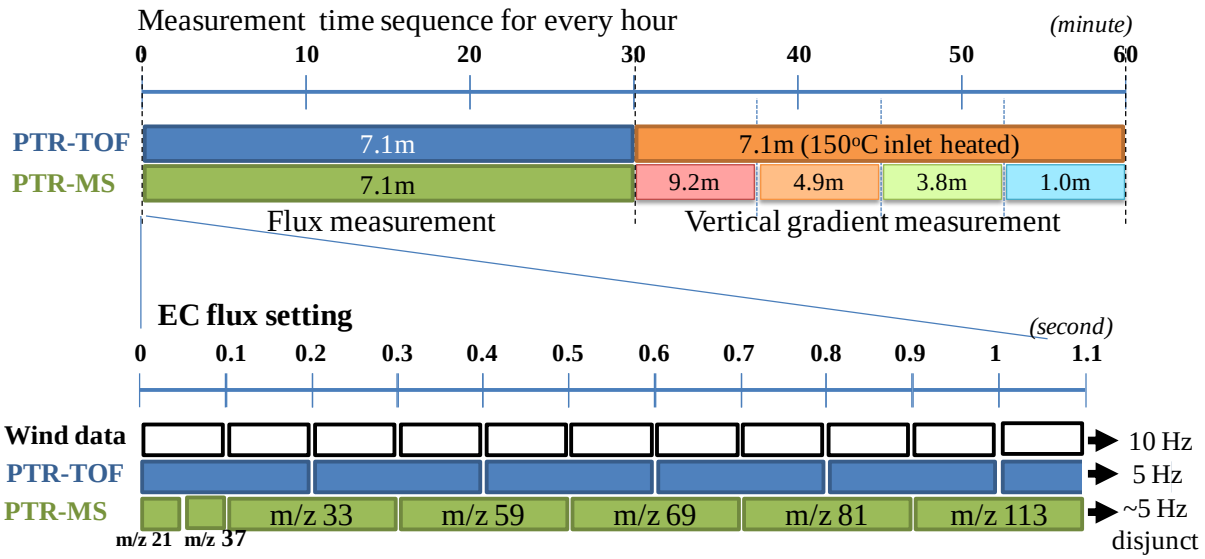

Figure 3. 2. Data acquisition sequence for the PTR-TOF-MS, PTR-MS, and 3-D sonic anemometer. The upper panel shows the hourly measurement scheme. The lower panel describes the data collecting sequence of one cycle corresponding to 1.1 seconds, which was repeated for first 30 minutes of each hour to measure fluxes. Data from the sonic anemometer and PTR-TOF-MS were collected at 10 Hz and 5Hz, respectively. PTR-MS flux data (*m/z* 33, 59, 69, 81 and 113) were sampled with dwell times of 0.2 seconds (overall 5Hz disjunct) after collecting the primary ion signal (*m/z* 21 and 37) for the first 0.1 seconds.

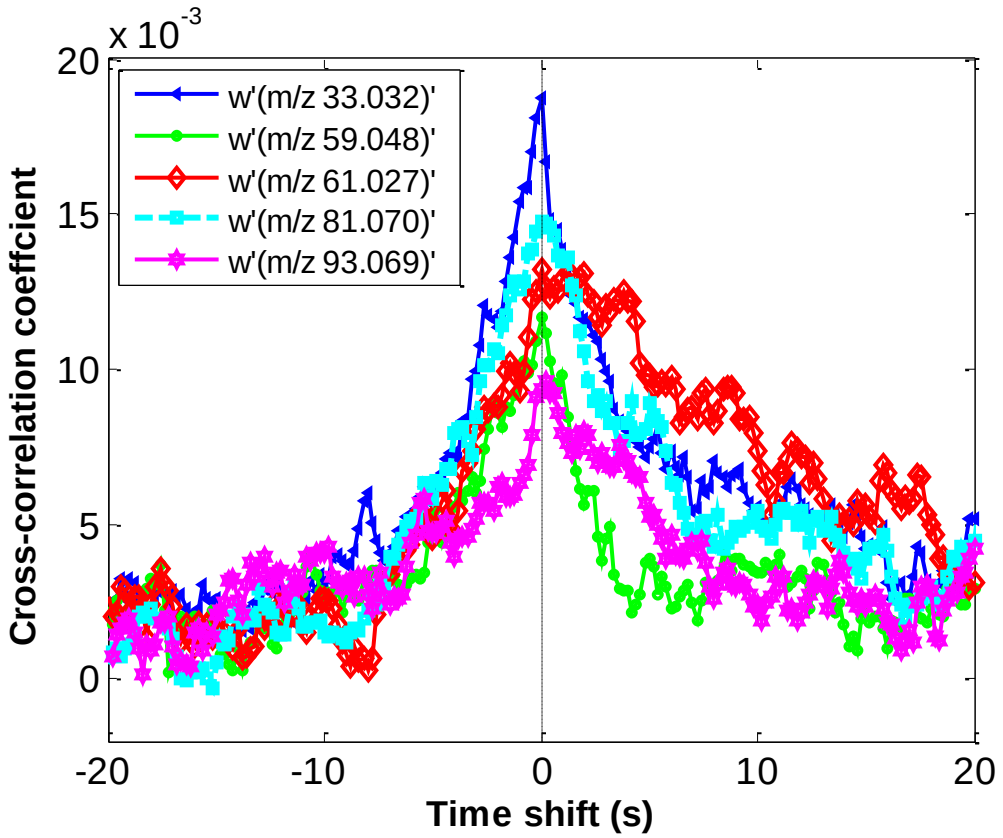

Figure 3. 3. Cross-correlation plots of vertical wind speed and concentration for the five most dominant flux compounds (m/z 33.032, 59.048, 61.027, 81.070 and 93.069) observed by PTR-TOF-MS, averaged over 10:00 – 16:00 PST throughout the whole measurement campaign.

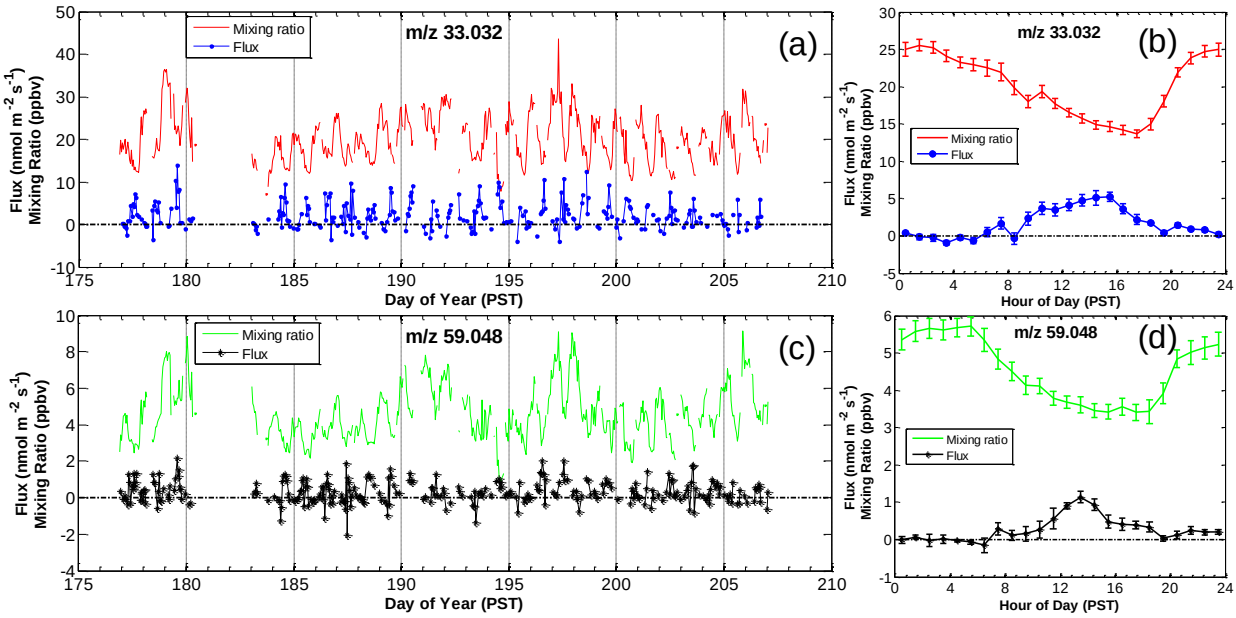

Figure 3. 4. Time series (26 June to 26 July 2012) of mixing ratios and fluxes for (a) *m/z* 33.032(methanol) and (c) *m/z* 59.048 (acetone) from PTR-TOF-MS measurements. Hourly averaged diurnal cycles of mixing ratios and fluxes of *m/z* 33.032 and *m/z* 59.048 are shown in (b) and (d), respectively. Error bars in (b) and (d) denote standard errors of all measurements at the respective hour of the day.

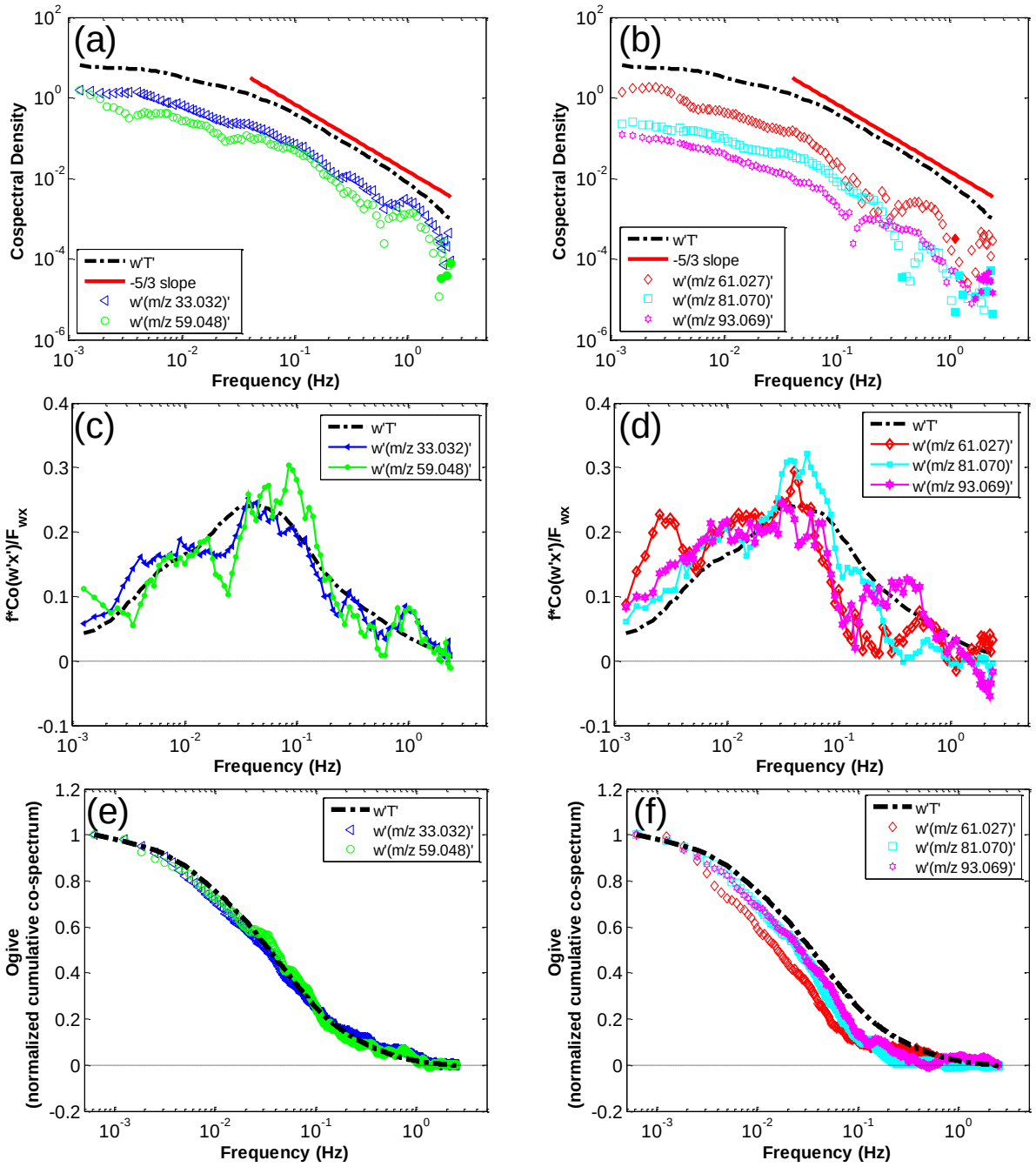

Figure 3. 5. Cospectral density (a, b), frequency weighted covariance normalized cospectra (c, d), and normalized cumulative cospectra or ogive (e, f), of five dominant BVOCs (colored open symbols) and sensible heat (black broken line) binned into 100 evenly spaced intervals along the frequency axis. Each closed symbol in (a) and (b) represents negative values.

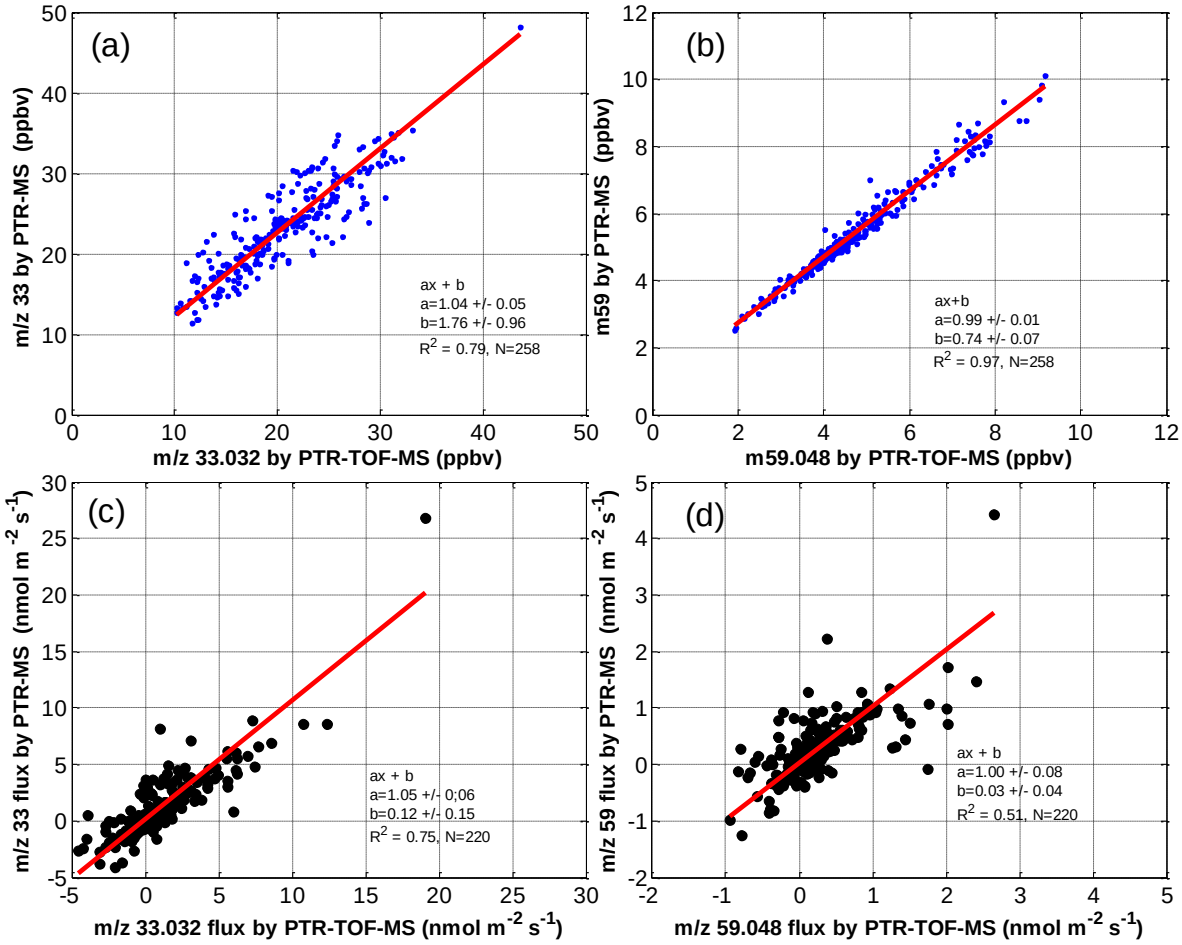

Figure 3. 6. PTR-MS and PTR-TOF-MS mixing ratio (a, b) and flux (c, d) inter-comparison for methanol (a, c) and acetone (b, d). Best fit is shown in red with fitting parameters given in the legends (slope, intercept and R-square).

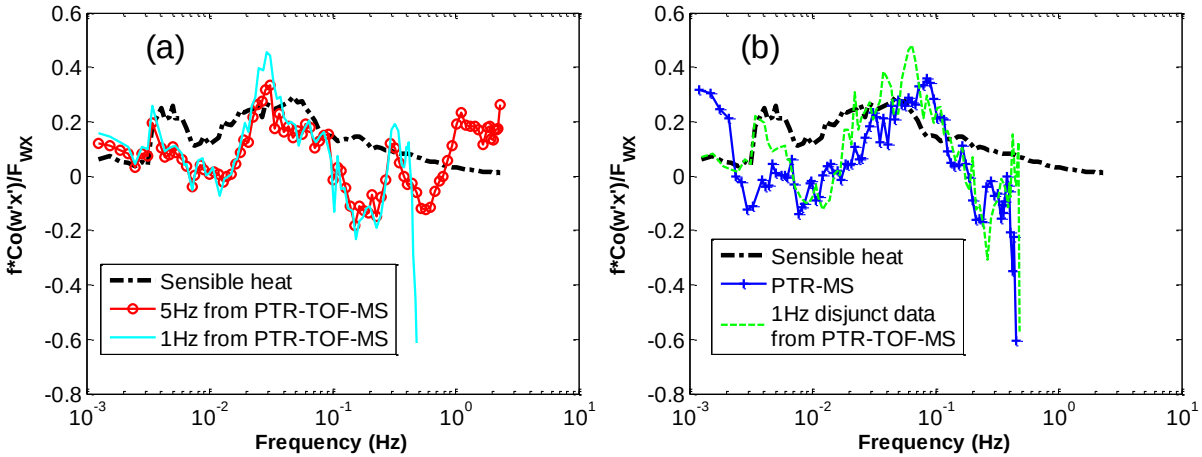

Figure 3. 7. Normalized co-spectra for vertical wind speed with sensible heat (broken black line) and acetone (*m/z* 59.048 for PTR-TOF-MS and *m/z* 59 for PTR-MS) for 14:00 PST on 22nd July, 2010, smoothed by averaging into 100 equally-spaced logarithmic bins. (a) Acetone data are shown for 5 Hz (red line with open circle) and 1 Hz (cyan solid line) for PTR-TOF-MS data. (b) Acetone data are shown for PTR-MS (blue line with plus) and 1Hz disjunct data from PTR-TOF-MS (green dotted line).

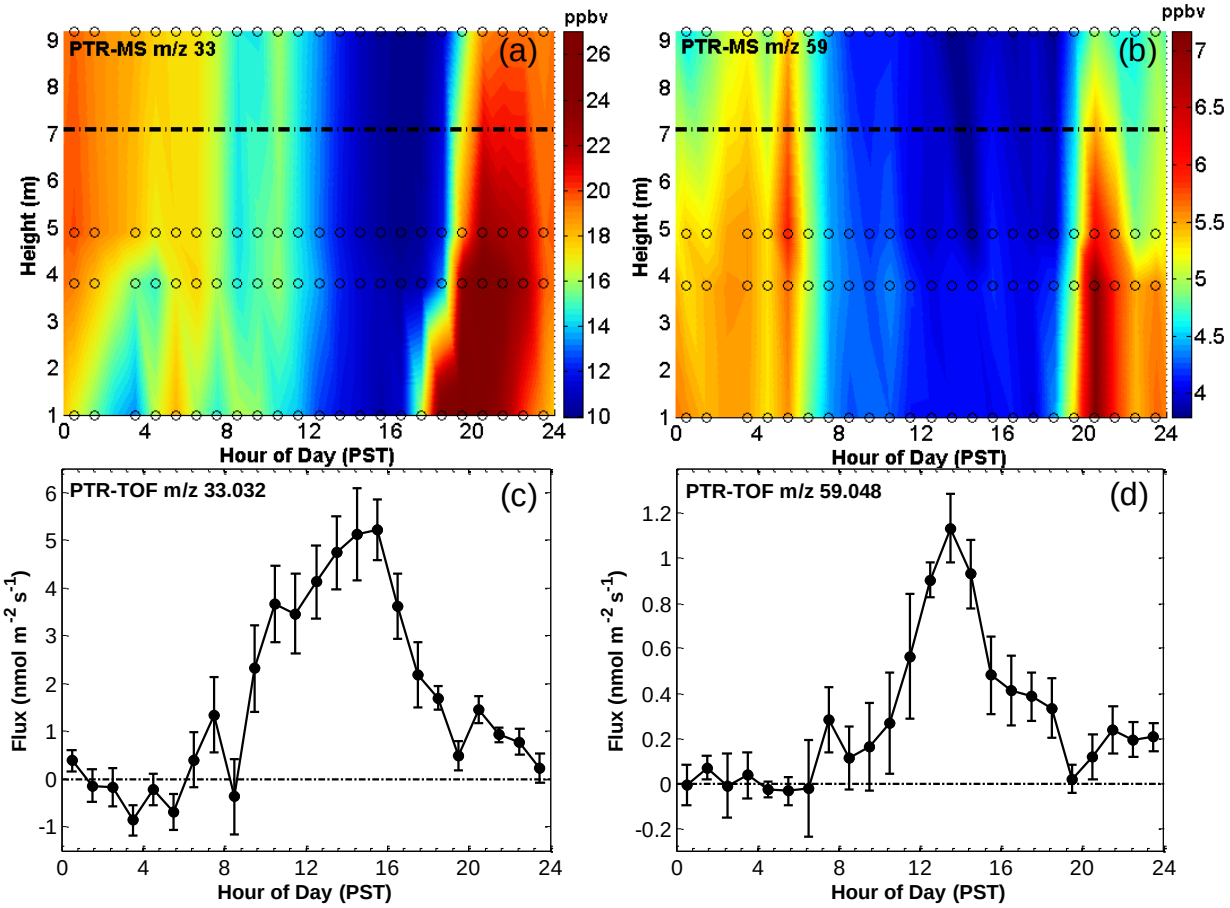

Figure 3. 8. Mean vertical gradient (a and b, PTR-MS) and flux (c and d, PTR-TOF-MS) diurnal patterns of methanol and acetone respectively. Interpolated gradient measurements (a and b) are color coded with actual measurement timing and vertical positions shown as open circles, and flux measurement height shown as a broken black line. Flux diurnal patterns of methanol and acetone shown in (c) and (d) agree well with observed vertical gradients during day and night. Error bars in (c) and (d) denote the standard errors of all measurements at the respective hour of the day.

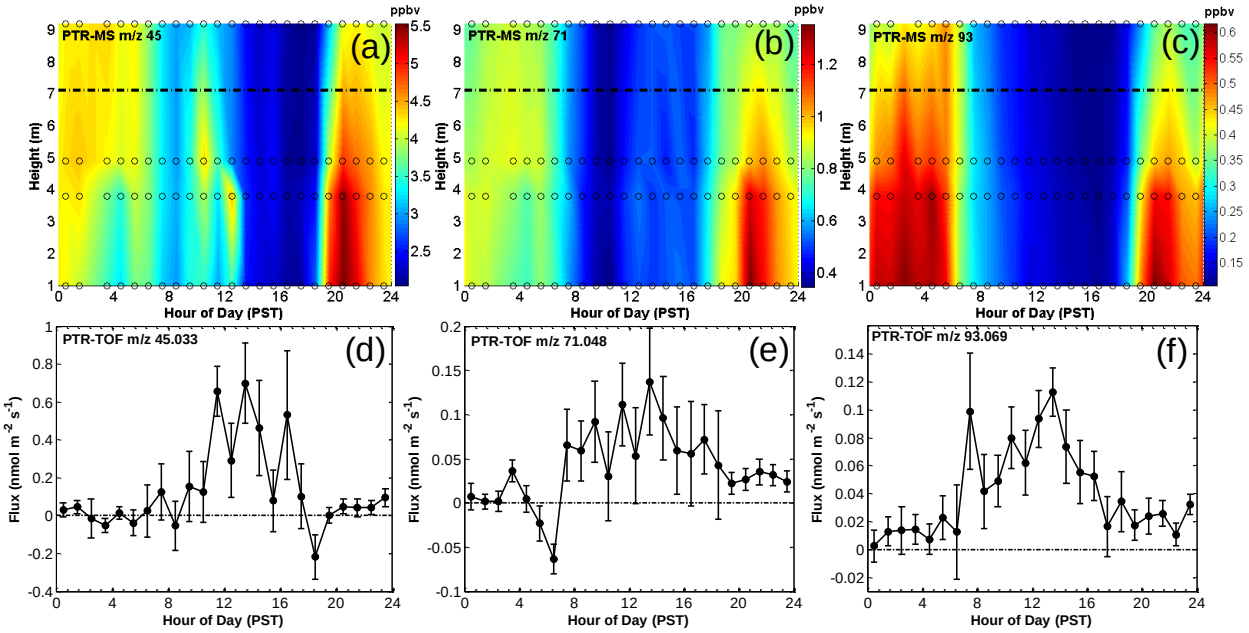

Figure 3. 9. Mean vertical gradient (a, b, and c, PTR-MS) and mean flux (d, e, and f, PTR-TOF-MS) diurnal patterns of acetaldehyde, MVK+MACR and para-cymene+toluene respectively. Symbols, color coding and error bars as in figure 3.8.

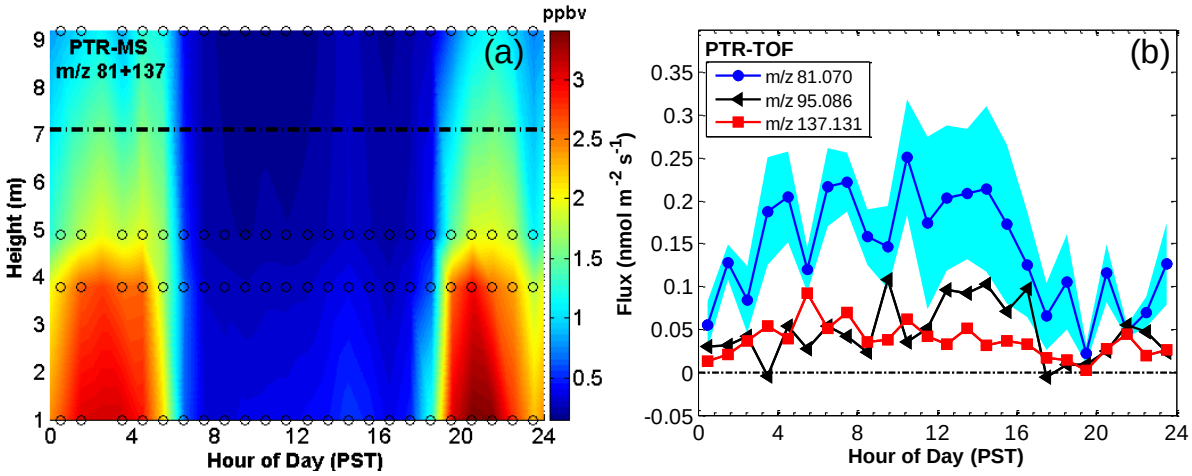

Figure 3. 10. (a) Monoterpenes vertical gradient from PTR-MS as a sum of *m/z* 81 and 137, and (b) flux of individual *m/z* of 81.070 (in blue circle), 95.086 (in black triangle) and 137.131 (in red square) from PTR-TOF-MS with standard errors of *m/z* 81.070 (shaded as cyan). Gradient pattern and flux both show emission throughout the day and *m/z* 81.070 (main fragment of monoterpenes) shows the largest flux among the 3 ions.

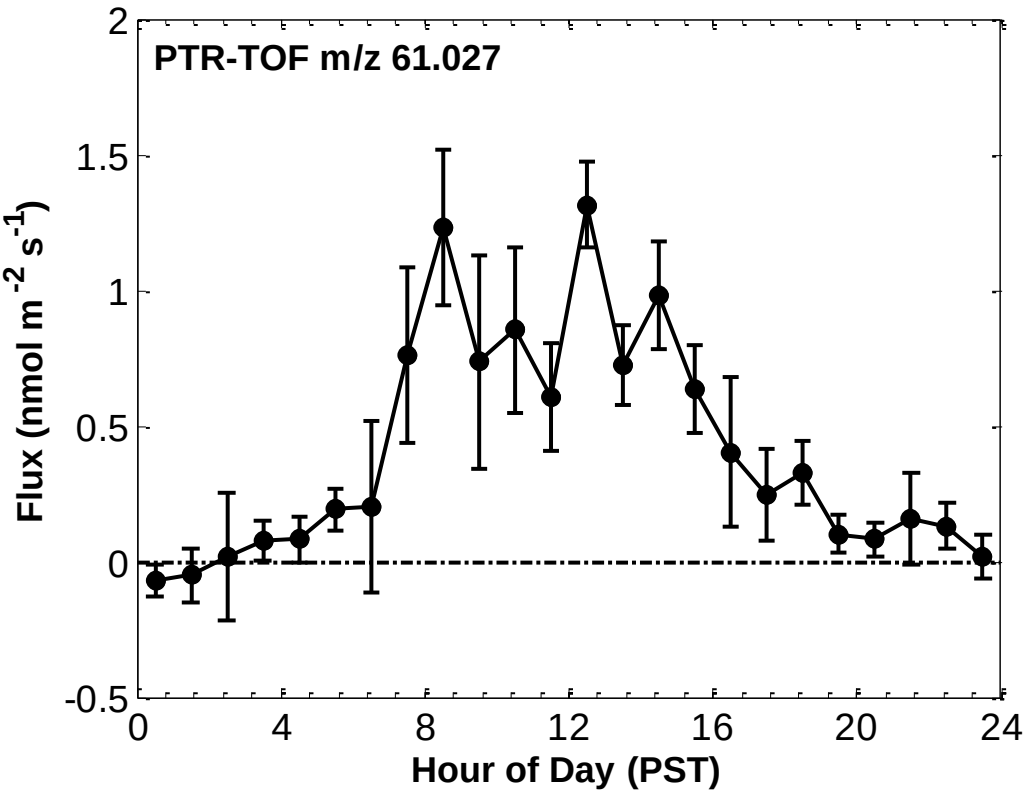

Figure 3. 11. Diurnal variation of *m/z* 61.027 (acetic acid) fluxes with standard errors.

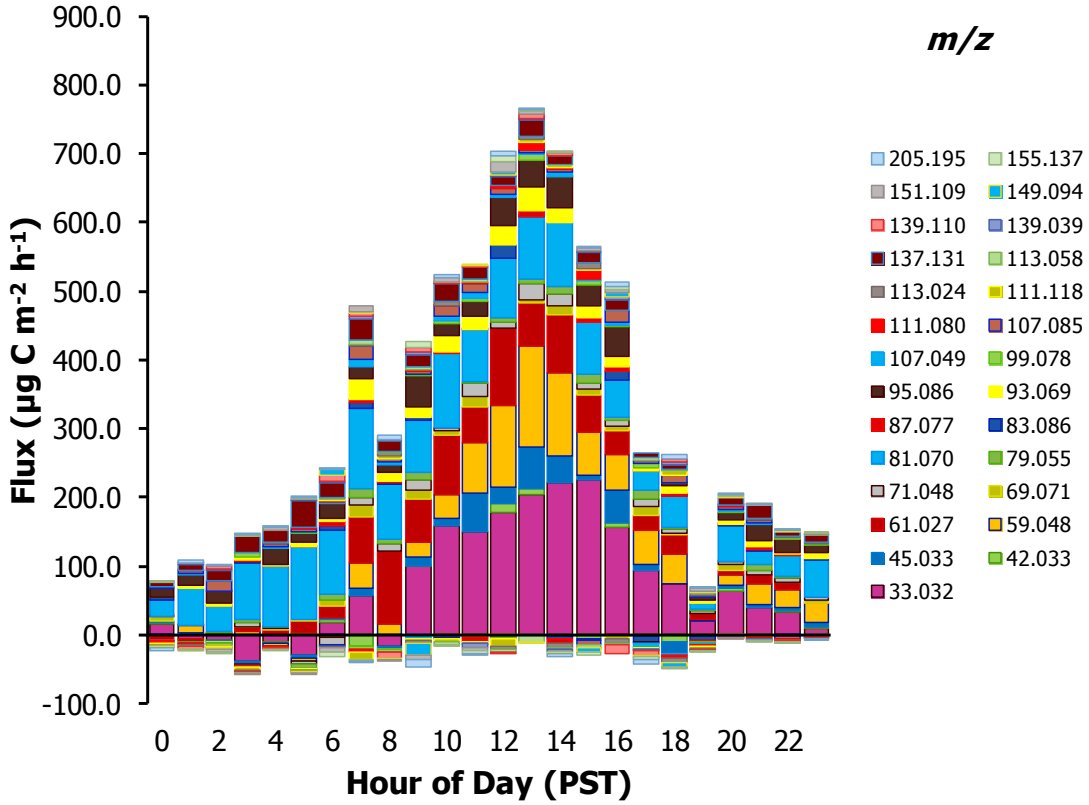

Figure 3. 12. Total and fractional BVOC diurnal flux measured by PTR-TOF-MS on a carbon mass basis. Staged bar plots of 27 masses with the largest fluxes are shown throughout the day with *m/z* indicated in the legend.

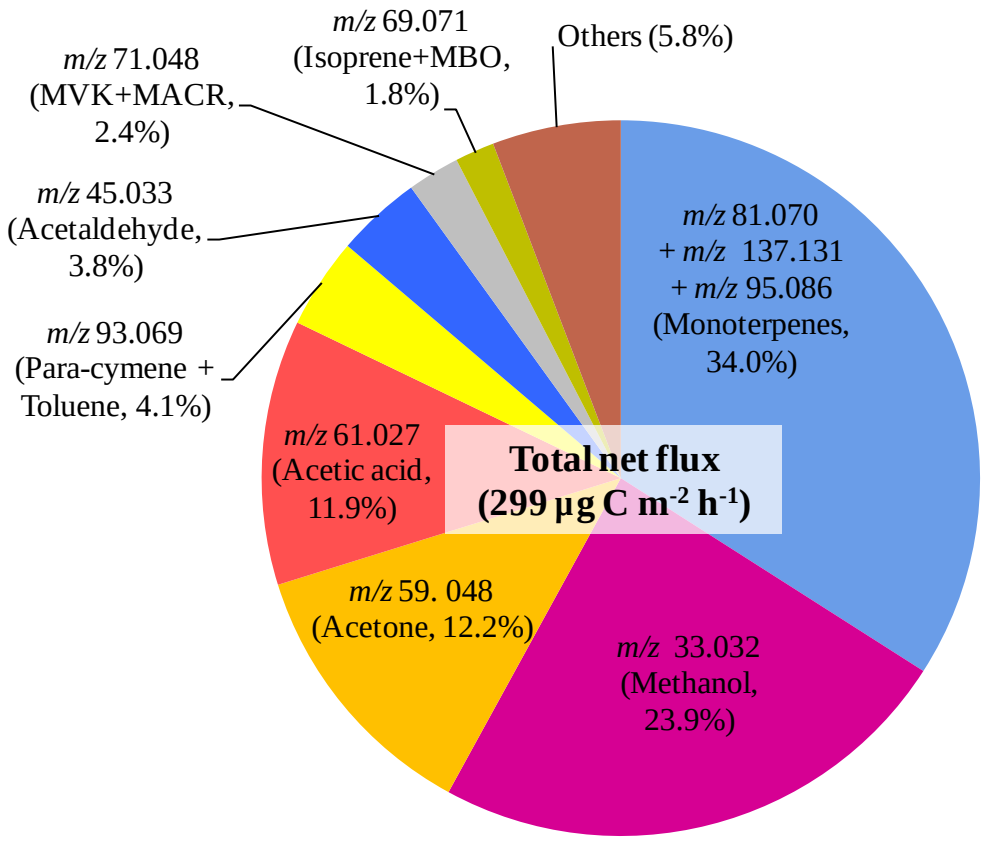

Figure 3. 13. Fractional contribution to the total flux for 27 ion species selected.

Chapter 4: Observational Evidence for active atmosphere-biosphere exchange of the vast majority of VOCs

Abstract

Numerous volatile organic compounds (VOC) and their oxidation products (OVOC) exist in Earth's atmosphere, and biogenic VOC (BVOC) emissions contribute up to 90% of the total global source. In spite of their critical role in tropospheric chemistry in terms of ozone production and secondary organic aerosol (SOA) formation, studies for evaluating their exchanges (emission/deposition) between the atmosphere and ecosystem have been mostly limited to only a few dominant species such as isoprene and monoterpenes due to lack of appropriate measurement techniques. Here, we report direct measurements of the full range of VOCs with molecular weight between 10 and 1278 using a PTR-TOF-MS coupled to the eddy covariance method to determine ecosystem scale exchange, and demonstrate at least 494 VOC species have bi-directional flux. Moreover, we found that at least 186 different compounds are significantly deposited to the ecosystem. This first observational evidence for active ecosystem scale exchange of the vast majority of VOC provides a major challenge to current BVOC emission models and possibly regional air quality and global climate models, which do not account for contributions from this extremely large range of species observed.

4.1. Introduction

On the global scale, up to 90% of Earth's volatile organic compounds (VOC) are emitted from biogenic sources and mostly from vegetation, so called BVOC (Guenther et al., 1995).VOC play a critical role in tropospheric chemistry, associated with ozone production and secondary organic aerosol (SOA) formation which affects human health, regional air quality, and global climate (Chameides et al., 1988; Andreae and Crutzen, 1997; Jang et al., 2002). Once BVOCs are emitted from plants to the atmosphere, they start being oxidized until they form carbon dioxide (CO_2) mainly through carbon monoxide (CO), are deposited, or transform into SOA. Consequently, numerous species of VOCs and their oxidation products (OVOC) must exist in the gas phase in the atmosphere (Goldstein and Galbally, 2007). A few studies have shown the existence of very reactive and/or unexplored VOCs in the air in and above forest canopies that are responsible for O3 chemical loss and missing OH reactivity (Kurpius and Goldstein, 2003; Di Carlo et al., 2004; Holzinger et al.,2005). Intuitively, it seems reasonable that these newly produced or unknown VOCs in the air should be actively exchanged between the atmosphere and ecosystem. For example, one should expect all of the water soluble species to deposit at rates proportional to the Henry's Law coefficients. Previous BVOC flux field observations have mainly been focused on a few dominant BVOCs such as methanol, isoprene, and terpenes, and the number of compounds which could be measured at nearly maximum capability by current technique (e.g. PTRMS) was generally limited to at most 17 species (Ruuskanen et al., 2011). Understanding of VOC deposition is still particularly uncertain due to a lack of direct flux measurement, but this loss process may actually dominate the removal of VOC from the atmosphere (Hallquist et al., 2009; Goldstein and Galbally, 2007). One study has recently reported measurable ecosystem-scale deposition of a few OVOCs, either formed from VOC oxidation in the atmosphere or directly emitted from the ecosystem, in deciduous forest (Karl et al., 2010).

In this chapter, we present observational evidence of active exchange for the vast majority of VOCs, which is a very novel and challenging finding.

4.2. Experiment

4.2.1 Field site and instrument

An intensive VOC flux measurement field campaign took place in an orange grove in California's Central valley during summer 2010 (24 June to 26 July) as part of a one-year continuous field campaign (Oct. 2009 – Nov. 2010). Details of the site location, environmental conditions, and experimental setup have been described in Chapter 3, Fares et al. (2012 a and b), and Park et al. (2012). Briefly, to measure ambient concentrations of volatile organic compounds (VOC) and their ecosystem-scale fluxes, we deployed a proton transfer reaction-time of flight-mass spectrometer (PTR-TOF-MS) and a quadrupole PTR-MS along with a three-dimension sonic anemometer. Both PTR instruments use hydronium ions (or protonated water, H_3O^+) to chemically ionize the compounds of interest through a proton transfer reaction, thus two PTR

systems detect any compound that has higher proton affinity than that of water. Detailed description of the instrument and measurement principles has been published elsewhere (for PTR-TOF-MS: Jordan et al., 2009; Graus et al., 2010, for PTR-MS: Lindinger et al., 1998; de Gouw and Warneke., 2007).

Through an inter-comparison study between two PTR instruments in addition to spectral analysis from PTR-TOF-MS flux data as described in Chapter 3, we concluded that PTR-TOF-MS is a powerful new tool for quantifying ecosystem fluxes for a wide range of VOCs (Park et al., 2012). As an example, figure 4.5 shows good agreement of the vertical gradients measured by PTR-MS and eddy covariance (EC) flux by PTR-TOF-MS for the sum of methyl-vinyl-ketone and methacrolein (MVK+MACR), but PTR-MS was not able to measure eddy covariance flux of MVK+MACR due to an instrumental limitation which allows observation of only a small number of compounds with fast enough time resolution for flux measurements (4 or 5 compounds in 1 second).

For PTR-TOF-MS eddy covariance flux measurements, we collected VOC concentration data at 5Hz and identified at least 664 significant signals for VOCs following the procedure described by Holzinger et al, (2010) with mass to charge ratios (*m/z*) between 10 and 1278 (resolving power ~5000 m/Δm). Most VOCs observed showed lower concentration during daytime than nighttime indicating these compounds accumulated at night in a shallow atmospheric boundary layer (Table 4.1). We determined the fluxes for 555 species excluding those masses due to the instrument's primary ions and impurities and found the vast majority of VOCs had bi-directional exchange, such that their net flux was due to a combination of emission and deposition.

4.2.2 Determination of ion species exchanging between the ecosystem and atmosphere

A total of 664 significant mass peaks were identified by IDL (Interactive Data Language) routines according to Holzinger et al. (2010). These included major primary ions (e.g. $(H_2O)H^+$, $(H_2O)_2H^+$, $(H_2O)_3H^+$), their isotopes (e.g. $H_2{}^{18}OH^+$, $H_2{}^{16}O{\cdot}H_2{}^{18}OH^+$), impurities such as $O_2{}^+$, NO^+, N_2H^+, and ammonium ions (e.g. $NH_3{}^+$, $NH_3NH_3H^+$). After excluding all above mentioned peaks, we applied the flux calculation routines described in Chapter 3 to the remaining 555 peaks above m/z 31 (this includes protonated formaldehyde). In the following we outline the method applied to determine whether species represented by these mass peaks were exchanged between the atmosphere and the ecosystem. This is a non-trivial analysis especially for species with bi-directional or small fluxes.

As a first step, we investigated co-variances of vertical wind speed with lag time corrected VOC data using the following procedure: (i) within the limits of ± 30 seconds, we shifted the wind data in steps of 0.2 s, basically in the same manner as a standard lag time correction for the eddy covariance method; (ii) we calculated the absolute value of the covariance between VOC data and time-shifted wind data; (iii) we averaged the absolute values of the covariance for all 30 min flux periods (n ≈ 150) between 10:00 and 16:00 PST. An example of this treatment for *m/z*

127.073 ($C_7H_{10}O_2H^+$) is shown in figure 4.1b, whereas figure 4.1a shows the results of averaging the covariance (NOT the absolute value of the covariance) of VOC with time shifted wind data for exactly the same set of measurements. Figure 4.1a indicates that the net flux (the co-variance at 0 second) for the one month period is very small. The value of ~ 0.005 nmol m^{-2} s^{-1} represents an upward flux (emission) but the signal is clearly within the noise level. From figure 4.1a, it is hard to argue that there is an ecosystem flux at all, because the covariance at a time shift of 0 seconds does not emerge above the noise level, a good proxy of which is the variability observed between -30 and -20 or 20 and 30 second time shifts, respectively, in figure 4.1a. In contrast, the sharp peak at 0 seconds in Figure 4.1b (absolute value covariance) implies that there is an exchange with an average magnitude of 0.054 nmol m^{-2} s^{-1}. Note that information about whether the flux is up or down is lost in this representation. If we determine the noise level between -30 and -20 sec (0.042 ± 0.002 nmol m^{-2} s^{-1}, mean ± standard deviation), the peak at 0 seconds exceeds 6 times the standard deviation of the noise. However, we used the noise time window from two 20 second periods from -180 s to -160 s and from 160 s to 180s for all ion species analyzed, because the covariance should become uncorrelated as the time shift becomes larger than the duration of the eddies that drive the transport. By this definition, which is similar to the signal to noise ratio (S/N), the absolute value co-variance peak exceeded 4 times the standard deviation of the noise; thus S/N=4 (Fig. 4.1c and Table 4.1). From figure 4.1 we conclude that the species detected at m/z 127.073 is both emitted and taken up by the ecosystem, though the net exchange is close to zero during daytime for the one month period of measurements.

In order to confirm whether there is real ecosystem exchange for the compounds which have bi-directional and low fluxes, we first examined the time shifted absolute value co-variances of lag time corrected vertical wind speed with concentration data of each compound as described above. Most compounds showed a sharp maximum co-variance peak at 0 seconds, indicating either upward or downward fluxes (Fig. 4.1, a typical example). As a second step we quantified the significance of the co-variance between time-shifted vertical wind speed and VOC mixing ratio which should become uncorrelated as the time shift becomes larger than the duration of the eddies that drive the transport. Therefore, for such long time-shifts, the computed covariance between the two is a measure of the noise level and can be used to determine the significance of a measured flux. We determined that an ion species has a meaningful flux if the average daytime absolute value of the co-variance at 0 second (Fig. 4.1) exceeds 3 times the standard deviation of two 20 second time windows from -180 s to -160 s and from 160 s to 180s plus the average of the two time windows. This definition is similar to a signal to noise ratio of 3 (hereafter S/N=3). Of the 555 species analyzed, 494 ion species (~ 89 %) passed this criterion. The number of ion species with flux above a signal to noise ratio from 3 to 10 is shown in Fig. 4.2 (numbers of species indicated above bar).

To examine a 24h-mean net flux, we i) took the mean flux for each species in every one hour time bin, ii) plotted diurnal trend (e.g. MVK+MACR in figure 4.5b), and then iii) took average for 24h data as a 24h-mean net flux of each species. For estimating a 24h-mean gross emission (/deposition), we had the first 2 steps the same manner as above, added up only emissions (/deposition) from diurnal trend, and then divided by 24. For example in figure 4.5b, there are only 2 points of depositions in diurnal trend, so a 24h-mean gross deposition for MVK+MACR was determined by (sum of those 2 deposition fluxes)/24.

4.3. Results and Discussion

4.3.1 Fluxes of 494 chemical species

On a molar basis, the net flux (Fig. 4.2, green bar) of 494 ion species contributed 97% of the total net flux of 4.43 nmol m^{-2} s^{-1} for all 555 ion species observed, indicating mass fluxes for the ion species below S/N=3 are minor contributions to the total. We found that the gross deposition for species above S/N=3 is surprisingly substantial, with a total magnitude of -3.24 nmol m^{-2} s^{-1} counteracting 42 % of the gross emission of species above S/N=3, and exceeding the gross emission of 3.03 nmol m^{-2} s^{-1} above S/N=8 which includes the 10 dominant BVOCs fluxes measured. This result strongly supports the idea that many unexplored VOCs exist in the atmosphere and they are actively exchanged at the atmosphere-biosphere interface, thus their presence and oxidation products may be significant for regional photochemistry and SOA formation (Goldstein and Galbally, 2007; Hallquist et al.,2009).

Most reported BVOC flux field observations tend to measure the dominant VOCs which are included in our top 10 major species exceeding S/N=8. These dominant species were almost exclusively emissions throughout the day except for small depositions of a few compounds in the early morning and evening (Fig. 4.3a). On a molar basis, the 24h-mean total net flux of these 10 major species contributed 63% to the total of all 555 observed compounds (Figs. 4.2 and 4.3a). Methanol fluxes were the largest (37%), followed by acetic acid (9.3%, *m/z* 33.032), acetone (6.3%, *m/z* 59.048), monoterpenes (MTs; 5.3%, sum of *m/z* 81.07, 95.086, 137.131), acetaldehyde (3.0%, *m/z* 45.033), para-cymene (1.0%, *m/z* 93.069), methyl-vinyl-ketone+methacrolein (MVK+MACR; 0.9 %, *m/z* 71.048), and isoprene+methyl-butenol (ISOP+MBO; 0.6 %, *m/z* 69.027). For the additional 484 distinct masses above S/N=3 (but below S/N=8) exchanging with the ecosystem, we classified them into 4 groups by selecting the mass to charge ratio ranges of 31-69 (n=61), 69-136 (n=141), 136-237 (n=141), and 237-1278 (n=141), hereafter called as M31-69, M69-136, M136-237, and M237-1278, respectively. For grouping these, we simply assumed that M31-69, M69-136, M136-237, and M237-1278 have at least 2, 5, 10, and 15 carbons, respectively, and chose the mass ranges such that the same number of species was included in each group above *m/z* 69. The mass to charge ratio of 237 has been previously observed in the gas phase by PTR-MS as a β-caryophyllene oxidation product (Lee et al., 2006). In addition, many compounds observed as concentrations and fluxes in the range M237-1278 are expected to be highly uncertain since those species are less volatile (low vapor pressure), sticky and not calibrated by standard gases, and are currently not well understood. Thus, further research in this m/z range is recommended.

All 484 of these species were observed to have fluxes that were bi-directional throughout the day (Fig 4.3b). Both emission and deposition fluxes were maxima during daytime in contrast to the concentration diurnal trend which was generally lower during day and higher at night due to buildup in the shallow nighttime boundary layer. Although their 24h-mean total net flux was an emission (1.61 nmol m^{-2} s^{-1}) and smaller than the total net emission of 10 major species (2.82 nmol m^{-2} s^{-1}) described above, their 24h-mean total gross emission was ~1.6 times larger than that of 10 major species. Their 24h-mean total gross deposition is almost similar magnitude of

emission of 10 major species (Fig 4.3b and Table 2), indicating significant depositions. Surprisingly, a 24h-mean net deposition occurred for at least 186 masses, but no single species accounted for more than 1.6 % of the total observed deposition on a molar basis. We did not find any compounds uniformly deposited throughout the day. More net depositing species were observed in the higher *m/z* group; 18, 40, 57, and 71 species for M31-69, M69-136, M136-237, and M237-1278, respectively (Fig 4.4 and Table 4.2), suggesting heavier molecules deposit more efficiently. For these 186 species observed to have net deposition, the exchange velocity (or deposition velocity) was evaluated according to V_{ex}= (flux) / (ambient concentration). To examine V_{ex} diurnal trends for these masses and each group, we took the median V_{ex} for each depositing species in every one hour time bin, plotted diurnal trends for each species, and then took the average for every hour from all depositing species in each group. For example, every one hour data bin includes 18 median V_{ex} data from 18 species deposited for M31-69 (Fig. 4.4a). Based on this analysis, a 24h-mean V_{ex} in M136-237 (-0.41 cm s^{-1}) was the fastest and the maximum hourly average V_{ex} was between -1 and -1.5 cm s^{-1} for all groups. During daytime two V_{ex} maxima commonly appeared, first in the morning hours 09:00 – 12:00 PST and second in the afternoon hours 14:00 – 17:00 PST. Interestingly, however, low V_{ex} in hours 12:00 – 15:00 were observed for all groups (Fig. 4.4). This implies that direct emission from the ecosystem and/or within-canopy (or below measurement height) photochemical production depresses the net deposition when both temperature and sun light intensity are maximum, presumably causing direct BVOC emission from plants along with active photochemistry. Recently, Karl et al.,(2010) reported significant deposition of MVK+MACR and a few other OVOCs including acetaldehyde above deciduous forests, but those only accounted for a small fraction of what we observed as deposition. In contrast to Karl et al's results, we observed MVK+MACR to have a net emission with bi-directional flux; clear emission during daytime with small deposition in the early morning (yellow bars in Figs. 4.3a and c), in excellent agreement with vertical gradient observations performed simultaneously at the site using a separate instrument (Fig. 4.5). The exchange velocity range we observed for the 186 depositing species (Fig. 4.4) was generally lower or at the low end of the values reported above deciduous forests (Karl et al., 2010). This contrasting result implies that the emission and deposition characteristics in a broader array of systems should be further studied to better understand the atmosphere-biosphere exchange in various ecosystems.

4.3.2 Fluxes on a carbon mass basis

In contrast to our molar basis analysis above, when considering carbon mass flux the heavier compounds observed are generally more important. For example, of the 10 major species (Fig 4.3a and c) observed, monoterpene emission is the largest on a mass basis rather than methanol emission (the largest on a molar basis) because it has ten times the number of carbon atoms per molecule. We estimated carbon mass fluxes for each group (Fig 4.3d) using the expected carbon numbers assumed above. A 24h-mean total gross carbon emission of 484 species (842 µg C m^{-2} h^{-1}) is at least 2.8 times larger than that of 10 major species (294 µg C m^{-2} h^{-1}), and a 24h-mean total gross carbon deposition is also 2 times larger (Fig 4.3c and d). The carbon mass flux of 484 species is more substantial than on a molar basis. This estimate is conservative and likely is an

underestimation because more carbons may be expected in each class than the carbon numbers we assumed, and some fragments from parent ions also would make the carbon number larger than we used in the calculation. Therefore, we consider this magnitude of carbon fluxes to be a minimum estimate. The 24h-mean gross emission of the M31-69 group was the largest and gross emissions decreased as the *m/z* group number increased. The deposition was almost equivalent among 3 groups except for M69-136 (Fig 4.3d and Table 4.2), indicating deposition in the higher *m/z* range is more significant than at lower *m/z*.

4.3.3 Fluxes for 162 identified molecular formulas classified as hydrocarbons and oxidized hydrocarbons.

We identified the chemical formulas for 162 observed hydrocarbons and oxidized hydrocarbons (Table 4.1). To do this, three different criteria were applied; i) absolute maximum covariance peak exceeding S/N=3 criterion, ii) does not include ion species above *m/z* 237 (highly uncertain concentration estimation because they tend to be low vapor pressure, sticky and not calibrated by standard gases, and currently not well understood), iii) can be identified as an exact molecular formula (ion mass range within ± 3 mDa) with a combination of carbon (C), hydrogen (H), and oxygen (O) atoms using the database created by Holzinger et al. (2010) which comprises ~18,000 molecular formulas. These three criteria were satisfied for 494, 353, and 162 ions, respectively. For criteria iii), we found a few peaks overlapped with possible empirical formulas including organic nitrogen and sulfur compounds. For example, three empirical formulas could be matched at *m/z* 175.037 within an ion mass range of ± 3 mDa, i.e. $C_{10}H_6O_3H^+$ (175.039 Da), $C_5H_6N_2O_5H^+$ (175.036 Da), and $C_6H_{10}N_2S_2H^+$ (175.035 Da). However, we assumed those masses were completely hydrocarbons or oxidized hydrocarbons, thus $C_{10}H_6O_3H^+$ was considered as the match for m/z 175.037 from the example above. A total of 30 mass peaks out of 162 had similar overlaps, thus 28 mass peaks were overlapped with 2 compounds and the other 2 mass peaks with 3 compounds (Table 4.1).

Diurnal trends of total VOC (162 identified ion species) fluxes are shown for the whole measurement period (Fig. 4.6) with all compounds that were not specifically identified summarized in groups of pure hydrocarbons (C_xH_y) and oxygenated VOCs (OVOCs) containing one, two, and three or more oxygen atoms (i.e. C_xH_yO, $C_xH_yO_2$, and $C_xH_yO_{3+}$). The fluxes shown are expressed in mass C units: µg C m^{-2} h^{-1}. The carbon numbers were inferred from the ion species detected by PTR-TOF-MS, but 10 carbons were assumed for *m/z* 81.070 and *m/z* 95.086 because these masses are known to mainly be due to fragmentation of monoterpenes ($C_{10}H_{16}H^+$). For example, para-cymene has ten carbons if monitored unfragmented ion at *m/z* 135.116 ($C_{10}H_{14}H^+$), and in this case the correct carbon number was definitely assigned. However the main fragment detected at *m/z* 93.069 ($C_7H_8H^+$) has only 7 carbons and in this case the carbon mass flux of this ion species was calculated assuming only 7 carbons. Therefore, total carbon fluxes may be underestimated because we did not consider neutral (undetected) fragments.

Considering all 162 compounds as completely pure hydrocarbons or oxygenated hydrocarbons, the 24-h average total net flux for these 162 species contributed 77% to the total

of the 555 species identified on a molar basis. Using the expected molecular formula from 152 VOCs identified (excluding the 10 major species), we calculated carbon mass fluxes and summarized them in groups of pure hydrocarbons (C_xH_y) and OVOCs containing one, two, and three or more oxygen atoms (i.e. C_xH_yO, $C_xH_yO_2$, $C_xH_yO_{3+}$). By adding up all contributions to the total net flux over a day, a 24-h mean net emission flux of 426 µg C m^{-2} h^{-1} was estimated during the campaign, and the total net flux of 152 species accounted for about one third of the total observed flux (Fig. 4.7, left pie). Pure hydrocarbons (C_xH_y; n=40) comprised 15 % of the total carbon flux of these 162 species, and compounds containing one to three or more oxygen (C_xH_yO; n=30, $C_xH_yO_2$; n=44; and $C_xH_yO_{3+}$; n=38) contributed 12.7, 3.2, and 1.8 %, respectively. Although the total flux of these 152 species was a net emission of 139 µg C m^{-2} h^{-1}, it is intriguing to look at the contributions of oxygenated hydrocarbons and pure hydrocarbons to emissions and depositions separately. For gross emission in each category, total OVOC (at least one oxygen containing compounds) emissions dominated, but pure hydrocarbon (C_xH_y) emission was individually the largest, followed by C_xH_yO, $C_xH_yO_2$, and $C_xH_yO_{3+}$, indicating the vast unknown VOCs either photochemically produced below the measurement height or directly emitted from the ecosystem are extremely significant (Fig. 4.7, right upper pie). Moreover, we also found more substantial deposition fluxes for oxygenated hydrocarbons (71%) than pure hydrocarbons (29%), and $C_xH_yO_2$ deposition exceeded C_xH_y (Fig. 4.7, right lower pie). This result suggest that on average the parent or less oxygenated VOCs either emitted/produced from the ecosystem or advected from upwind sources are photochemically oxidized above the region and then removed by dry deposition of secondary compounds containing oxygen.

4.4. Summary

To our knowledge, we made the first direct measurements showing that a broad range of VOCs are significantly deposited from the atmosphere to an ecosystem and this deposition is dominated by OVOCs. In addition, less than half the total gross emission from this ecosystem is represented by the 10 main BVOCs observed. Furthermore, the vast majority of emitted and deposited species are generally not measured by current techniques (e.g. PTR-MS or Gas Chromatography system). These findings demonstrate the importance of using a comprehensive approach to understanding ecosystem-scale VOC exchanges. Moreover, the lower flux and concentration species are not in current BVOC emission models, but their size, chemical formulae, and sum, suggest they should be important for SOA formation and O_3 chemistry, and their presence in the atmosphere may also account for a significant amount of the missing OH chemical reactivity and O_3 chemical loss observed in forest environments.

4.5. References

Andreae, M. O., and Crutzen, P. J.: Atmospheric aerosols: Biogeochemical sources and role in atmospheric chemistry, Science, 276, 1052-1058, 1997.

Chameides, W. L., Lindsay, R. W., Richardson, J., and Kiang, C. S.: The Role of Biogenic Hydrocarbons in Urban Photochemical Smog - Atlanta as a Case-Study, Science, 241, 1473-1475, 1988.

de Gouw, J., and Warneke, C.: Measurements of volatile organic compounds in the earth's atmosphere using proton-transfer-reaction mass spectrometry, Mass Spectrom Rev, 26, 223-257, doi:10.1002/Mas.20119, 2007.

Di Carlo, P., Brune, W. H., Martinez, M., Harder, H., Lesher, R., Ren, X. R., Thornberry, T., Carroll, M. A., Young, V., Shepson, P. B., Riemer, D., Apel, E., and Campbell, C.: Missing OH reactivity in a forest: Evidence for unknown reactive biogenic VOCs, Science, 304, 722-725, 2004.

Fares, S., Park, J. H., Gentner, D. R., Weber, R., Ormeño, E., Karlik, J., and Goldstein, A. H.: Seasonal cycles of biogenic volatile organic compound fluxes and concentrations in a California citrus orchard, Atmos. Chem. Phys. Discuss., 12, 17987-18027, doi:10.5194/acpd-12-17987-2012, 2012a.

Fares, S., Weber, R., Park, J.-H., Gentner, D., Karlik, J., and Goldstein, A. H.: Ozone deposition to an orange orchard: Partitioning between stomatal and non-stomatal sinks, Environmental Pollution, 169, 258-266, doi:10.1016/j.envpol.2012.01.030, 2012b.

Goldstein, A. H., and Galbally, I. E.: Known and unexplored organic constituents in the earth's atmosphere, Environ Sci Technol, 41, 1514-1521, 2007.

Graus, M., Muller, M., and Hansel, A.: High Resolution PTR-TOF: Quantification and Formula Confirmation of VOC in Real Time, J Am Soc Mass Spectr, 21, 1037-1044, doi: 10.1016/j.jasms.2010.02.006, 2010.

Guenther, A., Hewitt, C. N., Erickson, D., Fall, R., Geron, C., Graedel, T., Harley, P., Klinger, L., Lerdau, M., Mckay, W. A., Pierce, T., Scholes, B., Steinbrecher, R., Tallamraju, R., Taylor, J., and Zimmerman, P.: A Global-Model of Natural Volatile Organic-Compound Emissions, J Geophys Res-Atmos, 100, 8873-8892, 1995.

Hallquist, M., Wenger, J. C., Baltensperger, U., Rudich, Y., Simpson, D., Claeys, M., Dommen, J., Donahue, N. M., George, C., Goldstein, A. H., Hamilton, J. F., Herrmann, H., Hoffmann, T., Iinuma, Y., Jang, M., Jenkin, M. E., Jimenez, J. L., Kiendler-Scharr, A., Maenhaut, W., McFiggans, G., Mentel, T. F., Monod, A., Prevot, A. S. H., Seinfeld, J. H., Surratt, J. D., Szmigielski, R., and Wildt, J.: The formation, properties and impact of secondary organic aerosol: current and emerging issues, Atmos Chem Phys, 9, 5155-5236, 2009.

Holzinger, R., Lee, A., Paw, K. T., and Goldstein, A. H.: Observations of oxidation products above a forest imply biogenic emissions of very reactive compounds, Atmos Chem Phys, 5, 67-75, 2005.

Holzinger, R., Kasper-Giebl, A., Staudinger, M., Schauer, G., and Rockmann, T.: Analysis of the chemical composition of organic aerosol at the Mt. Sonnblick observatory using a novel high mass resolution thermal-desorption proton-transfer-reaction mass-spectrometer (hr-TD-PTR-MS), Atmos Chem Phys, 10, 10111-10128, doi: 10.5194/acp-10-10111-2010, 2010.

Jang, M. S., Czoschke, N. M., Lee, S., and Kamens, R. M.: Heterogeneous atmospheric aerosol production by acid-catalyzed particle-phase reactions, Science, 298, 814-817, 2002.

Jordan, A., Haidacher, S., Hanel, G., Hartungen, E., Mark, L., Seehauser, H., Schottkowsky, R., Sulzer, P., and Mark, T. D.: A high resolution and high sensitivity proton-transfer-reaction time-of-flight mass spectrometer (PTR-TOF-MS), Int J Mass Spectrom, 286, 122-128, doi: 10.1016/j.ijms.2009.07.005, 2009.

Karl, T., Harley, P., Emmons, L., Thornton, B., Guenther, A., Basu, C., Turnipseed, A., and Jardine, K.: Efficient Atmospheric Cleansing of Oxidized Organic Trace Gases by Vegetation, Science, 330, 816-819, doi:10.1126/science.1192534, 2010.

Kurpius, M. R., and Goldstein, A. H.: Gas-phase chemistry dominates O-3 loss to a forest, implying a source of aerosols and hydroxyl radicals to the atmosphere, Geophys Res Lett, 30, 1371, doi:10.1029/2002gl016785, 2003.

Lee, A., Goldstein, A. H., Kroll, J. H., Ng, N. L., Varutbangkul, V., Flagan, R. C., and Seinfeld, J. H.: Gas-phase products and secondary aerosol yields from the photooxidation of 16 different terpenes, J Geophys Res-Atmos, 111, D17305, doi:10.1029/2006jd007050, 2006.

Lindinger, W., Hansel, A., and Jordan, A.: On-line monitoring of volatile organic compounds at pptv levels by means of proton-transfer-reaction mass spectrometry (PTR-MS) - Medical applications, food control and environmental research, Int J Mass Spectrom, 173, 191-241, 1998.

Park, J. H., Goldstein, A. H., Timkovsky, J., Fares, S., Weber, R., Karlik, J., and Holzinger, R.: Eddy covariance emission and deposition flux measurements using proton transfer reaction-time of flight-mass spectrometry (PTR-TOF-MS): comparison with PTR-MS measured vertical gradients and fluxes, Atmos. Chem. Phys. Discuss., 12, 20435-20482, doi:10.5194/acpd-12-20435-2012, 2012.

Ruuskanen, T. M., Mueller, M., Schnitzhofer, R., Karl, T., Graus, M., Bamberger, I., Hortnagl, L., Brilli, F., Wohlfahrt, G., and Hansel, A.: Eddy covariance VOC emission and deposition fluxes above grassland using PTR-TOF, Atmos Chem Phys, 11, 611-625, doi:10.5194/acp-11-611-2011, 2011.

Table 4. 1. Mixing ratio and eddy covariance flux measured for 162 selected species.

Mass to charge observed (*m/z*)	Possible empirical formulae	Δ mDa[a]	Mixing ratio [nmol mol^{-1}] 24-h mean (day/night)	EC flux [µg C m^{-2} h^{-1}] 24-h mean net flux (gross emission/deposition)	S/N criterion
31.018	CH_2OH^+	-0.16	0.36 (0.31 / 0.41)	0.86 (1.76 / -0.9)	5
33.032	CH_4OH^+	1.39	19.89 (16.85 / 24.55)	71.5 (75.9 / -4.39)	10
41.038	$C_3H_4H^+$	0.28	0.39 (0.2 / 0.51)	10.96 (11.58 / -0.62)	3
43.018	$C_2H_2OH^+$	-0.16	1.03 (0.96 / 1.25)	10.92 (11.49 / -0.58)	5
43.054	$C_3H_6H^+$	0.23	0.37 (0.27 / 0.46)	9.7 (9.86 / -0.16)	7
44.997	CO_2H^+	-0.09	0.19 (0.14 / 0.23)	-0.78 (0.9 / -1.68)	3
45.033	$C_2H_4OH^+$	0.89	2.92 (2.77 / 3.18)	11.46 (12.82 / -1.36)	8
47.012	$CH_2O_2H^+$	0.86	0.17 (0.19 / 0.16)	-1.12 (0.35 / -1.47)	5
47.047	$C_2H_6OH^+$	2.34	0.77 (0.65 / 0.93)	1.67 (2.93 / -1.26)	4
53.039	$C_4H_4H^+$	-0.22	0.08 (0.07 / 0.1)	2.13 (3.66 / -1.54)	4
57.034	$C_3H_4OH^+$	-0.61	0.28 (0.2 / 0.36)	4.33 (6.36 / -2.03)	3
57.069	$C_4H_8H^+$	0.48	0.11 (0.07 / 0.14)	2.81 (4.66 / -1.85)	7
59.048	$C_3H_6OH^+$	0.94	4.52 (3.73 / 5.35)	36.48 (37.02 / -0.54)	10
61.027	$C_2H_4O_2H^+$	1.21	4.9 (5.05 / 5.47)	35.68 (36.11 / -0.43)	8
63.043	$C_2H_6O_2H^+$	1.26	0.061 (0.058 / 0.067)	-0.17 (0.57 / -0.75)	3
67.055	$C_5H_6H^+$	-0.67	0.058 (0.03 / 0.081)	2.64 (3.6 / -0.95)	4
68.997	$C_3O_2H^+$	0.41	0.037 (0.036 / 0.038)	0.62 (0.93 / -0.31)	5
69.034	$C_4H_4OH^+$	-0.61	0.052 (0.038 / 0.063)	0.26 (1.33 / -1.07)	6
69.071	$C_5H_8H^+$	-0.82	0.28 (0.19 / 0.34)	5.31 (5.45 / -0.14)	8
71.013	$C_3H_2O_2H^+$	-0.34	0.04 (0.04 / 0.05)	0.43 (1.23 / -0.8)	5
71.048	$C_4H_6OH^+$	0.84	0.3 (0.2 / 0.36)	7.05 (7.67 / -0.62)	8
71.086	$C_5H_{10}H^+$	-0.27	0.049 (0.032 / 0.06)	1.33 (2.39 / -1.05)	5
73.029	$C_3H_4O_2H^+$	-0.69	0.2 (0.15 / 0.15)	-0.23 (1.67 / -1.9)	4
73.063	$C_4H_8OH^+$	2.19	0.38 (0.3 / 0.45)	5 (6.17 / -1.18)	3
77.022	$C_2H_4O_3H^+$	1.52	0.044 (0.038 / 0.052)	0.83 (1.39 / -0.55)	5
77.039	$C_6H_4H^+$	-0.52	0.08 (0.05 / 0.12)	4.89 (6.05 / -1.15)	4
	$C_3H_8SH^+$	2.85			
79.003	$CH_2O_4H^+$	-0.11	0.026 (0.025 / 0.028)	0.04 (0.29 / -0.25)	3
79.055	$C_6H_6H^+$	-0.37	0.1 (0.06 / 0.14)	4.14 (4.65 / -0.51)	4
81.036	$C_5H_4OH^+$	-2.01	0.05 (0.027 / 0.068)	3.19 (3.42 / -0.23)	4
81.070	$C_6H_8H^+$	-0.12	0.5 (0.23 / 0.73)	65.62 (65.62 / 0)	10
83.014	$C_4H_2O_2H^+$	-0.74	0.032 (0.027 / 0.035)	0.09 (0.85 / -0.76)	3
83.050	$C_5H_6OH^+$	-0.86	0.09 (0.03 / 0.14)	1.84 (2.62 / -0.78)	4
83.086	$C_6H_{10}H^+$	-0.57	0.13 (0.08 / 0.16)	1.72 (2.79 / -1.07)	4

85.028	$C_4H_4O_2H^+$	0.21	0.08 (0.06 / 0.1)	0.52 (1.53 / -1.01)	3
85.064	$C_5H_8OH^+$	0.89	0.07 (0.03 / 0.1)	1.71 (2.76 / -1.06)	4
85.103	$C_6H_{12}H^+$	-1.32	0.027 (0.019 / 0.032)	0.44 (1.86 / -1.42)	3
87.043	$C_4H_6O_2H^+$	1.26	0.22 (0.16 / 0.28)	2.46 (3.38 / -0.92)	6
89.024	$C_3H_4O_3H^+$	-0.48	0.04 (0.04 / 0.04)	0.9 (1.37 / -0.47)	5
89.059	$C_4H_8O_2H^+$	1.21	0.09 (0.08 / 0.1)	0.55 (1.81 / -1.26)	4
91.052	$C_7H_6H^+$	2.63	0.037 (0.017 / 0.054)	2.28 (2.76 / -0.48)	3
	$C_2H_6N_2O_2H^+$	-1.40			
91.055	$C_7H_6H^+$	-0.67	0.057 (0.021 / 0.088)	1.93 (3.06 / -1.13)	5
	$C_4H_{10}SH^+$	2.70			
93.034	$C_6H_4OH^+$	-0.11	0.056 (0.042 / 0.071)	4.17 (5.19 / -1.02)	4
93.069	$C_7H_8H^+$	0.78	0.14 (0.04 / 0.22)	17.41 (17.41 / 0)	8
95.049	$C_6H_6OH^+$	0.54	0.056 (0.032 / 0.074)	4.47 (4.81 / -0.34)	4
95.086	$C_7H_{10}H^+$	-0.47	0.25 (0.17 / 0.32)	20.11 (20.3 / -0.19)	9
97.028	$C_5H_4O_2H^+$	0.11	0.061 (0.032 / 0.086)	1.47 (2.53 / -1.06)	4
97.065	$C_6H_8OH^+$	-0.21	0.07 (0.02 / 0.1)	1.29 (2.56 / -1.26)	4
97.102	$C_7H_{12}H^+$	-0.42	0.038 (0.017 / 0.054)	0.93 (2.03 / -1.11)	3
99.043	$C_5H_6O_2H^+$	0.66	0.08 (0.04 / 0.12)	1.74 (2.57 / -0.84)	4
101.024	$C_4H_4O_3H^+$	-0.68	0.041 (0.035 / 0.047)	1.64 (2.24 / -0.6)	7
101.058	$C_5H_8O_2H^+$	1.71	0.08 (0.04 / 0.11)	0.88 (1.63 / -0.74)	5
103.038	$C_4H_6O_3H^+$	0.97	0.036 (0.033 / 0.038)	0.15 (1.02 / -0.87)	5
103.074	$C_5H_{10}O_2H^+$	1.36	0.042 (0.033 / 0.041)	1.4 (2.18 / -0.78)	5
105.071	$C_8H_8H^+$	-1.12	0.055 (0.019 / 0.085)	1.14 (2.67 / -1.53)	5
	$C_5H_{12}SH^+$	2.25			
107.049	$C_7H_6OH^+$	0.14	0.053 (0.012 / 0.087)	1.65 (2.49 / -0.84)	4
107.085	$C_8H_{10}H^+$	0.53	0.08 (0.01 / 0.12)	5.6 (6.19 / -0.59)	4
109.028	$C_6H_4O_2H^+$	0.41	0.025 (0.022 / 0.027)	0.79 (1.72 / -0.93)	3
109.066	$C_7H_8OH^+$	-1.21	0.034 (0.015 / 0.046)	0.45 (1.47 / -1.02)	6
109.101	$C_8H_{12}H^+$	0.18	0.033 (0.011 / 0.049)	0.31 (1.95 / -1.64)	5
111.044	$C_6H_6O_2H^+$	0.06	0.037 (0.021 / 0.048)	1.19 (1.87 / -0.68)	5
111.080	$C_7H_{10}OH^+$	0.44	0.056 (0.033 / 0.071)	0.72 (1.67 / -0.95)	3
111.118	$C_8H_{14}H^+$	-1.17	0.031 (0.023 / 0.037)	-1.24 (0.89 / -2.13)	3
113.024	$C_5H_4O_3H^+$	-0.68	0.064 (0.063 / 0.064)	-0.01 (1.48 / -1.49)	4
113.058	$C_6H_8O_2H^+$	1.71	0.049 (0.03 / 0.061)	-0.19 (1.2 / -1.39)	5
113.134	$C_8H_{16}H^+$	-1.52	0.017 (0.015 / 0.019)	-0.16 (0.93 / -1.09)	7
115.016	$C_8H_2OH^+$	1.84	0.03 (0.03 / 0.03)	-0.09 (1.37 / -1.46)	5
	$C_3H_2N_2O_3H^+$	-2.18			
115.038	$C_5H_6O_3H^+$	0.97	0.034 (0.029 / 0.038)	0.19 (0.87 / -0.67)	4
117.055	$C_5H_8O_3H^+$	-0.38	0.02 (0.018 / 0.021)	0.01 (0.65 / -0.64)	3
117.089	$C_6H_{12}O_2H^+$	2.01	0.034 (0.024 / 0.033)	0.51 (1.62 / -1.11)	5
119.032	$C_4H_6O_4H^+$	1.89	0.014 (0.012 / 0.015)	0.91 (1.11 / -0.2)	3
119.086	$C_9H_{10}H^+$	-0.47	0.041 (0.024 / 0.05)	-0.16 (1.96 / -2.11)	4
	$C_6H_{14}SH^+$	2.90			

121.031	$C_7H_4O_2H^+$	-2.59	0.031 (0.016 / 0.046)	0.32 (1.51 / -1.2)	3
	$C_4H_8O_2SH^+$	0.78			
121.064	$C_8H_8OH^+$	0.79	0.031 (0.014 / 0.045)	0.99 (1.73 / -0.74)	5
121.101	$C_9H_{12}H^+$	0.18	0.072 (0.023 / 0.112)	2.54 (3.34 / -0.8)	4
123.080	$C_8H_{10}OH^+$	0.44	0.026 (0.017 / 0.033)	0.88 (1.68 / -0.8)	4
123.117	$C_9H_{14}H^+$	-0.17	0.019 (0.008 / 0.027)	2.34 (2.74 / -0.4)	3
125.023	$C_6H_4O_3H^+$	0.32	0.023 (0.019 / 0.026)	1.1 (1.71 / -0.61)	3
125.059	$C_7H_8O_2H^+$	0.71	0.017 (0.009 / 0.023)	0.89 (1.38 / -0.49)	4
125.095	$C_8H_{12}OH^+$	1.09	0.022 (0.01 / 0.03)	0.39 (2.08 / -1.7)	4
125.132	$C_9H_{16}H^+$	0.48	0.019 (0.015 / 0.022)	-0.28 (1.69 / -1.97)	3
127.073	$C_7H_{10}O_2H^+$	2.36	0.03 (0.02 / 0.038)	1.6 (2.13 / -0.54)	4
129.055	$C_6H_8O_3H^+$	-0.38	0.015 (0.012 / 0.017)	0.35 (0.94 / -0.59)	5
129.069	$C_{10}H_8H^+$	0.88	0.029 (0.018 / 0.033)	0.24 (1.68 / -1.44)	4
131.105	$C_7H_{14}O_2H^+$	1.66	0.017 (0.014 / 0.019)	1.51 (2.18 / -0.67)	4
133.028	$C_8H_4O_2H^+$	0.41	0.013 (0.011 / 0.014)	0.22 (1.37 / -1.15)	6
133.100	$C_{10}H_{12}H^+$	1.18	0.046 (0.021 / 0.065)	4.13 (4.29 / -0.16)	5
	$C_5H_{12}N_2O_2H^+$	-2.85			
135.046	$C_8H_6O_2H^+$	-1.94	0.015 (0.009 / 0.02)	0.82 (1.44 / -0.62)	3
	$C_5H_{10}O_2SH^+$	1.43			
135.080	$C_9H_{10}OH^+$	0.44	0.041 (0.023 / 0.048)	1.29 (1.91 / -0.62)	3
135.116	$C_{10}H_{14}H^+$	0.83	0.094 (0.055 / 0.102)	2.28 (3.12 / -0.83)	6
137.059	$C_8H_8O_2H^+$	-0.64	0.017 (0.011 / 0.021)	0.46 (1.15 / -0.69)	4
137.097	$C_9H_{12}OH^+$	-0.91	0.034 (0.015 / 0.049)	3.23 (3.54 / -0.32)	4
137.131	$C_{10}H_{16}H^+$	1.48	0.12 (0.05 / 0.18)	15.94 (15.94 / 0)	10
139.039	$C_7H_6O_3H^+$	-0.03	0.021 (0.015 / 0.025)	0.75 (1.51 / -0.76)	5
139.075	$C_8H_{10}O_2H^+$	0.36	0.023 (0.013 / 0.031)	0.9 (1.59 / -0.7)	5
139.110	$C_9H_{14}OH^+$	1.74	0.032 (0.005 / 0.051)	-0.15 (1.64 / -1.78)	4
141.053	$C_7H_8O_3H^+$	1.62	0.019 (0.015 / 0.02)	0.94 (1.57 / -0.63)	6
	$C_2H_8N_2O_5H^+$	-2.40			
143.036	$C_6H_6O_4H^+$	-2.11	0.019 (0.018 / 0.021)	0.55 (1.04 / -0.49)	3
145.049	$C_6H_8O_4H^+$	0.54	0.011 (0.01 / 0.013)	-0.47 (0.5 / -0.97)	4
145.120	$C_8H_{16}O_2H^+$	2.31	0.015 (0.014 / 0.016)	0.01 (1.1 / -1.09)	6
147.117	$C_{11}H_{14}H^+$	-0.17	0.015 (0.012 / 0.016)	-0.94 (1.22 / -2.16)	4
149.133	$C_{11}H_{16}H^+$	-0.52	0.015 (0.008 / 0.02)	0.7 (1.61 / -0.91)	3
151.038	$C_8H_6O_3H^+$	0.97	0.019 (0.015 / 0.022)	-0.04 (1.39 / -1.43)	5
	$C_4H_{10}N_2S_2H^+$	-2.19			
151.109	$C_{10}H_{14}OH^+$	2.74	0.018 (0.008 / 0.024)	1.04 (2.36 / -1.32)	6
	$C_5H_{14}N_2O_3H^+$	-1.28			
151.151	$C_{11}H_{18}H^+$	-2.87	0.013 (0.01 / 0.015)	1.02 (1.64 / -0.62)	4
153.125	$C_{10}H_{16}OH^+$	2.39	0.025 (0.012 / 0.035)	1.36 (2.62 / -1.27)	3
155.072	$C_8H_{10}O_3H^+$	-1.73	0.014 (0.014 / 0.014)	0.57 (1.19 / -0.62)	4
159.012	$C_2H_6O_8H^+$	1.55	0.012 (0.012 / 0.011)	-0.06 (0.14 / -0.2)	4
	$C_6H_6O_3SH^+$	-0.96			

159.064	$C_7H_{10}O_4H^+$	1.19	0.016 (0.015 / 0.016)	0.52 (1.09 / -0.57)	5
159.136	$C_9H_{18}O_2H^+$	1.96	0.012 (0.011 / 0.014)	0.75 (1.71 / -0.97)	4
161.057	$C_{10}H_8O_2H^+$	2.71	0.017 (0.016 / 0.018)	0.14 (1.15 / -1.01)	4
	$C_5H_8N_2O_4H^+$	-1.32			
161.097	$C_{11}H_{12}OH^+$	-0.91	0.013 (0.012 / 0.015)	0.1 (1.52 / -1.42)	3
	$C_8H_{16}OSH^+$	2.46			
163.040	$C_9H_6O_3H^+$	-1.03	0.015 (0.013 / 0.016)	-0.68 (0.76 / -1.44)	4
163.111	$C_{11}H_{14}OH^+$	0.74	0.011 (0.009 / 0.012)	1.66 (2.27 / -0.62)	5
163.150	$C_{12}H_{18}H^+$	-1.87	0.011 (0.009 / 0.013)	0.57 (1.7 / -1.13)	3
165.089	$C_{10}H_{12}O_2H^+$	2.01	0.015 (0.01 / 0.018)	0.63 (1.83 / -1.2)	5
	$C_5H_{12}N_2O_4H^+$	-2.02			
167.072	$C_9H_{10}O_3H^+$	-1.73	0.009 (0.007 / 0.01)	0.75 (1.38 / -0.63)	4
	$C_6H_{14}O_3SH^+$	1.64			
167.145	$C_{11}H_{18}OH^+$	-1.96	0.015 (0.013 / 0.016)	0.73 (1.73 / -1)	4
171.067	$C_8H_{10}O_4H^+$	-1.81	0.01 (0.009 / 0.011)	0.48 (1.01 / -0.53)	3
171.136	$C_{10}H_{18}O_2H^+$	1.96	0.016 (0.014 / 0.017)	-0.27 (1.02 / -1.29)	4
173.062	$C_{11}H_8O_2H^+$	-2.29	0.015 (0.014 / 0.015)	-0.87 (0.58 / -1.45)	3
173.152	$C_{10}H_{20}O_2H^+$	1.61	0.014 (0.013 / 0.015)	0.48 (1.52 / -1.04)	4
175.037	$C_{10}H_6O_3H^+$	1.97	0.015 (0.014 / 0.015)	0.13 (1.29 / -1.16)	3
	$C_5H_6N_2O_5H^+$	-2.05			
	$C_6H_{10}N_2S_2H^+$	-1.19			
175.150	$C_{13}H_{18}H^+$	-1.87	0.012 (0.011 / 0.013)	-0.24 (1.43 / -1.67)	3
	$C_{10}H_{22}SH^+$	1.50			
177.054	$C_{10}H_8O_3H^+$	0.62	0.015 (0.015 / 0.016)	0.41 (1.85 / -1.45)	4
	$C_6H_{12}N_2S_2H^+$	-2.54			
177.165	$C_{13}H_{20}H^+$	-1.22	0.014 (0.012 / 0.015)	1.14 (2.44 / -1.3)	6
179.179	$C_{13}H_{22}H^+$	0.43	0.01 (0.009 / 0.011)	0.37 (1.79 / -1.42)	4
181.050	$C_9H_8O_4H^+$	-0.46	0.009 (0.009 / 0.01)	-0.67 (0.53 / -1.2)	5
181.085	$C_{10}H_{12}O_3H^+$	0.92	0.007 (0.006 / 0.008)	-0.43 (0.58 / -1.01)	4
181.120	$C_{11}H_{16}O_2H^+$	2.31	0.01 (0.008 / 0.011)	0.33 (1.49 / -1.16)	3
	$C_6H_{16}N_2O_4H^+$	-1.72			
183.080	$C_{13}H_{10}OH^+$	0.44	0.011 (0.009 / 0.012)	1.29 (2.01 / -0.72)	4
185.081	$C_9H_{12}O_4H^+$	-0.16	0.01 (0.01 / 0.011)	0.09 (0.79 / -0.7)	3
185.153	$C_{11}H_{20}O_2H^+$	0.61	0.012 (0.011 / 0.012)	0.32 (1.64 / -1.33)	3
187.168	$C_{11}H_{22}O_2H^+$	1.26	0.01 (0.009 / 0.011)	-1.66 (0.66 / -2.33)	6
189.055	$C_{11}H_8O_3H^+$	-0.38	0.012 (0.012 / 0.012)	0.32 (1.25 / -0.93)	4
189.164	$C_{14}H_{20}H^+$	-0.22	0.012 (0.011 / 0.013)	0.62 (1.38 / -0.76)	4
191.180	$C_{14}H_{22}H^+$	-0.57	0.013 (0.012 / 0.014)	0.03 (1.67 / -1.65)	5
197.134	$C_{15}H_{16}H^+$	-1.52	0.014 (0.013 / 0.014)	0.02 (1.4 / -1.38)	4
	$C_{12}H_{20}SH^+$	1.85			
199.169	$C_{12}H_{22}O_2H^+$	0.26	0.01 (0.01 / 0.011)	0.08 (1.27 / -1.2)	4
201.184	$C_{12}H_{24}O_2H^+$	0.91	0.013 (0.011 / 0.015)	-0.8 (1.2 / -2)	4
203.179	$C_{15}H_{22}H^+$	0.43	0.01 (0.009 / 0.011)	-1.6 (1.15 / -2.75)	4

205.049	$C_{11}H_8O_4H^+$	0.54	0.006 (0.006 / 0.007)	-1.03 (0.41 / -1.44)	4
205.195	$C_{15}H_{24}H^+$	0.08	0.02 (0.017 / 0.023)	0.8 (1.93 / -1.14)	4
209.023	$C_{13}H_4O_3H^+$	0.32	0.011 (0.01 / 0.012)	0 (1.87 / -1.87)	3
	$C_5H_8N_2O_5SH^+$	-0.33			
209.152	$C_{13}H_{20}O_2H^+$	1.61	0.013 (0.013 / 0.014)	0.31 (1.32 / -1.02)	3
	$C_8H_{20}N_2O_4H^+$	-2.42			
211.005	$C_{12}H_2O_4H^+$	-2.41	0.018 (0.018 / 0.018)	0.08 (1.28 / -1.2)	5
	$C_9H_6O_4SH^+$	0.96			
211.116	$C_8H_{18}O_6H^+$	1.62	0.007 (0.007 / 0.007)	0.09 (0.85 / -0.76)	4
	$C_{12}H_{18}OSH^+$	-0.89			
211.133	$C_{12}H_{18}O_3H^+$	-0.13	0.01 (0.009 / 0.01)	-1.01 (0.54 / -1.55)	5
213.092	$C_{14}H_{12}O_2H^+$	-0.99	0.009 (0.009 / 0.009)	-0.46 (0.81 / -1.27)	6
213.185	$C_{13}H_{24}O_2H^+$	-0.09	0.009 (0.009 / 0.01)	1.37 (2.12 / -0.74)	6
215.073	$C_{13}H_{10}O_3H^+$	-2.73	0.01 (0.01 / 0.01)	-0.69 (1.17 / -1.86)	5
	$C_{10}H_{14}O_3SH^+$	0.64			
215.201	$C_{13}H_{26}O_2H^+$	-0.44	0.009 (0.008 / 0.009)	-0.38 (0.93 / -1.31)	4
217.195	$C_{16}H_{24}H^+$	0.08	0.009 (0.009 / 0.01)	-0.94 (1.04 / -1.98)	6
219.045	$C_{15}H_6O_2H^+$	-0.94	0.13 (0.13 / 0.1)	-1.26 (4.83 / -6.09)	4
	$C_{12}H_{10}O_2SH^+$	2.43			
219.213	$C_{16}H_{26}H^+$	-2.27	0.011 (0.01 / 0.012)	-0.71 (1.86 / -2.56)	3
221.047	$C_{11}H_8O_5H^+$	-2.55	0.018 (0.019 / 0.016)	0.36 (1.49 / -1.13)	4
223.062	$C_{11}H_{10}O_5H^+$	-1.90	0.023 (0.02 / 0.028)	-1.6 (1.2 / -2.8)	5
225.126	$C_{16}H_{16}OH^+$	1.39	0.012 (0.011 / 0.013)	-1.45 (0.47 / -1.92)	3
	$C_{11}H_{16}N_2O_{3-}H^+$	-2.63			
227.035	$C_{13}H_6O_4H^+$	-1.11	0.008 (0.008 / 0.008)	1.74 (2.54 / -0.8)	3
227.202	$C_{14}H_{26}O_2H^+$	-1.44	0.009 (0.009 / 0.01)	-2.31 (0.59 / -2.9)	3
229.084	$C_{14}H_{12}O_3H^+$	1.92	0.012 (0.01 / 0.014)	0.26 (1.36 / -1.11)	3
	$C_9H_{12}N_2O_5H^+$	-2.10			
	$C_{10}H_{16}N_2S_2H^+$	-1.24			
229.216	$C_{14}H_{28}O_2H^+$	0.21	0.011 (0.009 / 0.015)	0.91 (1.94 / -1.02)	3
231.210	$C_{17}H_{26}H^+$	0.73	0.011 (0.01 / 0.011)	0.33 (1.58 / -1.25)	4

[a] The difference between the exact ion mass and the measured mass in mDa.

Table 4. 2. Summarized flux for the 10 major ion species including monoterpenes (*m/z* 81.070 + 137.131 + 95.086), methanol (*m/z* 33.032), acetone (*m/z* 59.048), acetic acid (*m/z* 61.027), para-cymene (*m/z* 93.069), acetaldehyde (*m/z* 45.033), MVK+MACR (*m/z* 71.048), and isoprene+MBO (*m/z* 69.071) and 4 groups of ion species summed as *m/z* ranges 31-69 (M31-69), 69-136 (M69-136), 136-237 (M136-237), and 237-1278 (M237-1278). Data are separated into fluxes on a molar and carbon mass basis (left four columns) and flux and exchange velocity (V_{ex}) by 4 groups for the 186 species which showed a 24-h net deposition flux (right 3 columns).

Group	# of species	Molar basis	Carbon mass basis	Depositing species		
		Net flux 24h mean [nmol m^{-2} s^{-1}] (gross emission/deposition)	Net flux 24h mean [µg C m^{-2} h^{-1}] (gross emission/deposition)	# of species	Net flux 24h mean [nmol m^{-2} s^{-1}] (gross emission/deposition)	24-h mean V_{ex} [cm s^{-1}]
10 majors	10	2.82 (2.95 / -0.13)	287 (294 / -7.7)	0		
M31-69	61	1.09 (2.97 / -1.88)	94 (257 / -163)	18	-0.27 (0.39 / -0.66)	-0.19
M69-136	141	0.45 (1.06 / -0.61)	96 (229 / -132)	40	-0.07 (0.18 / -0.24)	-0.24
M136-237	141	0.06 (0.42 / -0.37)	24 (183 / -158)	57	-0.07 (0.12 / -0.19)	-0.41
M237-1278	141	0.02 (0.27 / -0.25)	11 (174 / -163)	71	-0.05 (0.1 / -0.15)	-0.32

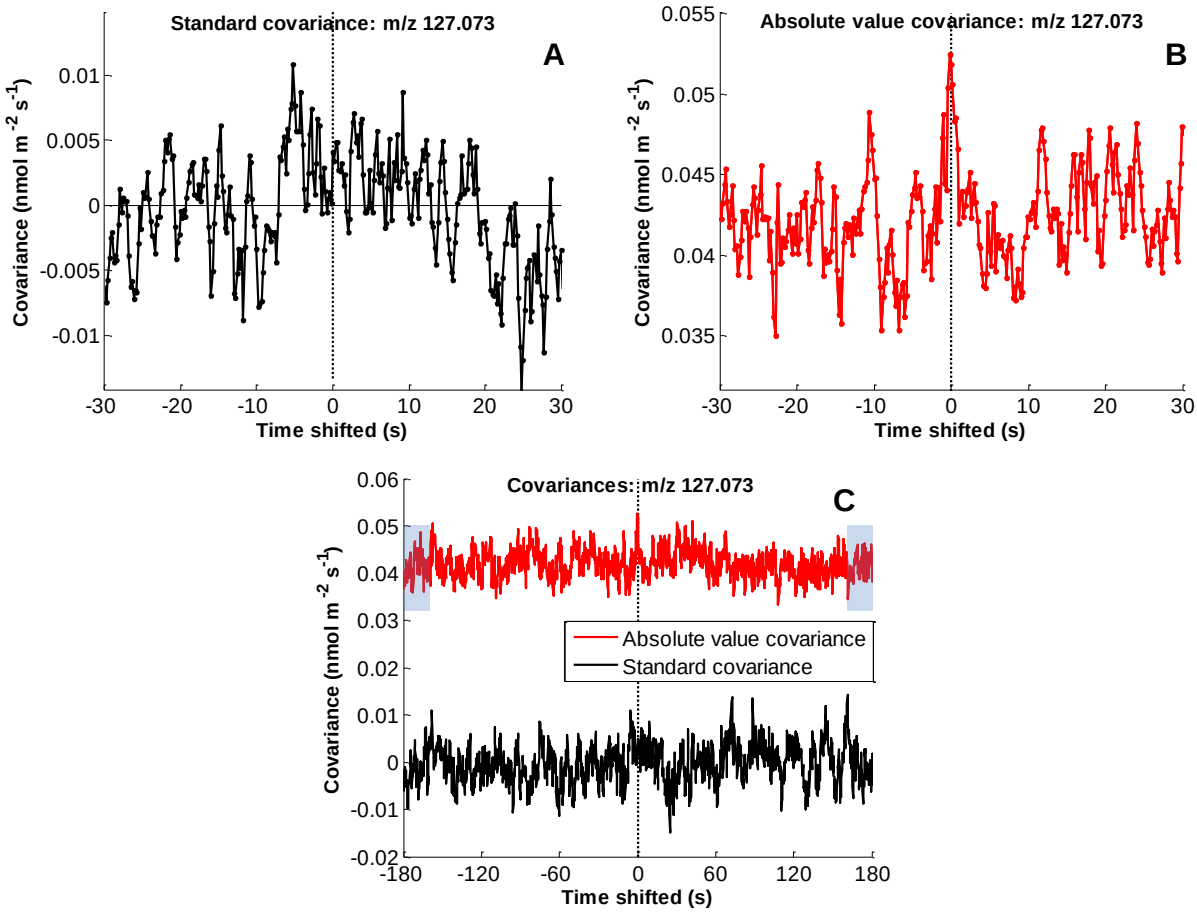

Figure 4. 1. Time shifted covariance plots of vertical wind speed and *m/z* 127.073 ($C_7H_{10}O_2H^+$) observed by PTR-TOF-MS, averaged over 10:00 – 16:00 PST throughout the whole measurement campaign with (A) standard co-variance analysis in ± 30 s time window, (B) absolute value co-variance analysis ± 30 s, and (C) both analyses (standard co-variance in black line and absolute value co-variance in red line) in ± 180 s for each 30 min data period. The shaded area in C is assumed to represent the noise of signal for absolute value co-variance analysis. A sharp peak at 0 s in B and C (red line) indicates apparent exchange for *m/z* 127.073 when analyzing the absolute value covariance, which is not observed in A and C (black line) due to bi-directional exchange masking the flux.

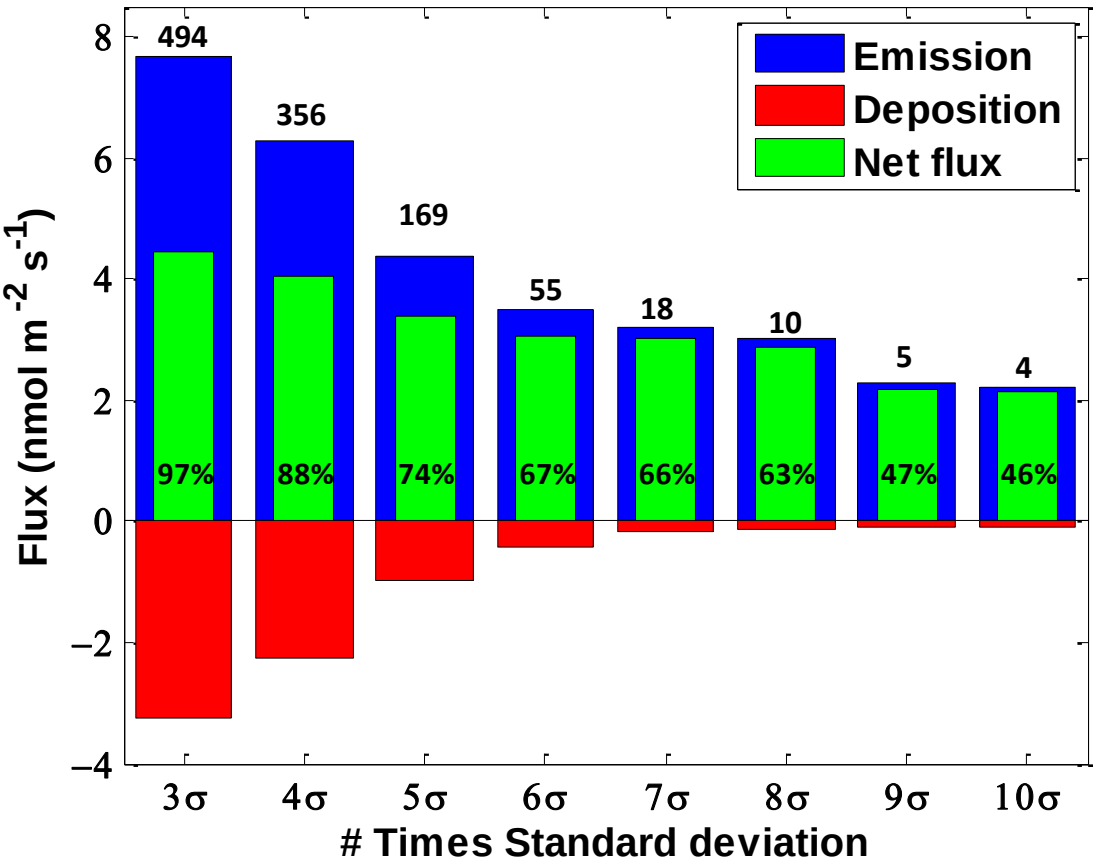

Figure 4. 2. Flux contribution by identified ions (out of 555) which had flux exceeding a signal to noise ratio of three or more sigma (σ, standard deviation of the noise). Blue, red, and green bars indicate gross emission, gross deposition and net exchange, respectively. The number of ions in each bin is indicated above. Percent shown in the green bars indicates the flux contribution to total net flux of 555 ions on a molar basis.

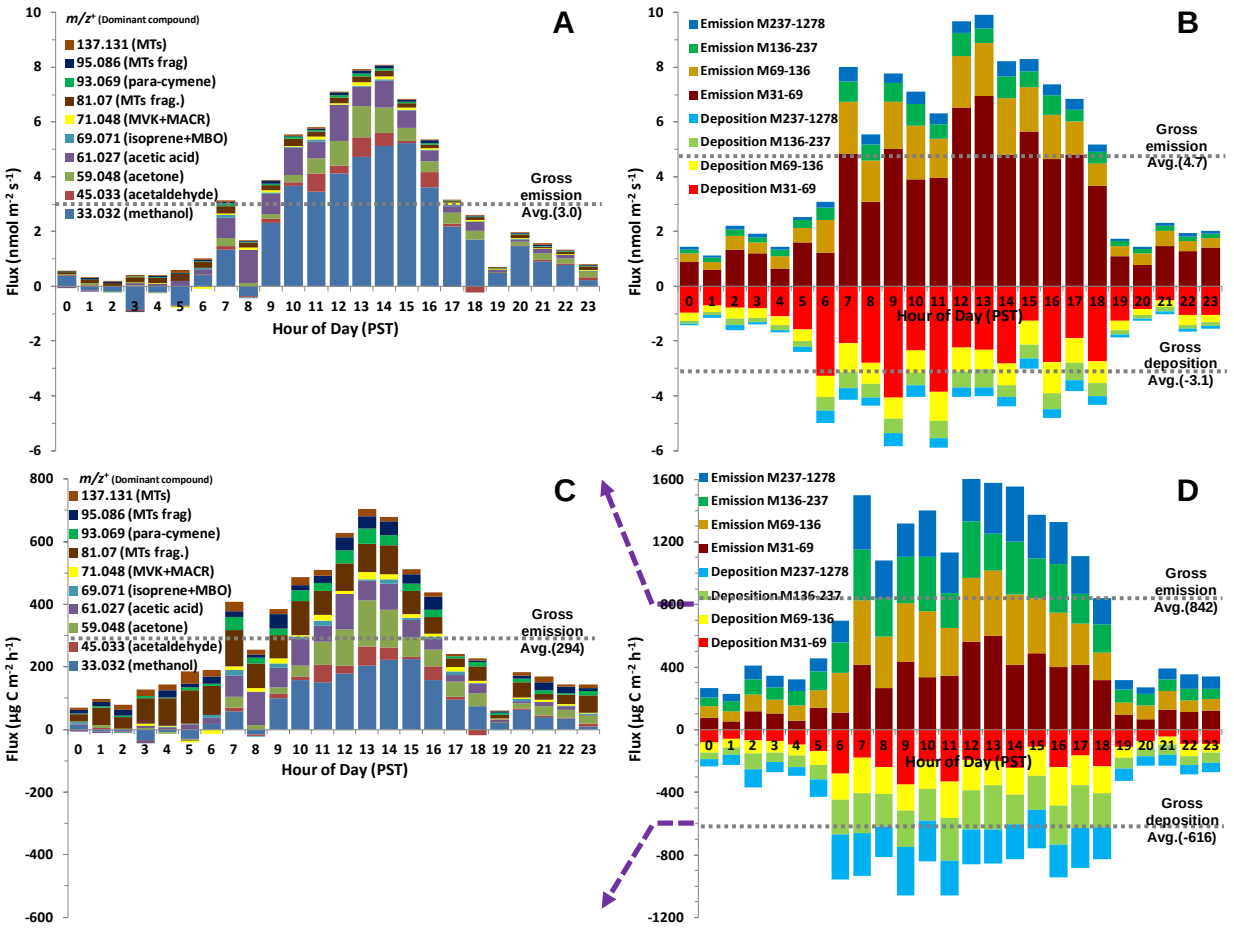

Figure 4. 3. Total and fractional BVOC diurnal emission and deposition flux on a molar basis for (A) 10 major species, (B) 4 different mass ranges categorized as m/z 31-69 (n=61), m/z 69-136 (n=141), m/z 136-237 (n=141) and m/z 237-1278 (n=141), and on a carbon mass basis for (C) 10 majors and (D) 4 classes. Staged bar plots of 10 masses and 4 classes with the largest fluxes are shown as diurnal cycles with *m/z* (or *m/z* range) indicated in the legend. The y scale in (C) is half of (D).

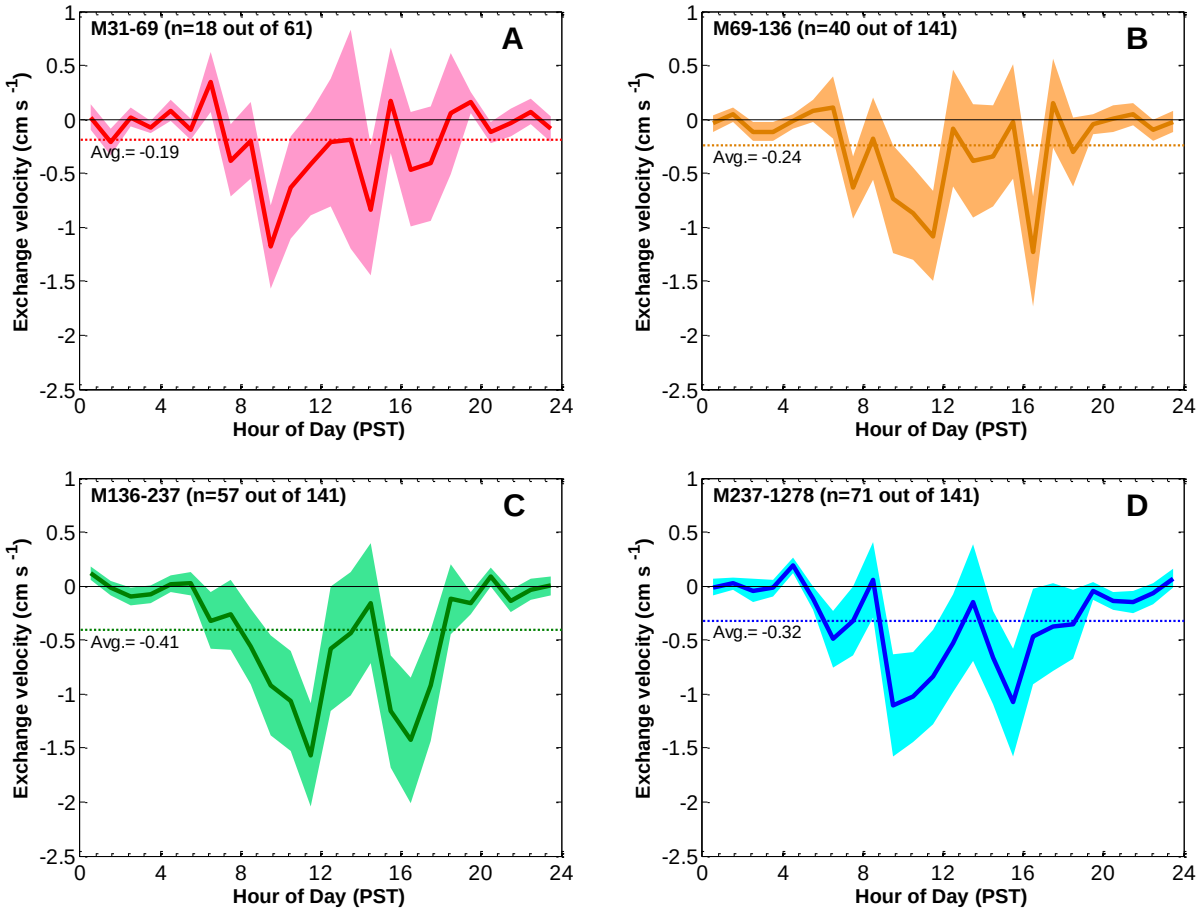

Figure 4. 4. Mean diurnal cycle of exchange velocity for (A) M31-69, (B) M69-136, (C) M136-237, and (D) M237-1278. Dotted lines indicate the 24-h mean exchange velocity for each group, and the shaded area indicates standard error of the mean.

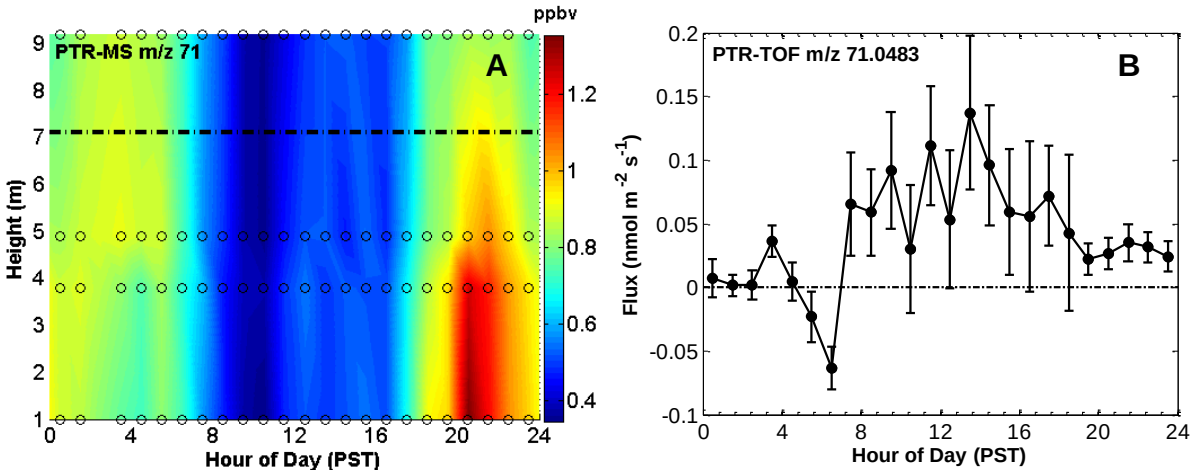

Figure 4. 5. Mean vertical gradient measured by PTR-MS (A) and flux measured by PTR-TOF-MS (B) of the diurnal pattern for the sum of methlyvinylketon and methacrolein (MVK+MACR) (Park et al., 2012). Interpolated gradient measurements (A) are color coded with actual measurement timing and vertical positions shown as open circles, and flux measurement height shown as a broken black line. Flux diurnal patterns of MVK+MACR shown in B agree well with observed vertical gradients during day and night with net emission. Error bars in B denote the standard errors of all measurements at the respective hour of the day.

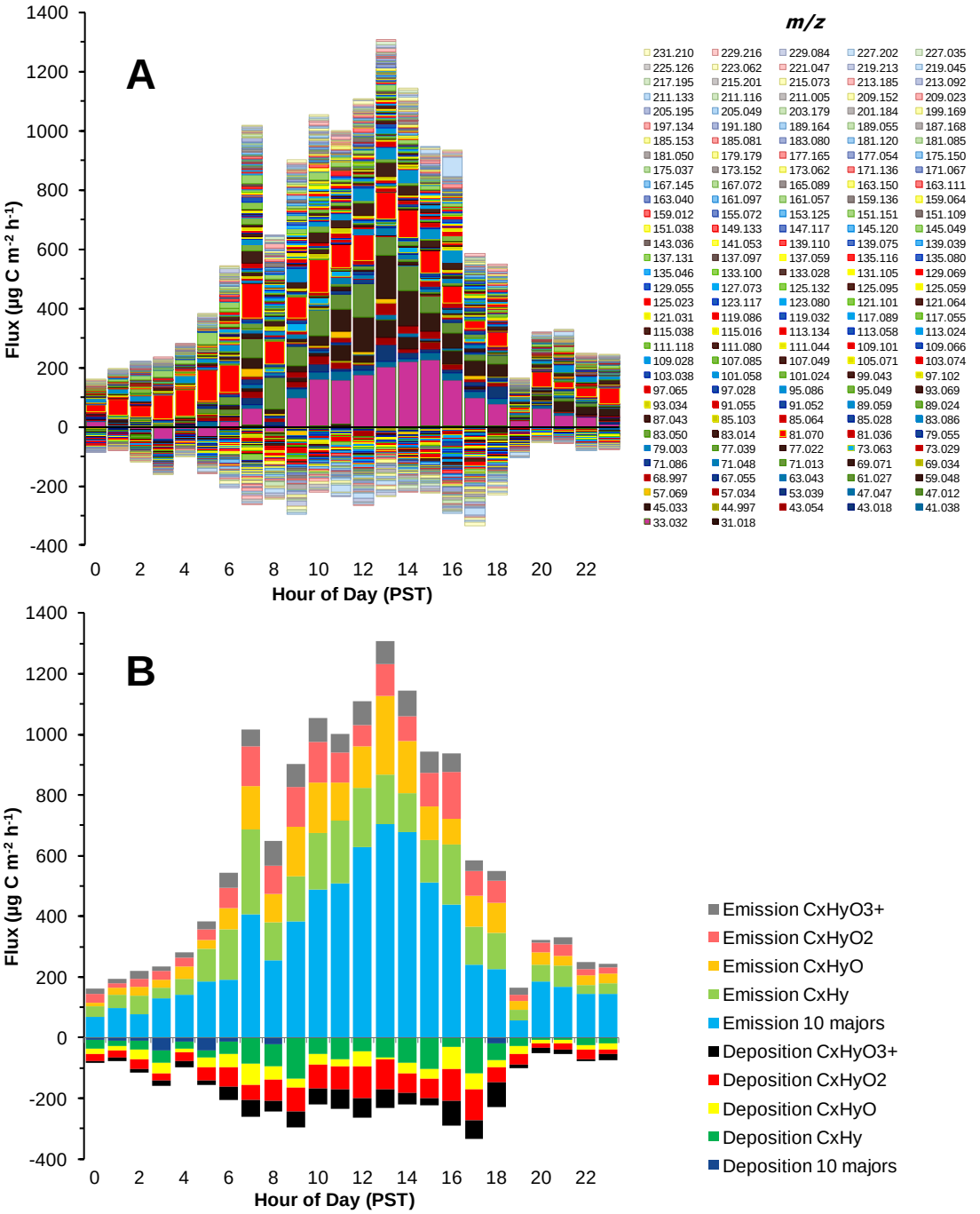

Figure 4. 6. Total and fractional VOC diurnal flux measured by PTR-TOF-MS on a carbon mass basis. Staged bar plots of (A) 162 ion species selected with the largest fluxes are shown as diurnal cycles with *m/z* indicated in the legend and (B) 4 hydrocarbon groups classified by the number of oxygen they contained in addition to 10 major dominant compounds at the site.

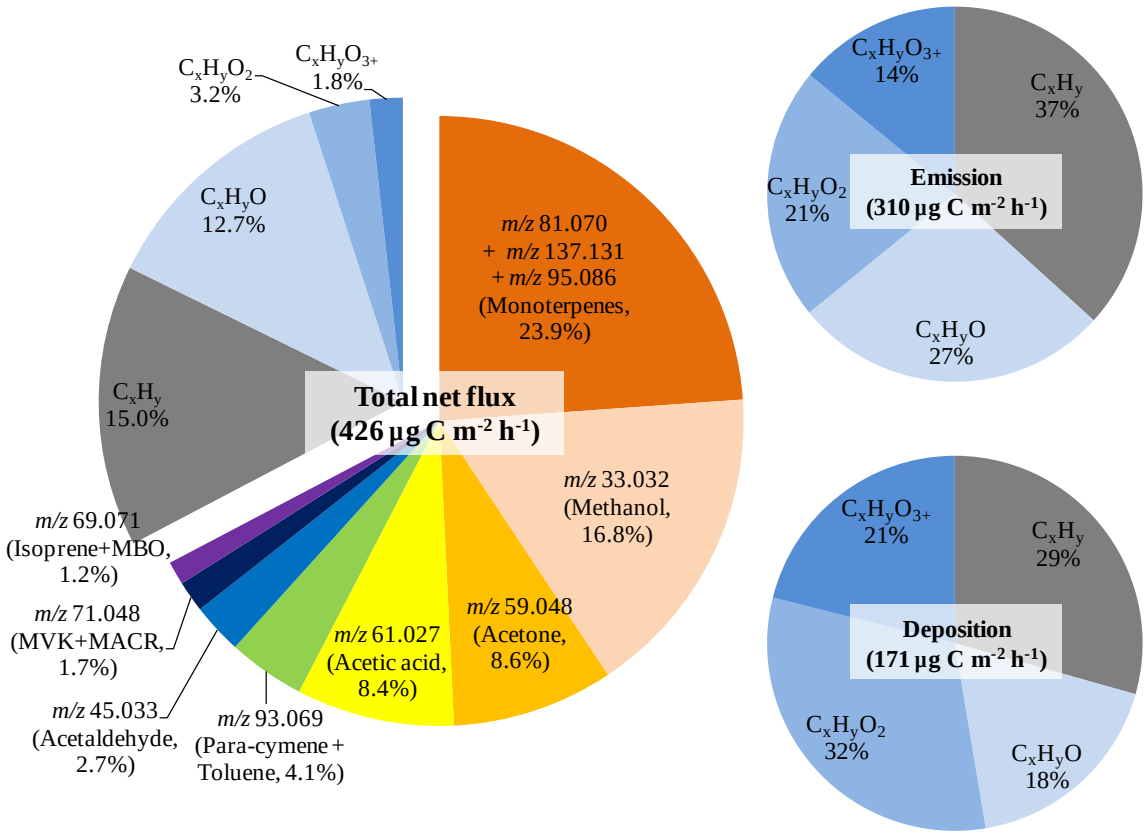

Figure 4. 7. Fractional contribution to the total flux for the VOC with the highest fluxes (162 species) shown in pie chart on left. 10 species were specifically identified, and the remaining 152 masses were categorized by number of oxygen in the molecule as C_xH_y, C_xH_yO, $C_xH_yO_2$, and $C_xH_yO_{3+}$. The two pies on the right separately show the contribution of categorized masses to emission and deposition.

Chapter 5: Summary and future work

5.1 Summary of this work

This dissertation presents novel measurements quantifying ecosystem-scale fluxes of diverse BVOC species and their oxidation products. In two different tree ecosystem; a Ponderosa pine forest (BEARPEX 2009) and an orange orchard (CITRUS 2010), BVOC concentration and eddy covariance flux measurements were conducted using two PTR systems (i.e. PTR-MS and PTR-TOF-MS).

In Chapter 2, I report the canopy-scale fluxes of 17 BVOC species, 3 of which were measured by the eddy-covariance method, and the rest of which were determined using the flux-gradient similarity method, generally called *K*-theory. In contrast to past studies using the flux gradient method for BVOC flux measurements which derived eddy diffusivity (*K*) from flux and vertical gradient measurements of water (H_2O), carbon dioxide (CO_2), or sensible heat, in this thesis a universal *K* was determined as the mean of individual *K*'s calculated from the PTR-MS EC flux and vertical gradient measurements of 3 dominant BVOCs (MBO, methanol, monoterpenes) during BEARPEX 2009 which should have similar source and sink profiles. Through the comparison between the *K*-theory and EC method along with historical measurements from the same site, quantifying BVOC fluxes using the flux-gradient relationship was demonstrated to be a useful method in the case where fast measurements were not available for a diverse range of species.

In Chapter 3, a state of the art instrument, PTR-TOF-MS, was confirmed to be a very powerful tool for determining the ecosystem-scale fluxes of the full range of VOC and OVOC. I demonstrated the capability of PTR-TOF-MS for accurate flux measurements of a much fuller range of VOC by spectral analysis based on EC flux measurement data, inter-comparison with PTR-MS EC fluxes, and qualitative comparison with PTR-MS vertical gradient measurements. This new instrument allows simultaneous measurement of an unprecedented range of BVOC emissions to the atmosphere while also observing their oxidation products and deposition.

In Chapter 4, the ecosystem-atmosphere exchange of the full range of VOC and their oxidation products in gas phase was investigated in an orange orchard during CITRUS 2010 based on PTR-TOF-MS EC flux measurement validated in Chapter 3. Existence of ecosystem exchange for the species having small concentration and bi-directional flux was proved by developing and applying the time-shifted absolute value covariance analysis which is a newly proposed method in this dissertation. At least 494 chemical compounds observed were actively exchanged between the biosphere and atmosphere. The fluxes of most compounds were bi-directional and a large number of species are clearly deposited.

5.2 Recommendations for future work

In this dissertation, I was able to augment our knowledge about what kinds of and how much VOCs and their oxidation products are vertically exchanged at the ecosystem-atmosphere interface.

Through field observations in two independent ecosystems (BEARPEX 2009 and CITRUS 2010), I found that on a carbon mass basis the total BVOC emission rate in Blodgett forest is at least 3 times greater than in the orange orchard even when a much larger number of compounds were accounted for in the CITRUS 2010 measurements (Figs. 2.10 and 3.12). Moreover, the chemical species dominantly emitted from the two sites were obviously different. I also discovered that many more compounds are actively exchanged than the relatively few species that had been observed previously. These results suggest that more comprehensive studies are required for understanding emission/deposition characteristics of VOCs coupled with photochemistry in diverse ecosystems, and raise main 3 questions that I suggest require further investigation:

1) What specific chemical compounds in different ecosystems can be measured by different PTR systems? What chemical formula and structures are responsible in each emitting /depositing species measured by PTR systems?

2) What environmental factors control the fluxes of reactive chemical compounds previously unmeasured, and what kinds of products will be generated through the biogeochemical processes within and above the plant canopy atmosphere?

3) How do these compounds impact regional atmospheric chemistry and global climate?

For the first question, specifying all the compounds measured by two PTR systems is still challenging even though distinguishing isobaric compounds has been improved in PTR-TOF-MS. For example, PTR-MS detects together benzaldehyde and xylene at *m/z* 107, but PTR-TOF-MS is able to separate them at *m/z* 107.049 and 107.085, respectively. However, neither instrument can distinguish isomers having the exact same molecular weight such as methyl-vinyl-ketone and methacrolein; both are detected at *m/z* 71 for PTR-MS and *m/z* 71.048 for PTR-TOF-MS. In addition, ion fragmentation also makes it more complicated to define what exact parent or original ion is responsible for each ion fragment since the fragmentation patterns for all individual chemical species are different and dependent on instrumental conditions (e.g. E/N ratio, temperature, pressure, etc…) used in the experiment. Therefore, further improvements and study on these issues are required.

To explore the second question, more comprehensive field measurements in addition to laboratory studies are recommended. For some dominant BVOC species directly emitted from plants such as isoprene and monoterpenes, the emission is known to be mainly driven by temperature and/or light. However, for the other larger number of species having small concentration and bi-directional fluxes shown in Chapter 4, it is not well understood yet what main controllers are responsible for their emission and deposition since those VOCs are mostly

unmeasured or neglected in previous studies. Consequently, their source and sink functions are not well defined. For very reactive oxygenated compounds, their canopy-scale emission (/deposition) is possibly due to not only direct emission (/uptake) from the plant or soil but also photochemical production within (/above) the canopy. In addition, they are also removed in the atmosphere by proceeding to further oxidation, nucleating to form SOA, or partitioning to existing particles. Thus, the drivers for their emission and deposition are not easy to identify from this research. Future intensive and cooperative field measurement campaigns measuring meteorological parameters and the full range of atmospheric chemical composition including atmospheric oxidants (e.g. O_3, OH, HO_2), aerosol, nitrogen oxides (e.g. NO_X, NO_y), and $CO/CO_2/H_2O$ along with VOC measurements (e.g. gas chromatography and PTR-MS/PTR-TOF-MS EC flux and vertical gradient) will continue to provide better knowledge on the second question. Controlled laboratory studies of uptake and emission for a fuller range of VOCs from a variety of plant species are also still needed, particularly as our ability to measure the VOCs continues to improve.

Finally, modeling work is recommended to address the third question. Particularly, to date BVOC emission models are taking account of a few dominant BVOC species observed from branch level measurements and/or some canopy-scale measurements (e.g. isoprene, monoterpenes, and sesquiterpenes). However, the vast majority of VOC (rather than these few species) as described in Chapter 4 are actively exchanged at the atmosphere-biosphere interface. Those minor species are not in current BVOC emission models, but their size and chemical formulae suggest they should be important for SOA formation and O_3 chemistry which affect regional air quality and global climate. Additionally, their presence in the atmosphere may also account for a significant amount of the missing OH chemical reactivity observed in forest environments, and this is critical to understanding atmospheric oxidative capacity in areas where these emissions are significant. Therefore, sensitivity analyses using a much larger number of reactive VOC should be considered in current BVOC emission and tropospheric chemistry models for better predicting their impacts on regional atmospheric chemistry and global climate.